Local synthesis of steroid hormones in human hair roots

Doctoral thesis

to obtain a doctorate (PhD)

from the Faculty of Medicine

of the University of Bonn

Kristina Dorzweiler, née Hegemann

from Soest (NRW), Germany

2025

Written with authorization of

the Faculty of Medicine of the University of Bonn

First reviewer: Prof. Dr. Ulrich Schweizer

Second reviewer: Prof. Dr. Lutz Schomburg

Day of oral examination: 28.01.2025

From the Institute of biochemistry and molecular biology

Table of Contents

List of abbreviations

ABC transporter family	Adenosine-triphosphate-binding cassette transporter family
Acetyl-CoA	Acetyl coenzyme A
AGA	Androgenetic alopecia
AKR	Aldo-keto reductases
AM	Ante meridiem
ANOVA	ANalysis of Variance
APM	Arrector pili muscle, musculus arrector pili
AR	Androgen receptor
AREs	Androgen-responsive elements
ATP	Adenosine triphosphate
β-Me	β-Mercaptoethanol
C3	Carbon 3
C17	Carbon 17
C18 steroid	18 carbons containing steroid
CAIS	Complete androgen insensitivity syndrome
cDNA	Complementary desoxyribonucleic acid
$CHCL_3$	Chloroform
Ci	Curie
cm	Centimeter
CO_2	Carbon dioxide
CT	Cycle Threshold
Ctrl	Control

CYP	Cytochrome P450
DABA	3,5-diamino benzoic acid dihydrochloride
DA	Diffuse Alopecia
DEPC	Diethyl pyrocarbonate
DHEA	Dehydroepiandrosterone
DHEAS	Dehydroepiandrosterone sulfate
°C	Degree Celsius
5α-DHT	5α-dihydrotestosterone
EC_{50}	Half-maximal respond of a compound
E1	Estrone
E2	17β-estradiol
E1S	Estrone sulfate
EDA	Ectodysplasin A
EDTA	Ethylenediaminetetraacetic acid
EMA	European Medicines Agency
ER	Estrogen receptor
ERα	Estrogen receptor α
ERβ	Estrogen receptor β
EREs	Estrogen-responsive elements
FBS	Fetal bovine serum
FDA	Food and Drug Administration
FGF5	Fibroblast growth factor 5
Fig.	Figure

FPHL	Female pattern hair loss
FSH	Follicle stimulating hormone
g	Gramm
GPER1	G-protein-coupled estrogen receptor 1
GRCh38	Genome Reference Consortium Human Build 38 Organism
$HCLO_4$	Perchloric acid
HDL	High-density lipoproteins
hESR2	Human estrogen receptor 2
H_2O	Water
HSD	Hydroxysteroid dehydrogenases
hHSD17B7	Human hydroxysteroid dehydrogenase 17 B7
hLARS2	Human Leucyl-tRNA synthetase 2
IRS	Inner root sheath
LARS2	Leucyl-tRNA synthetase 2
LH	Luteinizing hormone
LHR	Leydig cell luteinizing hormone receptor
LDL	Low-density lipoproteins
LDLr	Low-density lipoprotein receptor
LLLT	Low-level light therapy
M	Molar
MEM	Minimal essential medium
MeOH	Methanol
µg	Microgram

μL	Microliter
mL	Milliliter
mmol	Millimoles
μM	Micromolar
min	Minute
MOPS	3'Morpholinopropanesulfonic acid
MPB	Male Pattern Baldness
mRNA	messenger Ribonucleic Acid
MT-TI	tRNA isoleucine
MT-TL1	tRNA Leucin 1
MT-TS1	tRNA serin 1
N	Normal
Na_2EDTA	Disodium ethylenediaminetetraacetate
NaOAc	Sodium acetate - 3 H_2O
NGS	Next Generation Sequencing
NH_4OH	Ammonium hydroxide
nM	Nanomolar
ns	not significant
O_2	Oxygen
OAT	Organic anion transporter
OATP	Organic anion-transporting polypeptides
ORS	Outer root sheath
%	Percent

PAPS	3’phosphoadenosine 5’-phosphosulfate
PBS	Phosphate buffered saline
PCA	Principal Component Analysis
pH	Pondus hydrogenii
PM	Post meridiem
POR	Cytochrome P450 oxidoreductase
R^2	Coefficient of determination
rcf	Relative centrifugation force
R_f-value	Relate-to-front value
RIN	RNA Integrity Number
RNA	Ribonucleotide acid
rpm	Rounds per minute
RPM	Reads Per Million mapped reads
RT	Reverse transcriptase
qRT-PCR	Quantitative Reverse Transcriptase Polymerase Chain Reaction
SD	Standard Deviation
SDS	Sodium dodecyl sulfate
SDR	Short-chain dehydrogenases
sec	Second
SEM	Standard Error of the Mean
SERM	Selective estrogen receptor modulator
SHBG	Sex hormone binding globulin
SLC-transporters	Solute carrier transporters

StAR	Steroidogenic acute regulatory protein
STS	Steroid sulfatase
SULT2A1	Sulfotransferase Family 2A Member 1
^{3}H	Tritium
Tab.	Table
TLC	Thin-layer chromatography
TRMT10C	tRNA methyl transferase 10 C
tRNA	transfer RiboNucleic Acid
U	Units
UV	Ultraviolet
v:v:v	Volume:volume:volume
v:v	Volume:Volume

1. Introduction

1.1 Hair physiology, anatomy and the hair growth cycle

1.1.1 Hair physiology and anatomy

Most of the external human skin is able to produce hair (Randall 1994). It is the product of cell differentiation of trichocytes which are of epithelial origin (Langbein and Schweizer 2005). The hair density is determined during development and varies between individuals (Duverger and Morasso 2014). The type of hair changes with age from thin, unpigmented vellus hair where the arrector pili muscle (APM) is absent to strong, pigmented terminal hair (Duverger and Morasso 2014, Heilmann-Heimbach et al. 2016, Ramos and Miot 2015).

Hair serves as an important human feature that fulfills different tasks: Body and scalp hair is needed for heat regulation and to protect the skin from moisture, as well as against ultraviolet (UV-) radiation (Qi and Garza 2014). From a medical point of view, hair is considered as a skin appendage, consisting of specialized keratins like the nails from fingers and toes (Grymowicz et al. 2020, Langbein and Schweizer 2005, Lin et al. 2022).

A hair can be divided into two parts: Shaft and follicle (Grymowicz et al. 2020). The visible part of the hair protruding the skin is called shaft (Grymowicz et al. 2020). The hair follicle is located inside of the skin and hair production occurs within the hair follicle (Grymowicz et al. 2020, Langbein and Schweizer 2005). As illustrated in figure 1, the upper part of the hair follicle includes the infundibulum and isthmus, whereas the proximal end is referred to as the bulb (Fig. 1 A) (Grymowicz et al. 2020).

The three-layered hair (cuticle, cortex, medulla, see Fig. 1 B) is surrounded by two concentric cell layers, the inner (IRS) and outer (ORS) root sheaths (Fig. 1 A), that consist of keratinocytes and serve as a protective layer (Coulson-Thomas et al. 2014, Grymowicz et al. 2020, Langbein and Schweizer 2005, Mistriotis and Andreadis 2013, Santos et al. 2015).

Hair follicles contain epithelial and mesenchymal compartments and interaction of both drives hair follicle cycling and formation of the hair shaft (Ohnemus et al. 2006). The hair follicle is connected to the APM and to the sebaceous and apocrine glands (Fig. 1), which contribute to heat regulation and sebum secretion (Fuchs 2007, Mistriotis and Andreadis

2013, Sinclair et al. 2015). Together they form the pilosebaceous unit, where estrogen synthesis and metabolism take place (Ohnemus et al. 2006).

The hair bulb which contains melanocytes and cells of the ORS surrounds the dermal papilla, that contains mesenchymal cells, supplies nutrition for hair growth and regulates the size of the hair by controlling the number of matrix cells (Coulson-Thomas et al. 2014, Lin et al. 2022, Natarelli et al. 2023, Paus and Cotsarelis 1999). The hair bulb is referred to as active growth center of the hair and proliferation of matrix cells produce the hair shaft (Lin et al. 2022, Paus and Cotsarelis 1999).

The bulge region is the lowest part of the hair follicle and contains stem cells that regulate hair growth (Coulson-Thomas et al. 2014, Fuchs 2007, Mistriotis and Andreadis 2013, Sinclair et al. 2015).

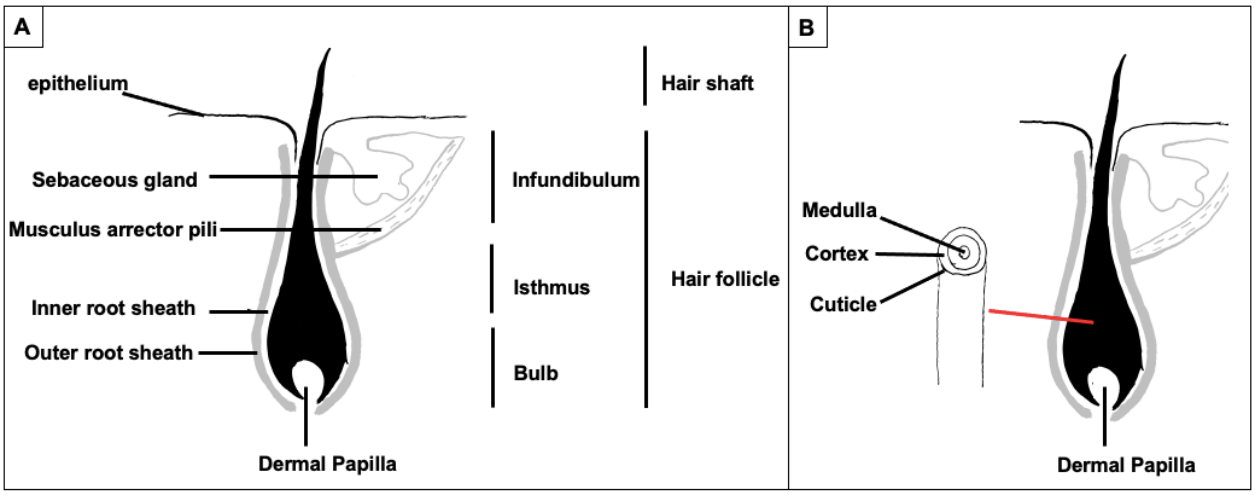

Fig. 1: Hair structure A Pilosebaceous unit and division of the hair into outer and inner part **B** Structure of the three-layered hair shaft. Own work.

1.1.2 The hair growth cycle

Hair formation is a cyclical process consisting of three main stages: Anagen, catagen and telogen (Grymowicz et al. 2020, Ohnemus et al. 2006), as illustrated in figure 2 (Fig. 2). The anagen phase lasts several years and is responsible for active hair follicle growth and hair formation (Grymowicz et al. 2020Ota et al. 2002). The catagen phase represents a transition phase, between anagen and telogen, of only a few weeks in which the hair starts to disconnect from the dermal papilla until the hair reaches the telogen state (Grymowicz et al. 2020, Pierard-Franchimont and Pierard 2013). The telogen phase lasts several

months and is referred to as a resting stage until the hair is finally shed (Grymowicz et al. 2020). Once in a telogen state, a new developing hair grows upwards pushing out the telogen hair (Natarelli et al. 2023).

The duration of the anagen phase determines the length of hair. Cycle length depends on the body area, as well as on various hormones (Duverger and Morasso 2014, Grymowicz et al. 2020, Higgins et al. 2009, Ohnemus et al. 2006, Mistriotis and Andreadis 2013, Sinclair 1998). In humans, different anagen to telogen ratios exist, depending on the body site (Higgins et al. 2014). For example, human eyelashes have shorter anagen phases than scalp hair, underlining the determining role of anagen phase in growth and length of hair (Higgins et al. 2014, Santos et al. 2015, Sinclair 1998).

Some animals display different hair growth patterns due to seasonal changes. Some animals get longer and thicker fur in preparation for colder months, as a result of a synchronized hair cycle (Pierard-Franchimont and Pierard 2013). In humans, hair formation follows an asynchronous rhythm, meaning that some hairs always reside in anagen state, whereas others are close to be shed and therefore hair density remains relatively stable in healthy humans (Natarelli et al. 2023, Pierard-Franchimont and Pierard 2013).

Human hair growth is subject to a gender dimorphism, regulated by a complex interaction of hormones, especially steroid hormones (Schweikert and Wilson 1974).

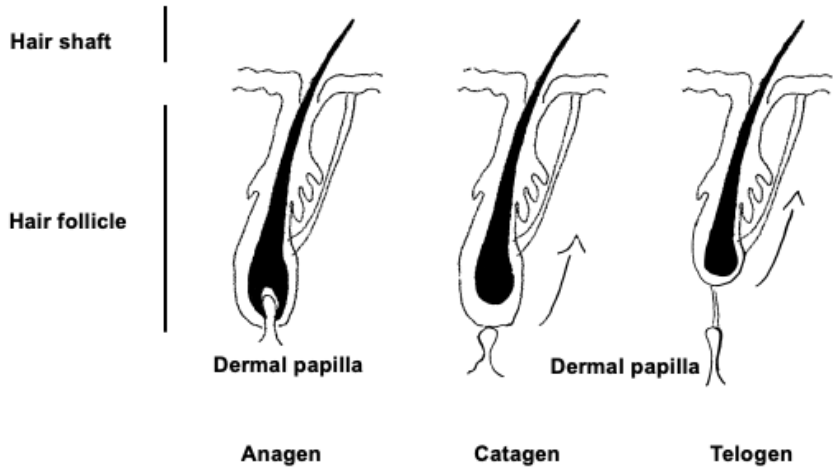

Fig. 2: Hair growth cycle. Own work.

1.2 Cholesterol as source of steroid hormones of the adrenal cortex and gonads

1.2.1 Cholesterol dietary intake, *de novo* synthesis and storage

The origin of all adrenal gland hormones and sex hormones of the gonads is the steroid cholesterol, which contains 27 carbons and therefore sometimes is referred to as C27 steroid (Miller and Auchus 2011, Samavat and Kurzer 2015, Turcu and Auchus 2015). Cholesterol is part of most biological membranes, except plants and bacteria, and contributes to their fluidity (Colardo et al. 2021, Enkavi et al. 2019).

Part of cholesterol is taken up through nutrition, mainly by eating animal products (exogenous or dietary cholesterol) (Xu et al. 2018). Cholesterol can also be derived from *de novo* synthesis in most human cells (Colardo et al. 2021). *De novo* synthesis derives from the mevalonate-isoprenoid pathway and sterol biosynthesis pathway, beginning with acetyl-coenzyme A (acetyl- CoA) and ending with the synthesis of cholesterol in nearly 30 enzymatic reactions (Bah et al. 2017, Cardoso and Perucha 2021, Colardo et al. 2021).

Lipoproteins are responsible for the transport of cholesterol within the body (Rassow et al. 2012). Depending on their content and amount of lipids and proteins, different types of lipoproteins can be distinguished, among these are the group of very low-density lipoproteins (VLDL), low-density lipoproteins (LDL) and high-density lipoproteins (HDL) (Rassow et al. 2012). LDL contain high amounts of cholesterol esters and reduced amounts of fatty acids, so that their density is higher than that of VLDL which in turn contain high amounts of fatty acids (Rassow et al. 2012). LDL is responsible for the peripheral distribution of esterified cholesterol (Rassow et al. 2012). The LDL-receptor (LDLR) mediates endocytosis of LDL molecules, leading to lysosomal hydrolysis of LDL and cholesterol esters, a process termed receptor-mediated endocytosis (Rassow et al. 2012). Unesterified cholesterol is then released from the lysosomal lumen and traffics to the endoplasmic reticulum where it can be further transported to the plasma membrane or mitochondria for the biosynthesis of steroid hormones (Kraemer et al. 2017, Martini and Pallottini 2007, Rassow et al. 2012). Cholesterol needs transporter proteins to cross cell membranes, for example (e.g.) the protein Niemann-Pick type C1 (NPC1), an endolysosomal membrane protein that helps to exit lysosomes, NPC1 like 1 (NPC1L1) which acts as an apical cholesterol transporter in the gut (Goldstein and Brown 2015, O'Neill et al. 2022) and steroidogenic acute regulatory protein (StAR), which is involved

in cholesterol import into the mitochondrial intermembrane space (Miller and Auchus 2011, Mostaghel 2013). The LDLR is transported in vesicles back to the plasma membrane where it can bind further LDL molecules (Rassow et al. 2012). To prevent free cholesterol accumulation, cholesterol can be esterified again and stored as cholesterol ester droplets in the cytosol (Colardo et al. 2021, Kraemer et al. 2013, Rassow et al. 2012, Walther and Farese 2009).

HDL are responsible for transporting excess cholesterol from the periphery to the liver in preparation for the excretion in the feces, a mechanism called reverse cholesterol transport (Ouimet et al. 2019, Papotti et al. 2021).

1.2.2 Steroid hormone synthesis (steroidogenesis)

The hormones of the adrenal cortex, including sex hormones, are derivatives of cholesterol (Maninger et al. 2009, Mostaghel 2013, Samavat and Kurzer 2015). The term “steroid” hormone is related to the shared sterane structure (Fuentes and Silveyra 2019). Sexual hormones induce male sexual development (Rizner and Penning 2014), determine male and female body features (Reisch et al. 2019) and are necessary for maintaining bone mineralization in humans (Chen et al. 2022, Lin et al. 2019, Manolagas et al. 2013). *De novo* steroidogenesis occurs in the adrenal cortex and the gonads, as well as in the placenta (Schiffer et al. 2019).

The synthesis of steroid hormones involves several functional classes of enzymes including cytochrome P450s (CYP), short-chain dehydrogenases (SDR) and aldo-keto reductases (AKR) (Mostaghel 2013, Penning 2011, Rizner and Penning 2014, Schiffer et al. 2019). SDR and AKR enzymes function as hydroxysteroid dehydrogenases (HSDs) (Rizner and Penning 2014, Schiffer et al. 2019).

1.2.2.1 Steroidogenesis in the gonads

In principle, steroidogenesis is always regulated by G protein-coupled receptor-mediated production of cyclic adenosine monophosphate (cAMP) and subsequent activation of StAR protein (Fuentes and Silveyra 2019, Miller and Auchus 2011, Mostaghel 2013). Gonadal steroid synthesis is regulated by the hypothalamic-pituitary-gonadal axis with the

stimulation of luteinizing hormone (LH) and follicle stimulating hormone (FSH) from the pituitary beginning at pubertal age (Schiffer et al. 2019, Tan et al. 2015). Gonadal steroidogenesis is cell type dependent, since each cell type is characterized by the expression of specific enzymes (Schiffer et al. 2019).

1.2.2.2 Steroidogenesis in Leydig cells

Two types of Leydig cells are distinguished: fetal and adult Leydig cells (Zirkin and Papadopoulos 2018). High amounts of androgens produced by fetal Leydig cells are responsible for the formation of male genitalia (Zirkin and Papadopoulos 2018). After birth, fetal Leydig cells are replaced by developing adult Leydig cells (Zirkin and Papadopoulos 2018). Through interaction of the luteinizing hormone receptor (LHR) and LH (secreted by the pituitary gland) on the surface of the Leydig cells, steroidogenesis is initiated (Zirkin and Papadopoulos 2018). Steroidogenesis in the Leydig cells follows the classical androgen biosynthesis pathway (see 1.2.2.4.) yielding androstenedione and testosterone as products (Schiffer et al. 2018). While Leydig cells produce only low amounts of androstenedione and dehydroepiandrosterone (DHEA), testosterone is the main product of Leydig cell-derived steroidogenesis (Schiffer et al. 2019). Testosterone is sythesized to a lesser extend in ovaries and adrenal glands (Schiffer et al. 2018, Schiffer et al. 2019, Tan et al. 2015, Turcu and Auchus 2017, Turcu et al. 2018). After its production, it is released into circulation and transported by sex hormone binding globulin (SHBG) (Schiffer et al. 2018).

Leydig cells also produce estrogens through aromatization (Fuentes and Silveyra 2019), which contribute to the negative feedback on the pituitary (Rassow et al. 2012).

1.2.2.3 Steroidogenesis in theca cells and granulosa cells

Main estrogen production comes from the ovaries and adrenal glands and to a lesser extend from tissues that also possess an aromatase activity like adipose tissue (Fuentes and Silveyra 2019, Rassow et al. 2012).

Ovarian steroidogenesis begins with the synthesis of androstenedione derived from the classical androgen biosynthesis pathway in the theca cells using pregnenolone as

substrate (Schiffer et al. 2018, Schiffer et al. 2019). In the theca cells, andostenedione is partly enzymatically converted to testosterone by the enzyme AKR1C (Schiffer et al. 2019). In the granulosa cells, theca cell-derived androstenedione and testosterone are used for further estrogen biosynthesis (Schiffer et al. 2019).

Estrogens belong to the group of C18 steroids, because they contain 18 carbons (Fuentes and Silveyra 2019). Estrone (E1) and 17β-estradiol (E2) share a common structure consisting of three cyclohexane and one cyclopentane ring systems with a phenolic hydroxyl group at C3, but differ in a ketone group for E1 and one hydroxyl group for E2 at C17 (Fuentes and Silveyra 2019, Samavat and Kurzer 2015).

As illustrated in figure 3, in the granulosa cells, androstenedione can serve as direct substrate for E1 synthesis (Fig. 3) requiring expression of the enzyme aromatase (P450aro, CYP19A1), which is controlled by stimulation of FSH (Fuentes and Silveyra 2019, Hilborn et al. 2017, Ramos and Miot 2015). E1 is then reduced to E2 by enzymes of the HSD family, namely HSD17B1 and HSD17B7 or E2 can be the product of aromatization from theca cell-derived testosterone (Fig. 3) regulated by FSH (Hilborn et al. 2017, Miller and Auchus 2011, Nokelainen et al. 1998, Ramos and Miot 2015, Samavat and Kurzer 2015, Schiffer et al. 2019).

Next to the androstenedione-derived synthesis, E1 can also be the product of desulfation from estrone sulfate (E1S, see Fig. 3) via the enzyme steroid sulfatase (STS) (Hilborn et al. 2017, Mueller et al. 2015). This reaction is reversible, so that E1 can be sulfated by SULT2E1 yielding E1S (Miller and Auchus 2011, Mueller et al. 2015).

E2 is the most important estrogen in premenopausal women, whereas E1 is predominantly synthesized during menopause (Cui et al. 2013, Samavat and Kurzer 2015). E2 can also be oxidized to E1 in the human endometrium catalyzed by HSD17B2 (Miller and Auchus 2011).

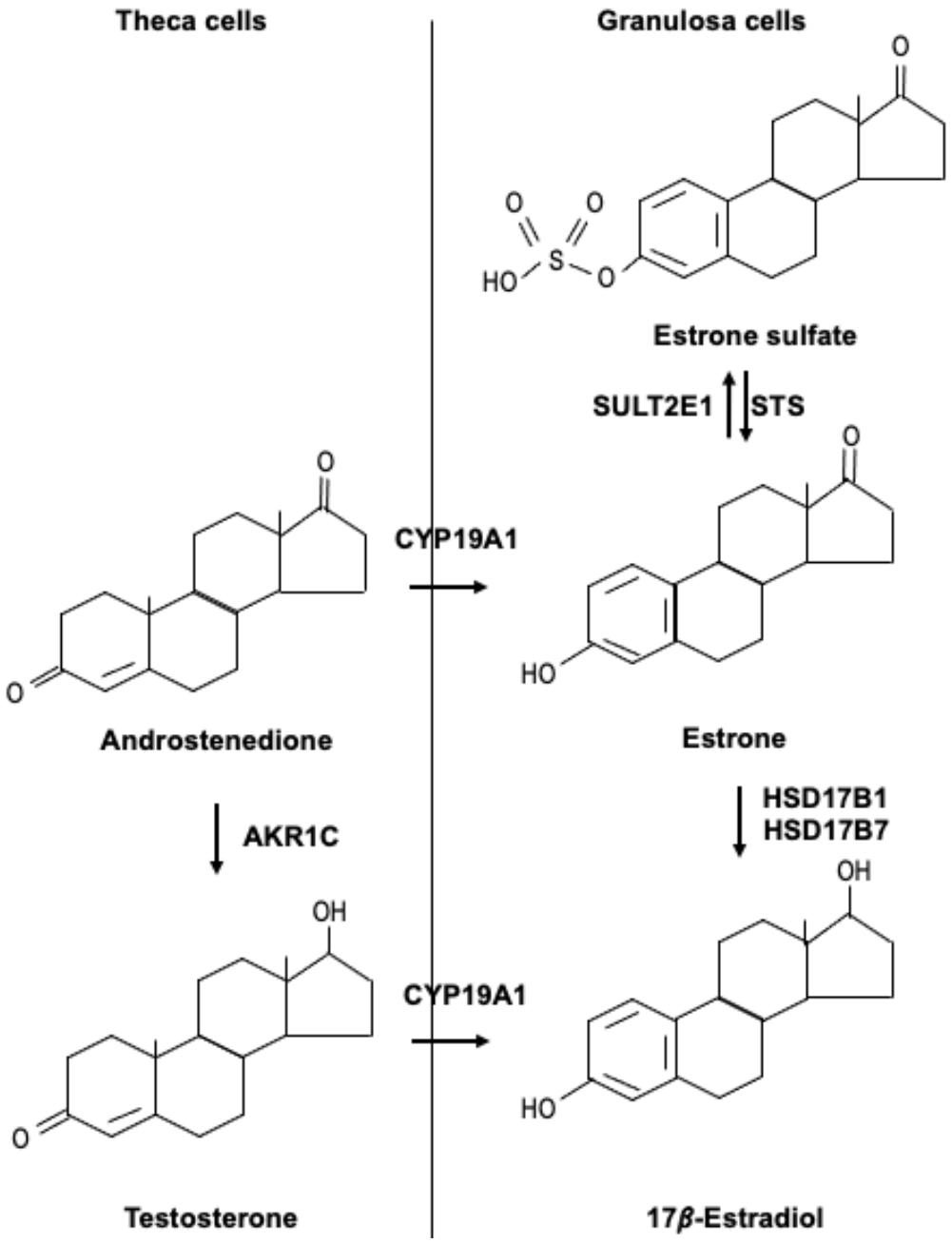

Fig. 3: Steroidogenesis in theca and granulosa cells. Own work.

1.2.2.4 Steroidogenesis in the adrenal zona reticularis

The adrenal cortex is subdivided into three zones: Zona glomerulosa, zona fasciculata and zona reticularis (Schiffer et al. 2019). Each zone expresses specific enzymes and therefore synthesizes a distinct group of steroid hormones: Mineralocorticoids are produced in the zona glomerulosa, the zona fasciculata is responsible for the synthesis of glucocorticoids and the zona reticularis, as well as the gonads, contribute to the formation

of sexual hormones (Schiffer et al. 2019, Turcu and Auchus 2015). Steroids containing 19 carbons (C19 steroids) are synthesized in the adrenal zona reticularis (Turcu and Auchus 2015).

Steroidogenesis from cholesterol in the adrenal cortex is hormone regulated (Maninger et al. 2009). Synthesis of the androgen precursors is induced by adrenocorticotropic hormone (ACTH) which release is stimulated by corticotropin-releasing hormone (CRH) in the hypothalamic-pituitary-adrenal axis in a G-protein-coupled receptor (GPCR)-mediated process (Kraemer et al. 2017, Rassow et al. 2012, Schiffer et al. 2019). ACTH also induces the synthesis of the glucocorticoid cortisol in the adrenal cortex (Rassow et al. 2012). Different to the synthesis of glucocorticoids and androgens, the synthesis of mineralocorticoids is rather controlled by the Renin-Angiotensin-System and aldosterone displays one hormone of the group of mineralocorticoids (Rassow et al. 2012).

The first step in steroid hormone biosynthesis is the transport of C27 cholesterol from the outer to the inner mitochondrial membrane regulated by StAR protein (Miller and Auchus 2011, Mostaghel 2013). At the inner mitochondrial membrane, cholesterol is enzymatically converted to pregnenolone via CYP11A (P450scc) by cleavage of the side chains between carbons 20 and 22 (Miller and Auchus 2011, Mostaghel 2013). Pregnenolone now serves as precursor for the synthesis of other steroid hormones like progesterone and is hydroxylated to 17α-hydroxypregnenolone catalyzed by CYP17A1 (P450c17) (Miller and Auchus 2011, Rassow et al. 2012, Turcu and Auchus 2015).

The most abundant steroid hormones of the adrenal cortex are DHEA (Hernandez-Pando et al. 1998, Kohalmy et al. 2007, Turcu and Auchus 2015, Schiffer et al. 2018), its sulfate ester dehydroepiandrosterone sulfate (DHEAS) and androstenedione (Arnold 2009, Rege et al. 2013, Schiffer et al. 2018). They share a low biological activity (Baulieu 1996, Turcu and Auchus 2017), but can be converted into more active steroid hormones in the periphery like testosterone and the more potent 5α-dihydrotestosterone (5α-DHT) or the estrogens E1 and E2 (Labrie et al. 2000, Oostdijk et al. 2015, Samavat and Kurzer 2015, Schiffer et al. 2018, Turcu and Auchus 2017).

Adrenal steroidogenesis follows the classical androgen biosynthesis pathway. The enzyme CYP17A1 that catalyzes the hydroxylation of pregnenolone into 17α-hydroxy-

pregnenolone is also involved in the synthesis of DHEA from 17α-hydroxypregnenolone, regulated by electron transport via cytochrome P450oxidoreductase (POR) and promoted by cytochrome b_5 (Miller and Auchus 2011). Next to the conversion from 17α-hydroxypregnenolone, DHEA can also be derived as the product of desulfation of DHEAS (Fig. 4), catalyzed by the enzyme STS (Hilborn et al. 2017, Mueller et al. 2015). This reaction is reversible catalyzed by SULT2A1 using 3'phosphoadenosine 5'-phosphosulfate (PAPS) as ubiquitous sulfate donor (Mueller et al. 2015, Naville et al. 1991, Schiffer et al. 2018). As illustrated in figure 4, DHEA can further be reduced to androstenediol by the enzyme HSD17B1 or oxidized to androstenedione with the help of HSD3B1 and HSD3B2 (Hilborn et al. 2017, Rainey and Nakamura 2008, Rege et al. 2013). Both, DHEA and andostenediol, share a common structure consisting of a benzene ring with a hydroxyl group at carbon 3 (C3), but differ in a ketone group for DHEA and a hydroxyl group for androstenediol at carbon 17 (C17) (Schiffer et al. 2019). Structurally, androstendione differs from androstenediol in two ketone groups instead of two hydroxyl groups at C3 and C17 (Schiffer et al. 2019).

The members of the HSD family HSD17B5 and HSD17B3 catalyze the enzymatic conversion of androstenedione to testosterone (Fig. 4) which can be converted to E2 by CYP19A1 (aromatase) in the periphery (Dufort et al. 1999, Hilborn et al. 2017, Ramos and Miot 2015, Samavat and Kurzer 2015). Furthermore, testosterone can be the product of androstenediol (Fig. 4) catalyzed by HSD3B1 and HSD3B2 (Hilborn et al. 2017, Schiffer et al. 2018). Testosterone can be further reduced to 5α-DHT mediated by 5α-reductase (SRD5A) (Turcu et al. 2018).

Steroid hormones share structural similarities to the secosteroid family, with vitamin D_3 (cholecalciferole) being an important family member in humans that is involved in e.g. bone mineralization (Rassow et al. 2012, Zgaga et al. 2019). Vitamin D_3 can be supplemented or synthesized within the human body after exposure of the skin to sunlight and 25-hydroxycholecalciferol (25(OH)D) displays the storage form of vitamin D_3, being hydroxylated in the liver (O'Sullivan et al. 2017, Zgaga et al. 2019). 25(OH)D is further hydroxylated to the active form 1,25-dihydroxycholecalciferol (calcitriol) in the kidney (Rassow et al. 2012).

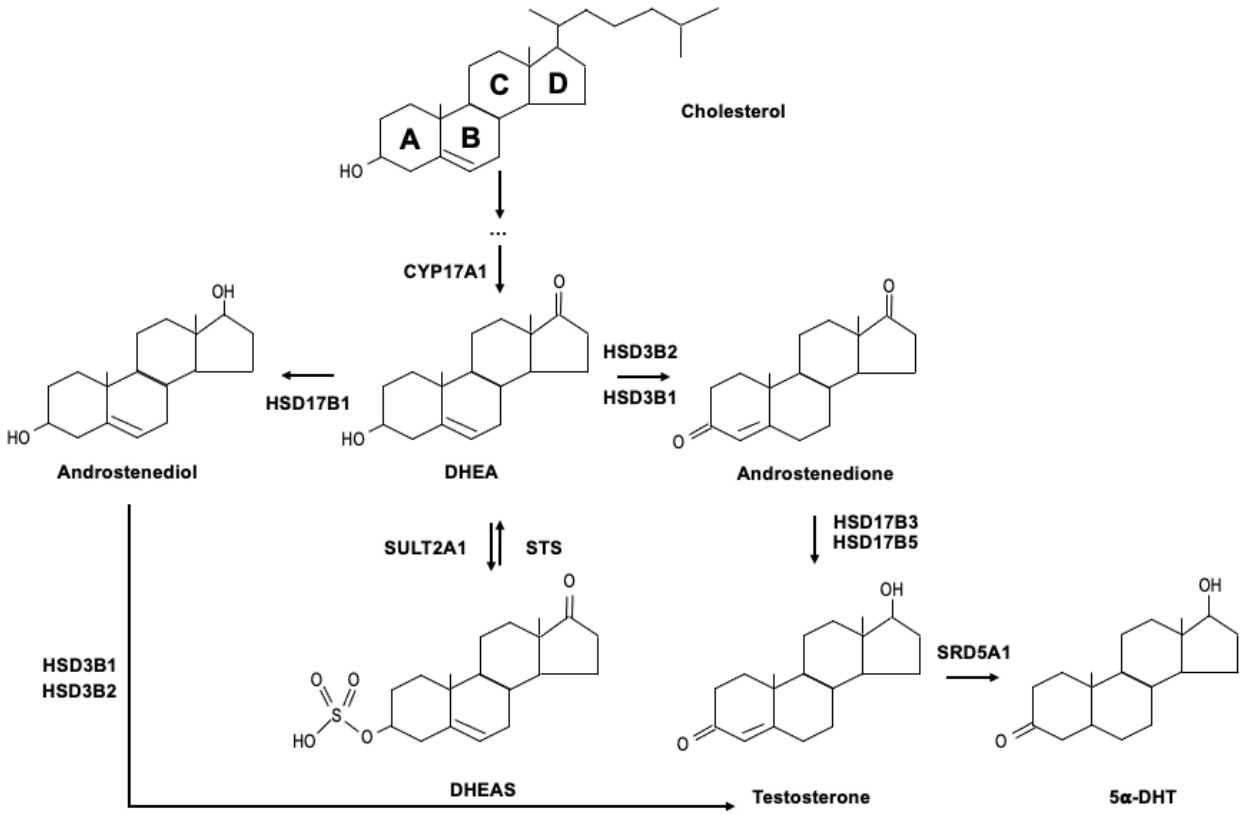

Fig. 4: Classical androgen biosynthesis pathway. Own work.

1.3 Steroid conjugation

1.3.1 Biotransformation

In order to prevent excessive amounts of intracellular cholesterol, cholesterol can be converted into bile acids and are conjugated to amino acids, leading to excretion of the conjugated bile (Martini and Pallottini 2007, Rassow et al. 2012).

Lipophilic steroids need to be structurally remodelled to be efficiently excreted in urine and bile, a process referred to as phase 1 and 2 metabolism (Schiffer et al. 2019). Enzymes involved in phase 1 and 2 reactions are generally thought to act sequentially (Rizner and Penning 2014).

Phase 1 metabolism consists of a series of different reactions leading to an alteration of steroid activity (Schiffer et al. 2019). Phase 1 includes A-ring reduction, followed by oxidation-, hydroxylation- and dehydroxylation reactions (Schiffer et al. 2019). These reactions involve enzymes of the HSD and CYP families (Schiffer et al. 2019).

In phase 2 reactions, steroids are conjugated, helping in increasing water-solubility of the steroid to facilitate the urinary and biliary excretion (Schiffer et al. 2019). Phase 2 metabolism includes reversible sulfation and irreversible glucoronidation reactions (Schiffer et al. 2019).

Circulating steroid conjugates are transported either to the kidney, where they are excreted in the urine or to the liver resulting in biliary excretion (Schiffer et al. 2019). Apart from this, salivary excretion of steroids is also a possible way for eliminating steroids (Schiffer et al. 2019).

1.3.2 Steroids in circulation and uptake of sulfated steroid hormones

After adrenal and gonadal steroidogenesis, both, androgens and estrogens are released into circulation, where estrogens circulate at lower and androgens at higher levels with most sexual steroids being transported as a complex containing albumin or SHBG (Schiffer et al. 2018, Schiffer et al. 2019).

The most abundant steroid in circulation is DHEAS, the product of DHEA sulfation by the enzyme SULT2A1 and cellular uptake of hydrophilic sulfated steroids needs transporter-mediated mechanisms for entering the cell membrane (Mueller et al. 2015, Schiffer et al. 2019). Cellular influx and efflux require transport proteins of the solute carrier (SLC) and adenosine-triphosphate (ATP)- binding cassette (ABC-transporter) families and there is evidence that both protein types are capable of bidirectional transport (Mueller et al. 2015, Roth et al. 2012).

Transporters of the SLC family like organic anion-transporting polypeptides (OATPs) and organic anion transporters (OATs) are known to mediate the uptake of sulfated steroids, where it is suggested that sulfation of steroids is needed to expedite circulatory transit and to facilitate cellular uptake via OATPs expressed by the corresponding target cells (Geyer et al. 2017, Hobkirk 1993, Mueller et al. 2015, Roth et al. 2012, Schiffer et al. 2018). Cellular efflux of substrates may be mediated by ABC transporters (Roth et al. 2012). One example of SLC transporters involved in steroid transport is SLCO2B1 (OATP2B1) and a well-studied substrate of SLCO2B1 is E1S (Medwid et al. 2021).

1.3.3 Transport of steroid hormones

There is evidence that androgens bind to some sort of endocytic receptor or transmembrane transporter at the cell surface (Foradori et al. 2008, Geyer et al. 2017). Studies in *Drosophila melanogaster* suggest, that cellular uptake of steroid hormones by facilitated diffusion is transporter-mediated (Okamoto et al. 2018). Hammes et al. described megalin-mediated endocytic uptake of steroid hormones in Brown Norway rat choriocarcinoma 16 (BN16) cells and in megalin knockout mice (Hammes et al. 2005). Our group recently described mutations in megalin in patients with partial androgen insensitivity syndrome (Marko et al. 2022). Testosterone is supposed to alter via an unknown mechanism the conformation of gap junctions (Foradori et al. 2008, Pluciennik et al. 1996). Furthermore, it is assumed that androgen metabolites induce changes in the membrane “flexibility” through exchanging charges and thereby possibly pass the cell membrane (Foradori et al. 2008, Żylińska et al. 1999). There is also the class of lipocalin proteins, that bind steroids and may serve as substrates for receptors (Jensen-Jarolim et al. 2016).

1.4 Steroids in signal transduction, hair growth and disease

1.4.1 Steroid receptors and their ligands

Steroid hormones are necessary for the beginning and maintenance of developmental changes and the initiation of sexual differentiation in humans, with vellus hair from prepubertal pubis, axillar, beard and chest growing into terminal hairs as a reaction to rising androgen levels (Grymowicz et al. 2020, Schiffer et al. 2019, Sinclair 1998).

Steroid hormones act via interaction with their nuclear receptors: Cortisol shows binding affinities for both, the glucocorticoid receptor (GR) and the mineralocorticoid receptor (MR), whereas aldosterone binds to the cytosolic MR (Rassow et al. 2012). Progesterone serves as ligand for the progesterone receptor (PR) (Yakin et al. 2023). Androgens like testosterone and 5α-DHT act via binding to the androgen receptor (AR), with 5α-DHT having higher binding affinity than testosterone (Chen et al. 2019, Tan et al. 2015). Furthermore, two highly homologous nuclear estrogen receptors (ER) α and β (ERα, ERβ) and the vitamin D-receptor (VDR) exist (Chen et al. 2022, Fuentes and Silveyra 2019, Rassow et al. 2012). Quite remarkably, G Protein-Coupled Estrogen Receptor 1 (GPER1)

has been described, with controversial findings on GPER1 functions (Chen et al. 2022, Fuentes and Silveyra 2019, Prossnitz an Barton 2011). GPER is supposed to promote phospholipase C (PLC)-mediated calcium mobilization from the endoplasmic reticulum (ER) (Hernández-Silva et al. 2020, Xu et al. 2019).

In principle, as mentioned before (1.2.2.1.), steroid receptors act via similar mechanisms, that involve G protein-coupled receptor-mediated activation of protein kinases and subsequent transcription of StAR, followed by StAR-regulated cholesterol transport to the inner mitochondrial membrane (Fuentes and Silveyra 2019, Miller and Auchus 2011, Mostaghel 2013). After interaction with the corresponding ligands, the PR interacts with progesterone-responsive elements (PREs), the AR binds to androgen-responsive elements (AREs), initiating male sexual development and differentiation, the ER interacts with estrogen-responsive elements (EREs) and the VDR binds to vitamin D-responsive elements (VREs) in regulatory regions of target genes in order to regulate their transcription (Chen et al. 2022, Elmlinger et al. 2001, Fuentes and Silveyra 2019, Rozmus et al. 2020, Sahu et al. 2014, Tan et al. 2015, Yakin et al. 2023).

The mammary gland expresses both ERα and ERβ and ERα serves as prognostic marker for the outcome of ER-positive breast cancer (Burns and Korach 2016). Experiments in mice and murine cells have demonstrated the importance of epithelial ERα expression for mammary gland development (Rusidzé et al. 2021), whereas deletion of ERβ did not result in developmental defects in mice (Krege et al. 1998), although the mammary gland of lactating mice lacking functional ERβ (ER$\beta^{-/-}$) was less well differentiated in comparison to wildtype mice (Förster et al. 2002). Marjon et al. suggest a role for GPER in the proliferation and growth of mammary tumors on the basis of experiments in GPER knockout mice (KO/PyMT) that showed smaller tumors in advanced tumor stages than GPER wildtype mice (WT/PyMT) (Marjon et al. 2015). Interestingly, high expression of GPER was shown to be associated with an aggressive subtype of triple negative breast cancer (TNBC) in humans and the expression increases with development and progression of ER-positive breast cancer (Xu et al. 2022). Zhang et al. showed that high expression of GPER1 mRNA was not associated with the overall survival of patients suffering from TNBC, but with a better overall survival of patients with ER-positive breast cancer (Zhang et al. 2022). And Martin et al. associated low cytoplasmic GPER

expression with adverse breast cancer-specific patient survival, whereas nuclear GPER expression was not (Martin et al. 2018).

There are several organic and inorganic molecules that are able to act as agonists or antagonists at steroid receptors: Cyproterone acetate and spironolactone display steroidal antiandrogens, with limited clinical application, that antagonize androgen actions by competing for AR binding (Tan et al. 2015). More extended clinical application can be seen for ER ligands like oral contraceptives (Soria-Jasso et al. 2019) and the class of selective estrogen receptor modulators (SERMs), which role as agonists or antagonists is dependent on the tissue where they act on (Fuentes and Silveyra 2019, Paterni et al. 2014). SERMs target both ER subtypes (Paterni et al. 2014). In its role as antagonists, SERMs compete with estrogens for the binding to the ER, thereby inhibiting binding of estrogens to the receptor (Wardell et al. 2014). After the successful binding to the ER, SERMs act as agonists and induce a conformational change in the ligand binding domain (Fuentes and Silveyra 2019).

Tamoxifen is one of the most used SERMs in the treatment of ER-positive breast cancer (Fuentes and Silveyra 2019). The compound is known to modulate estrogen signaling by competitively inhibiting the binding of estrogens to the ER and preventing estrogen action, therefore acting as antagonist in breast tissue (Freites-Martinez et al. 2018, Fuentes and Silveyra 2019, Gonzalez et al. 2016). Vice versa it fulfills its task as agonist in the uterus (Fuentes and Silveyra 2019).

Next to E1, E2 and SERMs, androstenediol can also serve as a ligand for the ER (Miller et al. 2013, Paterni et al. 2014).

1.4.2 Steroids in hair growth and disease

Stimulation of sebum secretion and hair growth is dependent on the local concentration of androgens in the skin (Schiffer et al. 2018). The impact of androgens on hair follicles depends on the hair location on the body, as known for follicles located in the eyelashes that are not androgen-regulated (Grymowicz et al. 2020).

Hirsutism is characterized by an excessive growth of terminal hair from a male patterned type that is mostly associated with an excess of androgen levels in the blood (hyperandro-

genemia) (Unluhizarci et al. 2023). Alopecia areata belongs to the non-scarring types of hair loss, beginning with loosing scalp hair as patches (Betz et al. 2015). It is associated with a deregulation of the immune system and with an increased local production of androgens (Betz et al. 2015, Schiffer et al. 2018). Complete androgen insensitivity syndrome (CAIS) also illustrates the determining effect of androgens on hair development in the human body (Krupp et al. 2012), since there is sparse or even a lack of pubic and axillary hair in case of CAIS, if there are mutations within the AR gene (Auer et al. 2022, Kapama et al. 2022).

Despite the role of male and female sexual hormones on the growth of body and sexual hair, all further considerations in this thesis regarding hair development and local steroid hormone metabolism concern human scalp hair.

There is evidence that estrogens play an important role in human scalp hair growth. In premenopausal women, circulating E1 and E2 levels are between 5 and 1000 pmol per liter blood plasma as mentioned in table 1 (Tab. 1) (Mueller et al. 2015, Schiffer et al. 2019). Higher E2 levels can be determined for pregnant women reaching a maximum in the third trimenon (Robinson and Klein 2012). During pregnancy, hair growth increases, whereas hair shedding decreases (Pierard-Franchimont and Pierard 2013). After pregnancy, estradiol decreases to normal levels again. It is believed, that observations on women who suffer from postpartum telogen effluvium can be explained with variations in hormone levels after delivery (Mirallas and Grimalt 2016).

As a result of a normal process of ageing, the amount of scalp hair and the hair diameter decrease with age (Robbins et al. 2012). But still, circulating E1 and E2 levels in postmenopausal women are lower than in premenopausal women (Tab. 1), with E1 achieving only a quarter of the former amount and E2 only a tenth (Mueller et al. 2015, Schiffer et al. 2019). E2 shows higher binding affinity for both, ERα and ERβ, and E1 shows lower affinity for both receptor types (Alemany 2021).

Tab. 1: Blood plasma levels of estrogens. Reference: Mueller et al. 2015.

Steroid	Premenopausal Women	Postmenopausal Women	Reference
E1S	2 – 5 nmol/ L	0.5 – 2 pmol/ L	(Mueller et al. 2015)
E1	15 – 500 pmol/ L	10 – 120 pmol/ L	
E2	5 – 1000 pmol/ L	5 – 80 pmol/ L	

1.4.3 E1 and E2 Formation in Isolated Human Hair Roots - Findings by Wehner and Schweikert

Steroids are subject to local activation and inactivation, as known for cortisol or vitamin D_3, as well as for 5α-DHT. As mentioned before, cortisol can serve as ligand for the MR, but since the cellular amount of cortisol is higher than the concentration of aldosterone, cortisol successfully competes with aldosterone for the MR binding (Rassow et al. 2012). In order to facilitate aldosterone binding to the MR, cortisol needs to be inactivated to cortisone, mediated by the enzyme 11β-hydroxy-dehydrogenase (Rassow et al. 2012). A similar mechanism is known for calcitriol, the active form of vitamin D_3. If a sufficient cellular amount of calcitriol is available, calcitriol is converted to 24,25-dihydroxycholecalciferol mediated by the enzyme CYP24A1, which competes with the enzyme 1α-hydroxylase for the VDR binding (Rassow et al. 2012).

Based on the hypothesis that hair may increase local E2 signaling through uptake and activation of E1S, Wehner and Schweikert identified the local synthesis of biologically active E1 and E2 from the biologically inert substrate E1S in human hair roots from healthy donors (Wehner and Schweikert 2014). In their experiments, Wehner and Schweikert investigated isolated scalp hair roots from men and women who reported no history of hair growth disorders and no use of oral or local steroids (Wehner and Schweikert 2014).

Their comparisons on hair from men and women from different anatomical sites and growth stages indicate that hair roots from scalp, beard and body possess enzymatic activity and are able to convert hormonally inactive steroids in the tissue into active steroid hormones (Wehner and Schweikert 2014). They showed that local E2 formation from E1S in the human scalp hair roots is higher than that resulting from the aromatization of androstenedione and testosterone (Wehner and Schweikert 2014). They also recognized,

that the metabolism is gender-, age-, site- and growth phase-dependent (Wehner and Schweikert 2014). They showed that estrogen formation in male anagen scalp hair roots was significantly lower than in female anagen scalp hair roots of people younger than 50 years (Wehner and Schweikert 2014). In contrast to that, comparable levels were observed in anagen hair roots of other anatomical sites (Wehner and Schweikert 2014). They found that estrogen formation in women older than 50 years was significantly lower than in women younger than 50 years, but higher in men older than 50 years (Wehner and Schweikert 2014). They propose, that local E2 formation from E1S could play an important role during the hair growth cycle, since they were not able to detect E2 in telogen hair (Wehner and Schweikert 2014).

1.5 Premature Hair Loss

1.5.1 Androgenetic alopecia (AGA) or *female pattern hair loss* (FPHL)

The term androgenetic alopecia (AGA) summarizes hair loss patterns occurring in men and women classified by Hamilton/Norwood and Ludwig (Hadshiew 2022, Ludwig 1977, Lutz 2018). Alopecia in women with increased androgen levels in the blood is called androgenetic alopecia and if blood androgen levels are normal the term FPHL is used, which is the most common cause of female hair loss (Davis and Callender 2018, Lutz 2012, Redler et al. 2017).

AGA is the most common hair loss in men (Heilmann-Heimbach et al. 2016). The enzyme SRD5A2 is associated with AGA (Ntshingila et al. 2023) as well as implicated to be involved in the pathophysiology of *male pattern baldness* (MPB), namely in the increase in the sensitivity to androgens (Heilmann-Heimbach et al. 2017).

Several genes are proposed to be involved in male hair loss, as described for MPB (Heilmann-Heimbach et al. 2017). Among these genes are fibroblast growth factor 5 (*FGF5*) and ectodysplasin A (*EDA*) (Heilmann-Heimbach et al. 2017). FGF5 is suggested to be involved in the misfunction of the regulation of the anagen to catagen transition (Heilmann-Heimbach et al. 2017, Higgins et al. 2014). It is also supposed to determine hair length in human hair follicles (Higgins et al. 2014). EDA is required for placode formation and therefore is necessary for the process of hair formation (Duverger and

Morasso 2014). Deregulation of EDA, resulting in decreased levels, is described for human hair growth disorders (Duverger and Morasso 2014, Heilmann-Heimbach et al. 2016). Mutations in the EDA gene are associated with hypohidrotic ectodermal dysplasia (HED), a disease that is characterized by failed development of hair and teeth, ranging from hypodontia to anodontia (Clarke et al. 1987).

AGA belongs to the non-scarring alopecia types and is characterized by a progressive loss of scalp hair (Sinclair 1998) starting in the “reproductive years”, in rare cases also during puberty (Davis and Callender 2018, Lutz 2018, Ramos and Miot 2015). Anagen phase is shortened in AGA (Paus and Cotsarelis 1999). It is caused either by genetic inheritance and/ or by hormonal imbalances (Lutz 2012). Terminal hairs change their appearance to intermediate or vellus hairs, a short, nonmedullated type of hair without association to the sebaceous gland (Duverger and Morasso 2014, Nestor et al. 2021, Ramos and Miot 2015).

Pathogenetically, two possible causes exist for the development of AGA: First, the hair loss can be caused by an increased sensitivity of the hair follicles against local 5α-DHT, which leads to a miniaturization of the hair follicles (Arias-Santiago et al. 2012, Lee et al. 2015, Lutz 2018, Paus and Cotsarelis 1999, Sinclair et al. 2015). And second, it can also occur in case of high androgen levels in the blood (Lutz 2018). The hair loss is clinically characterized by a diffuse and progressive thinning of the hair in the fronto-vertical or parietal area of the scalp, while the frontal hairline remains intact (Grymowicz et al. 2020, Lutz 2012, Lutz 2018, Nestor et al. 2021, Sinclair 1998). In AGA the amount of telogen hair is normally only increased in the central part of the scalp (Lutz 2012).

Interestingly, findings in epidemiology suggest associations of AGA with other somatic diseases: Arias-Santiago mentioned in 2010 and 2012 associations of greater prostate volume with early urinary flow changes in men with AGA (Arias-Santiago et al. 2012) as well as associations between AGA and cardiovascular risk factors of metabolic syndrome and carotid atheromatosis in men and women (Arias-Santiago et al. 2010).

1.5.2 Diffuse hair loss

In contrast to AGA, diffuse hair loss (diffuse alopecia (DA)) affects the scalp area uniformly (Qi and Garza 2014). Diffuse hair loss shows clinical variation and different stages and can be caused by several factors, including thyroid dysfunction, iron, zinc or biotin deficiencies or pharmacological side effects (Lutz 2012).

Since hair loss has been described to be associated with thyroid dysfunction (Cohen et al. 2023, Deo et al. 2016, Lutz 2012, Natarelli et al. 2023), laboratory testing in case of hair loss commonly includes thyroid stimulating hormone (TSH), thyroxine (T4) and trijodthyronine (T3) (Wolff et al. 2016). Furthermore, experiments in murine models have shown that mice, lacking thyroid hormone receptors, develop thinner fur than wildtype mice, although the overall number of hair follicles were similar, but in TR-deficient mice the number of hair follicles in anagen phase was significantly lower (Contreras-Jurado et al. 2014).

“Telogen effluvium” is one type of diffuse hair loss, in which a large number of hairs are simultaneously in telogen state (Qi and Garza 2014).

Another form of diffuse hair loss is called “anagen effluvium”, which is characterized by breaking off of hair instead of induced shedding of hair (Qi and Garza 2014).

And a third type of diffuse hair loss is referred to as “loose anagen syndrome” in which duration of anagen phase is shortened resulting in a reduced hair length (Qi and Garza 2014).

1.6 Confirmation of the type of hair loss and available therapies

1.6.1 Confirmation of the type of hair loss in a pluck trichogram

A trichogram serves as a method for differentiating the form of alopecia and to determine whether a therapy is successful or not (Lutz 2012, Ramos and Miot 2015). It is an analysis of epilated scalp hair roots under a microscope, standardized in the 1950s by Van Scott (Ramos and Miot 2015, Van Scott et al. 1957).

Since hair roots from different growth stages can be distinguished by appearance (Fig. 5), it is possible to assess the number of hair roots from each growth phase and to determine the percentage of hair of each hair growth stage (Ramos and Miot 2015).

In humans, a physiological trichogram of the capillitium shows at least 80 % of hair in an active growing stage (Lutz 2012) and maximal 14 % in the telogen phase (Lutz 2001, Lutz 2012). Sporadically, catagen or dystrophic hair can be counted or even broken off hair (Lutz 2012).

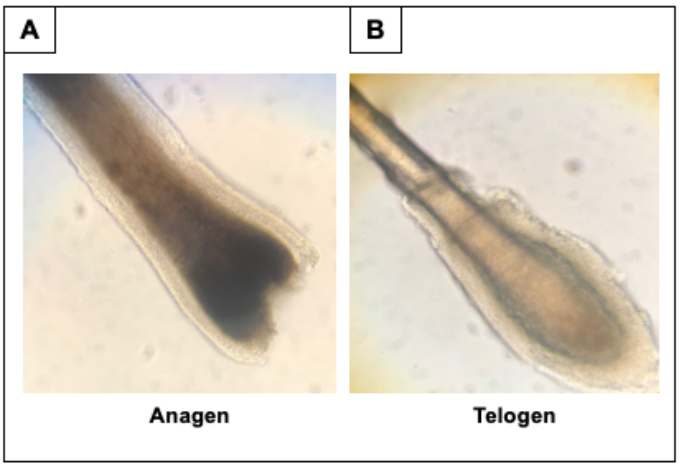

Fig. 5: Hair roots A Anagen hair root **B** Telogen hair root, 20x light microscope, own work.

In general, increasing telogen rates determined by pluck trichogram can be associated with moderate hair growth disorders, but the exact cause for the impaired growth has to be further specified (Lutz 2001). It is worth mentioning, that anagen and telogen rates show variations according to the activity of the hair loss (Lutz 2012). To avoid a distortion of results, the hair should not be washed for five days before carrying out a trichogram, otherwise most telogen hair would be mechanically shed in advance, because of the washing process and results would be falsely embellished (Lutz 2012, Ramos and Miot 2015).

1.6.2 Approved therapies

Hair loss represents a common symptom with a multitude of different origins. The demand for therapy options is understandably high, but there are only a few FDA- (Food and Drug Administration) and EMA- (European Medicines Agency) approved pharmaceuticals or devices available with potentially restricted efficacy. Topical minoxidil solution, oral finasteride and low-level light therapy (LLLT) represent FDA-approved options for treating androgenetic alopecia (Nestor et al. 2021, Panchaprateep and Lueangarun 2020, Paus and Cotsarelis 1999), with topical minoxidil and systemic finasteride also being drugs from the European guideline for the diagnostic and treatment of AGA (Wolff et al. 2016). The type of therapy chosen depends on the confirmed presence of a hyperandrogenemia (Lutz 2018).

1.6.2.1 Minoxidil

Minoxidil acts on potassium channels in smooth muscle leading to vasodilation, as well as it increases anagen state of the hair cycle and therefore has stimulating effects on hair formation and growth (Fabbrocini et al. 2018, Kaiser et al. 2023). The compound is a pro-drug that is converted into its active form inside of the hair (Fabbrocini et al. 2018). Minoxidil was actually approved by the FDA for the treatment of hypertension (Fabbrocini et al. 2018).

Topical minoxidil serves as a vasodilator and was shown to avoid hair loss by prolonging anagen phase and increasing hair diameter and hair density (Nestor et al. 2021, Paus and Cotsarelis 1999, Qi and Garza 2014, Trueb 2021). Furthermore, adipose-derived stem cells (ASC) pretreated with minoxidil and injected into mice were shown to promote hair growth in vivo (Choi et al. 2018).

The compound needs to be applied once or twice a day (Nestor et al. 2021), yielding variable effects in a minority of cases (Paus and Cotsarelis 1999).

Few side effects are mentioned for topical minoxidil treatment: skin irritation and contact allergic dermatitis (Sinclair 1998).

The compound can be used for both men and women (Qi and Garza 2014).

1.6.2.2 Finasteride

Finasteride is an inhibitor of the enzyme SRD5A type 2 (SRD5A2) that was originally shown to be effective in the treatment of prostate cancer (Vickers et al. 2010). Finasteride blocks the conversion of testosterone into its more active metabolite 5α-DHT (Fabbrocini et al. 2018).

The compound is not approved for the use in women (Fabbrocini et al. 2018).

1.6.2.3 Low-level light therapy

Low-level light therapy (LLLT, red light) has been proposed to stimulate hair growth, both in male and female hair loss diseases (Jimenez et al. 2014), but the exact molecular mechanisms are not completely understood (Fabbrocini et al. 2018, Jimenez et al. 2014).

A study by Jimenez et al. in 2014 revealed an increase in the density of terminal hair after 26 weeks treatment with the FDA-cleared HairMax Laser Comb® with a device emitting a wavelength of 655 nm (Jimenez et al. 2014).

LLLT has to be used three times a week with a treatment duration of 8 - 15 minutes (Jimenez et al. 2014).

1.6.3 Other options

Next to the approved therapies with topical minoxidil and oral finasteride, other pharmaceuticals have been described that may support the treatment of androgenetic alopecia. These options include cyproterone acetate (Fabbrocini et al. 2018, Lutz 2018) and spironolactone (Lutz 2018), the latter being tested as off-label drug, since it is not approved for any dermatologic conditions (Levy and Emer 2013).

1.7 Aim of the project

The overall aim of the current project was to test the hypothesis that hair loss may be correlated or even caused by a reduced enzymatical conversion of sulfated steroids into E2 in the human scalp hair root. More precisely, the project was supposed to confirm local steroid metabolism, as it was described by Wehner and Schweikert (Wehner and Schweikert 2014), with a focus on anagen scalp hair of healthy women, also in dependency of age.

Furthermore, the aim was to compare local steroid hormone metabolism in scalp hair roots of healthy women and women with a history of hair growth disorders (AGA or DA), and to investigate if AGA differs from DA. In this context, also gene expression data from hair roots were compared between the three observation groups (control, AGA, DA) in order to uncover potential transcriptional differences between control, AGA and DA. The analysis was supposed to give insights into the expression pattern of steroid hormone transporters or receptors and enzymes that are involved in the oxidation, reduction, conjugation and desulfation of steroid hormones that may affect the local concentration of steroids in hair roots and may influence the effects of steroid hormones on their corresponding receptors.

Since androstenediol shows binding affinity for the ER, another goal was to find out if DHEA may also represent a source of ER-signaling.

2. Materials and methods

2.1 General equipment and material

2.1.1 General equipment

Tab. 2: General equipment

Product	Name	Purchase
Cell culture hood	Hera Safe, Heraeus Type: HS 12/2 REF: 51010924 Fabric No.: 95110994	Thermo Scientific, Waltham (USA)
Centrifuge	Eppendorf 5430 Eppendorf 5810 R	Eppendorf, Hamburg (Germany) Eppendorf, Hamburg (Germany)
Heating Blocks	Thermomixer comfort MHR-20	Eppendorf, Hamburg (Germany) HLC BioTech
Homogenisator	Ultra Turrax T25	IKA-Werke GmbH & Co. KG, Staufen (Germany)
Ice Machine	Scotsman AF 80	Scotsman
Incubators	Galaxy S14	New Brunswick, an Eppendorf Company, Hamburg (Germany)
INTAS Science imaging	Gel imager	INTAS, Göttingen (Germany)
Mastercycler ® ep realplex		Eppendorf, Hamburg (Germany)
Microplate reader	Infinite M Plex	Tecan Deutschland GmbH, Crailsheim (Germany)
Microscope	Olympus BH-2	Olympus
Microwave	Type 7873	Severin
Nanophotometer	NanoDrop	Thermo Fisher
Photo machine	Mitsubishi P93D	Mitsubishi
Pipetboy	Accujet Pro	Brand
Pipettes	Eppendorf research Plus (2.5 µL, 10 µL,	Eppendorf, Hamburg (Germany)

	100 µL, 200 µL, 1000 µL)	
	Gilson (20 µL, 200 µL, 1000 µL)	Gilson International B.V., Limburg an der Lahn (Germany)
Power Supply	PAC 200	BioRad, Hertfordshire (United Kingdom)
Scale	Precision scale LPWQ-723i Serial No.: IT1402669	VWR International, Darmstadt (Germany)
	Serial No.: 50311283	Sartorius AG, Göttingen (Germany)
SpeedVac		ThermoFisher, Scientific Savant
Thermocycler	Mastercycler ep gradient S realplex 2	Eppendorf, Hamburg (Germany)
TriCarb liquid scintillation counter		PerkinElmer, Waltham, MA, USA
Vortex	Vortex Genie-2, Model G-560E; Serial No: 2-95848	Scientific Industries

2.1.2 General materials

Tab. 3: General materials

Product	Description	Article number	Purchase
Benchguard Extra	49 cm x 50 cm	115-9321	VWR International, Darmstadt (Germany)
Culture tubes with screw cap	glass	RG09	A. Hartenstein GmbH, Würzburg (Germany)
Disposal bags	small	86.1197	Sarstedt, Nümbrecht (Germany)

Gloves	Nitratex Microtouch, size M	4400053	Ansell Healthcare Europe N.V., Brussels (Belgium)
	Nitratex, size M	112-1845	
Liquid scintillation vials		AYX5.1	Carl Roth GmbH und Co. KG, Karlsruhe (Germany)
Objective slides	Mattrand	14000590	Engelbrecht Medizintechnik
Pipette filtertips biosphere	10 µL	70.3020.255	Sarstedt, Nümbrecht (Germany)
	20 µL	70.1114.210	
	200 µL	70.760.212	
	1000 µL	70.3050.255	
Pipette tips	10 µL	70.3010	Sarstedt, Nümbrecht (Germany)
	200 µL	70.3030.020	
	1000 µL	70.3050.020	
Seals	Microseal 'B' Seal	MSB1001	BioRad, Calofornia (USA)
Serological pipettes	10 mL	4488	Sarstedt, Nümbrecht (Germany)
	25 mL	4489	
	50 mL	86.1689.001	
Syringe filter	0.22 µm Filtropur S	83.1826.001	Sarstedt, Nümbrecht (Germany)
Syringes Omnifix-F Luer solo	Single-use, 0.01 - 1 mL	9161406V	B. Braun Melsungen AG, Melsungen (Germany)
TC-dish 35	Standard	83.3900	Sarstedt, Nümbrecht (Germany)
TLC Plates	Polygram Sil G 0.2 mm silica gel 20 x 20 cm	805013	Macherey-Nagel, Düren (Germany)
Tubes	Falcon 15 mL	62.554.502	Sarstedt,

	Falcon 50 mL	62.547.254	Nümbrecht (Germany)
Tubes, safe seal	1.5 mL	72.706	Sarstedt, Nümbrecht (Germany)
	2.0 mL	72.695.500	
Video printer paper	Mitsubishi K65HM	11001233	Diagramm Halbach
24 well plates	Corning primaria	734-0078	Corning B.V., Amsterdam (The Netherlands)
96-well microplates	Flat bottom black	738-0026	Th. Geyer

2.1.3 Chemicals

Tab. 4: Chemicals

Product	Description	Article Number	Purchase
Ammonium hydroxide, NH_4OH	100 mL	338818	Sigma-Aldrich Chemie GmbH, Taufkirchen (Germany)
Chloroform	2.5 L	133101.1612	Applichem, Darmstadt (Germany)
3,5-Diaminobenzoic acid dihydrochloride	100 g	113832	Sigma-Aldrich Chemie GmbH, Taufkirchen (Germany)
Dichloromethan	1L	1.06044-1000	Sigma-Aldrich Chemie GmbH, Steinheim (Germany)
17β-Estradiol	250 mg	E2758	Sigma-Aldrich Chemie GmbH, Taufkirchen (Germany)
Estrone	500 mg	E9750	Sigma-Aldrich Chemie GmbH, Taufkirchen (Germany)

Estrone sulfamate	2 mg	E9645	Sigma-Aldrich Chemie GmbH, Taufkirchen (Germany)
Ethanol	Technical		Werner Hofmann, Düsseldorf
Ethyl acetate	1L	1036491000	Merck KGaA, Darmstadt (Germany)
Formaldehyde solution	1 L	1.04003.1000	Merck KGaA, Darmstadt (Germany)
2-Mercaptoethanol	250 mL	4227.1	Carl Roth GmbH und Co. KG, Karlsruhe (Germany)
Methanol	Technical	1.06009.6025	Diagonal
3'Morpholinopropanesulfonic acid	500 g	A2947, 0500	Applichem
Notit A	100 g	30890.01	Serva Electrophoresis GmbH, Heidelberg (Germany)
p-anisaldehyde solution	p-Anisalde-hyd, Acid alcohol 5 mg/100 mL	SRA1	Sigma-Aldrich Chemie GmbH, Taufkirchen (Germany)
Peqlab Universal agarose	500 g	732-2789	VWR International, Darmstadt (Germany)
Percloric acid, $HCLO_4$	70 %, 50 mL	311421	Sigma-Aldrich Chemie GmbH, Taufkirchen (Germany)
Toluene	1L	1.08327	Merck KGaA, Darmstadt (Germany)

2.1.4 Isotope-labeled chemicals

Tab. 5: Isotope-labeled chemicals

Product/ Amount/ Lot	Description	Article number	Purchase
[1,2,6,7-3H(N)] Dehydroepiandrosterone / 250 μCi/ 210402	Specific activity: 76.1 Ci/ mmol; Solvent: Ethanol; Concentration: 1 mCi/ mL; Purity > 98 %	ART1607	Hartmann Analytic GmbH, Braunschweig (Germany)
[6,7-3H(N)] Estrone sulfate ammonium salt/ 50 μCi/ 200423	Specific activity: 40 Ci/ mmol; Solvent: Ethanol; Concentration: 1 mCi/ mL; Purity > 98 %	ART0821	Hartmann Analytic GmbH, Braunschweig (Germany)
[6,7-3H(N)] Estrone sulfate ammonium salt/ 50 μCi/ 210713	Specific activity: 40 Ci/ mmol; Solvent: Ethanol; Concentration: 1 mCi/ mL; Purity > 98 %	ART0821	Hartmann Analytic GmbH, Braunschweig (Germany)
[6,7-3H(N)] Estrone sulfate ammonium salt/ 50 μCi/ 210923	Specific activity: 40 Ci/ mmol; Solvent: Ethanol; Concentration: 1 mCi/ mL; Purity > 98 %	ART0821	Hartmann Analytic GmbH, Braunschweig (Germany)
[6,7-3H(N)] Estrone sulfate ammonium salt/ 50 μCi/ 220401	Specific activity: 40 Ci/ mmol; Solvent: Ethanol; Concentration: 1 mCi/ mL; Purity > 98 %	ART0821	Hartmann Analytic GmbH, Braunschweig (Germany)

2.1.5 Buffers, kits and solutions

Tab. 6: Buffers, kits and solutions

Product	Description	Article number	Purchase
HD Green Plus DNA Dye	5 x 1 mL	ISII-HD Green P	Intas
iScript™ cDNA Synthesis Kit		1708891	BioRad, Hercules, CA, USA
Phosphate Buffered Saline (PBS)	1x 10x	14190-169 14200-067	Life Technologies, Thermo Scientific
RiboRuler High Range RNA Ladder		SM1823	ThermoFisher
RNA Gel Loading Dye	2x	R0641	ThermoFisher
RNase-free DNase Set	50 preparations	79254	Qiagen, Hilden (Germany)
RNeasy Micro Kit		74004	Qiagen, Hilden (Germany)
Takyon Low Rox SYBR ® MasterMix dTTP Blue		UF-LSMT-B0701	Eurogentec, Seraing, Belgium

2.1.6 Oligonucleotide sequences for qRT-PCR

Tab. 7: Oligonucleotide sequences for qRT-PCR

Name	Sequence forward 5’ -> 3’	Sequence reverse 5’ -> 3’	Purchase
HSD17 B7	5’CATCTCGCAGTGCAAGGAAA	5’ATATTGCCGGCATCAACAGC	Eurofins
ESR2	5’GAGTCTGGTCGTGTGAAGGA	5’ACTTCTCTGTCTCCGCACAA	Eurofins
LARS2	5’AAACTGTATGAGGCTGGGCT	5‘AATCCAGTGGGCTTGCATG	Eurofins

2.1.7 Growth media and cell culture solutions

Tab. 8: Growth media and cell culture solutions

Product	Description	Article number	Purchase
Fetal bovine serum	500 mL, Lot: 42Q0008K	10270-106	Gibco, ThermoFisher Scientific
L-Glutamine	200 mM	25030-081	Gibco, ThermoFisher Scientific
MEM Non-essen-tial amino acid solution	100x	11140-035	Life Technologies, Thermo Scientific
Minimal Essential Medium	500 mL	21090-022	Life Technologies GmbH, Darmstadt (Germany)
Penicillin/ Streptomycin	5000 U/ mL	15070-063	Life Technologies, Thermo Scientific
Sodium pyruvate	100 mM	11360-039	Life Technologies, Thermo Scientific

2.1.8 Computer software

Tab. 9: Computer software

Product	Description	Purchase
EndNote	X8.2	Alfasoft
GraphPad Prism	Prism 6 for Mac OS X	Graphpad Software, Inc.
Microsoft Office	for Mac, Version 16.43 from 2020	Microsoft
Software qRT-PCR	Realplex	Eppendorf
Software Tecan reader	infinite 200Pro	Tecan Deutschland GmbH, Crailsheim (Germany)
Software TriCarb Scintillation Counter	QuantaSmart™ - 5.2	Perkin Elmer, Waltham, MA, USA

reMarkable 2	RM110, ™ and © 2020 reMarkable AS	reMarkable Norway

2.2 Methods

2.2.1 Design of the study

The study was approved by the ethics committee of the University of Bonn, reference number 272/16. Written informed consent was obtained from all participants prior to inclusion and is part of the scientific documentation.

Human anagen scalp hair roots were donated by 39 female volunteers (age range 19 - 72). Volunteers were classified into three observation groups: Control, androgenetic alopecia (AGA) and diffuse alopecia (DA). Personal data were replaced by a code consisting of letters and numbers, so that no data can be assigned to a specific person. Dr. med. Gerhard Alfons Lutz assisted with diagnosis and counseling of volunteers. Volunteers were included into the project either by Dr. med. Gerhard Alfons Lutz or by making an appointment on the basis of an informative flyer, that was available at the Institute for Biochemistry and Molecular Biology (IBMB) in Bonn or at different dermatologists in Bonn and Koblenz.

The combination of four aspects served to assign participating women to one of the three groups: Pluck trichogram, visual appearance, pull-test and anamnesis interview. The pluck trichogram served to determine the hair root state. Epilation sites for all three groups were first in the frontotemporal area and second from the occipital part of the scalp. The pluck trichogram was carried out as described (Lutz 2012). The hair was parted using a tail comb and fixed on both sides by hands. A cosmetically good result was achieved if a narrow column of nearly 100 hairs was lifted up with the comb and fixed with a rubber-faced surgical clamp near the scalp skin. The hair was suddenly epilated following the natural exit direction of the hair from the skin. The hair column was tape fixed on a lined objective slide followed by removal of the surgical clamp. The hair was covered with ice-cold 1x phosphate buffered saline (PBS) and a cover slip. Extending hair shafts were cut from the back of the slide and were discarded. The number of hairs in each growth phase was counted in a meander-shaped manner using a light microscope (Olympus BH-2) with a 5x objective and the number of hairs of each growth stage was calculated to 100 percent

(%). The ratio of telogen hair from both epilation sites served as marker for differentiating between a physiological state (control), AGA and DA. Women with a telogen rate below fourteen percent were considered healthy controls. A telogen rate above fourteen percent was associated with hair growth disorders (AGA and DA). According to the description by Lutz in 2012, a higher telogen rate only in the frontotemporal area was considered as AGA, a higher telogen rate in both epilation sites was considered as DA (Lutz 2012).

Next to the trichogram, hair density was assessed by visual appearance. In this context, the hair was parted in the central area, both parietal zones and the occipital area of the head using a comb and a visual diagnosis of the hair density was made.

A pull-test served to assess the activity of the hair loss by counting the lost hair that got stuck between the fingers when the hair was brushed with the hands.

To complete diagnosis, a structured anamnesis interview gave information of a potential history of hair growth disorders.

To rule out any subjective impressions concerning visual appearance of the hair growth state, the whole procedure was always carried out by the same first and second examiners.

Concerning impressions on the hair root state, the results made by pluck trichogram were strictly assigned to one of three observation groups, according to the percentages calculated.

Since hormone levels are variable during the day, pluck trichogram was always carried out between 9 AM and 11 AM, to reduce potentially fluctuating results concerning hormone levels.

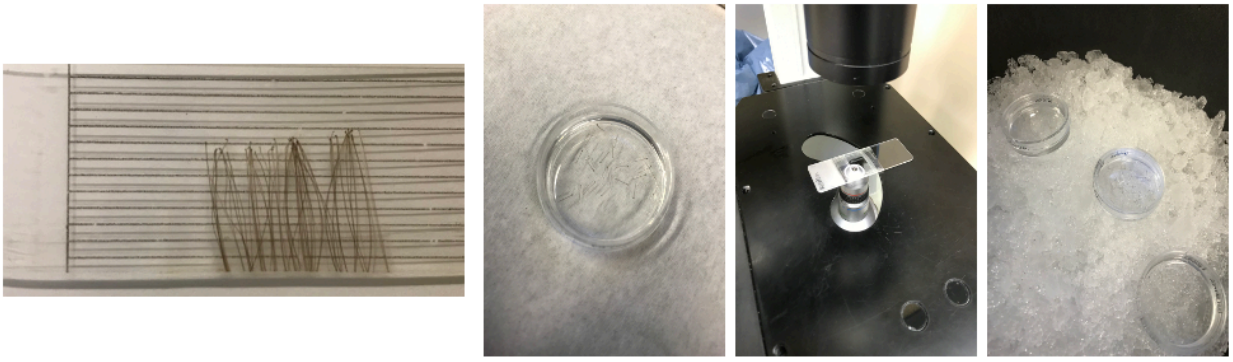

Fig. 6: Preparation of hair roots: Hair column tape fixed on a lined objective slide and separation of anagen and telogen hair. Own work.

2.2.2 Incubation of human scalp hair roots with isotope-labeled estrone-3-sulfate or dehydroepiandrosterone and extraction of steroid mixtures

It was shown that human scalp hair roots possess enzymatic activity through which conversion of steroid hormones can be catalyzed (Schweikert and Wilson 1974, Schweikert, Milewich et al. 1975, Wehner and Schweikert 2014).

The purpose of the following experiments was to investigate the formation of estrone (E1) and 17β-estradiol (E2) from estrone-3-sulfate (E1S) or the formation of androstenediol from dehydroepiandrosterone (DHEA) in isolated anagen scalp hair roots. Therefore, proximal ends of epilated hair containing the hair root (0.5 cm) were cut, and immediately transferred into ice-cold PBS (1x, Thermo Scientific) and separated according to the growth phase under a light microscope (Olympus BH-2) equipped with a 5x objective (Reinertson et al. 1957, Schweikert, Milewich et al. 1975, Van Scott 1957).

The necessary concentration of [1,2,6,7-^{3}H(N)] DHEA for the experiments was determined in a saturation analysis, where, according to Wehner and Schweikert (Wehner and Schweikert 2014), six isolated anagen scalp hair roots were incubated for 48 hours in 300 microliter (μL) minimal essential medium (MEM, Thermo Scientific) containing 50 nM, 100 nM, 500 nM and 1000 nM of [1,2,6,7-^{3}H(N)] DHEA (Hartmann Analytic, 76.1 Ci/ mmol) at 37 °C in an atmosphere of 5 % CO_2/ 95 % O_2 in a 24-well plate (Corning primaria, VWR). The volume of [1,2,6,7-^{3}H(N)] DHEA was calculated by multiplying the aimed concentration [nM] with the specific activity [Ci/ mmol] and by dividing this number by the concentration [mCi/ mL] of [1,2,6,7-^{3}H(N)] DHEA. To minimize the amount of isotope-

labeled substrate, concentrations higher than 100 nM were prepared with 100 nM of [1,2,6,7-^{3}H(N)] DHEA that were filled up with non-labeled DHEA (Sigma) to 500 nM and 1000 nM, respectively.

MEM was prepared as follows: To avoid any solvent effects during the incubation period, the different concentrations of [1,2,6,7-^{3}H(N)] DHEA were dried completely for fifteen minutes in a vacuum concentrator. The dried steroid was then dissolved completely in the necessary volume of MEM by incubation for 30 minutes under shaking at 37 °C. MEM was supplemented with 2 mM L-Glutamine (Thermo Scientific), 1 % penicillin/ streptomycin (5000 U/ mL, Thermo Scientific) and 10 % fetal bovine serum (FBS, Thermo Scientific). MEM containing steroids was in the following termed *substrate solution*.

A negative control containing substrate solution without hair roots was prepared for the lowest concentration (50 nM) of [1,2,6,7-^{3}H(N)] DHEA. Data values for the negative control were subtracted from all other data values as background.

A time course experiment served to specify the time that was necessary for the detection of androstenediol locally formed from DHEA. The experiment was performed as described before with a concentration of 100 nM of [1,2,6,7-^{3}H(N)] DHEA over a time period of 48 hours with time points at four hours, six hours, 24 hours and 48 hours.

The determined point in time was supposed to be in a linear range and was chosen on the basis of the here created XY-Plot (see results, figure 11 B).

In summary, experiments on androstenediol formation from DHEA were carried out in the following with 100 nM of [1,2,6,7-^{3}H(N)] DHEA over a time period of five hours.

According to the findings of Wehner and Schweikert (Wehner and Schweikert 2014) and the saturation and time course experiments for DHEA presented in this approach, anagen scalp hair roots were incubated for 48 hours in 300 µL MEM containing 50 nM [6,7-^{3}H(N)] estrone sulfate ammonium salt (E1S, Hartmann Analytic, specific activity 40 Ci/ mmol) or for five hours with 100 nM [1,2,6,7-^{3}H(N)] DHEA at 37 °C. The volume of [6,7-^{3}H(N)] E1S was calculated as previously described for [1,2,6,7-^{3}H(N)] DHEA.

As mentioned for DHEA experiments, also data for E1S experiments represent triplicate values and a negative control (also triplicate values) containing substrate solution without

hair roots was prepared for each sample, which was afterwards subtracted from all other data values as background.

After the incubation period, enzymatic reactions were stopped by placing the 24-well plate on ice. For [6,7-^{3}H(N)] E1S experiments, the conditioned medium was transferred into ice-cold glass tubes containing 1.5 mL chloroform ($CHCl_3$, Applichem) and 0.3 mL bi-distilled H_2O. The samples were stirred vigorously three times over a ten-minute period and incubated on ice for phase separation for fifteen minutes. The aqueous phases were transferred into new glass tubes and were extracted twice with 1.5 mL $CHCl_3$. The $CHCl_3$ layers were then combined and backwashed three times with bi-distilled H_2O, always shaking vigorously three times over a ten-minute period and left for phase separation on ice for fifteen minutes. The collected $CHCl_3$ extracts were used for steroid separation. The aqueous phases (liquid waste) were checked for isotope-labeled content, indicated by the number of counts per minute (cpm) detected by the liquid scintillation counter. Afterwards aqueous phases were discarded according to the isotope content and following the rules for isotope-labeled waste management in the corresponding laboratory. The amount of isotope-labeled content was documented in a list in the corresponding laboratory.

According to non-published pre-experiments of Wehner and Schweikert on androstenediol detection, the conditioned medium was transferred into ice-cold glass tubes containing 1.4 mL $CHCl_3$ and 0.7 mL technical methanol (MeOH, Diagonal). The samples were stirred vigorously three times over a ten-minute period and incubated on ice for phase separation for fifteen minutes. $CHCl_3$ extracts were further used for steroid separation and the remaining aqueous phases were managed according to the descriptions for E1S experiments.

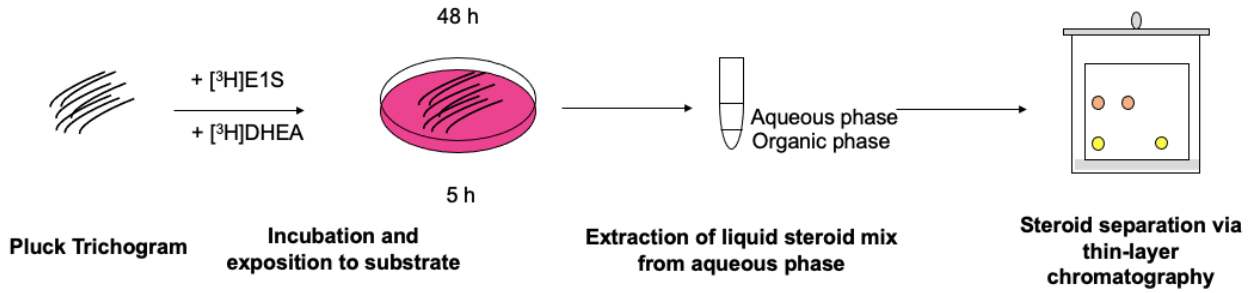

Fig. 7: Experimental workflow: Pluck trichogram, incubation of scalp hair roots, extraction of steroid mixture and steroid separation via thin-layer chromatography. Own work.

2.2.3 Steroid separation/ Thin-layer chromatography (TLC)

The collected $CHCl_3$ extracts contained a mixture of substrates (E1S or DHEA) and products (E1 and E2 in case of E1S or androstenediol in case of DHEA). In principle, DHEA can be converted into androstenedione, testosterone, androstenediol and 7α-hydroxy-DHEA. All of these metabolites can be detected using the solvent system dichloromethane/ ethyl acetate/ MeOH (85:15:1.7; v:v:v), which was tested before, in non-published experiments of Wehner and Schweikert. In this experiment, the focus laid on the detection of androstenediol.

In the second experiment, metabolites derived from E1S (E1 and E2) were detected, both in the same sample and on the same TLC plate and run. For separation of E1 and E2 the solvent system toluene/ ethanol (93:7; v:v) was used as described by Wehner and Schweikert (Wehner and Schweikert 2014).

Thin-layer chromatography (TLC) separated the formed steroid metabolites from each other. To describe the performance of separated compounds during a TLC, relate to front values (R_f values) can be calculated. R_f values are a characteristic property of a compound in a certain solvent system and describe the ratio of the distance the compound covers during the separation (a) and the distance between starting line and running front (b). Variations in R_f values can appear due to room temperature differences. R_f values were calculated by dividing a by b, yielding $R_f = a/b$.

Since the yield of formed steroid metabolite in hair roots is low, it was necessary to increase its amount for visualizing it after the TLC has been finished. Therefore, in case of E1 and E2 detection, 25 μg of a prepared mixture containing E1 and E2 (1 mg/ mL in MeOH, in the following termed *standard*) was added to a 0.5 mL aliquot of $CHCl_3$ extract. In case of DHEA metabolization, 25 μg of a standard containing testosterone (1 mg/ mL in MeOH) was added to a 0.5 mL aliquot of $CHCl_3$ extract. Testosterone showed a R_f value of 0.5 in this solvent system. In preliminary experiments of Wehner and Schweikert testosterone showed an equivalent R_f value and androstenediol showed a R_f value of 0.4 under the same conditions (non-published data from Wehner and Schweikert). These references were used in the here described experiments to assess androstenediol position after the TLC had been stopped.

The experimental design was the same for metabolite separation from DHEA and E1S. Aliquots of 0.5 mL $CHCl_3$ extract containing the corresponding standard were evaporated to dryness. The residues were redissolved in 75 µL $CHCl_3$ and spotted on a start line marked on plastic backed silica gel TLC plates (Ref. 805013, 20 cm x 20 cm, Macherey-Nagel). The TLC plate was transferred into a TLC chamber that was filled with the corresponding solvent system. The solvent system was filled in 30 minutes in advance to allow equilibration of the fume phase. The solvent system only covered the bottom of the TLC chamber and was not in direct contact to the start line, to prevent mixing of the samples and to allow separation of the samples in direction to the top of the TLC plate.

TLC was stopped when the running front reached the upper third of the plate (13 - 14 cm, calculated from the starting front). The running front was marked with a pencil and the plate dried at room temperature. Afterwards, p-anisaldehyde solution (5 mg p-anisaldehyde in 100 mL acid alcohol, Sigma) served to stain the formed metabolites during heating of the plate with a hair dryer. To evaluate the aimed metabolite, the colored area (E1 = red/ orange, E2 = yellow, Fig. 8) was scratched from the plate (R_f value calculated for androstenediol 0.4, R_f value E1 0.28, R_f value E2 0.15). The powder was transferred into liquid scintillation vials and 4 mL scintillation cocktail (Rotiszint eco plus, C. Roth) were added. Vials were capped and samples were stirred vigorously to release the sample from the powder into the liquid scintillation cocktail.

Corresponding energies of each spot were analyzed using a TriCarb liquid scintillation counter (Perkin Elmer) and the amount of ^3H of each spot was given as cpm. These cpm values were calculated to bequerel (Bq). Calculated Bq values were then transformed into picomol (pmol) using the specific activities of the used substrates. These values later served for normalization on the DNA-content.

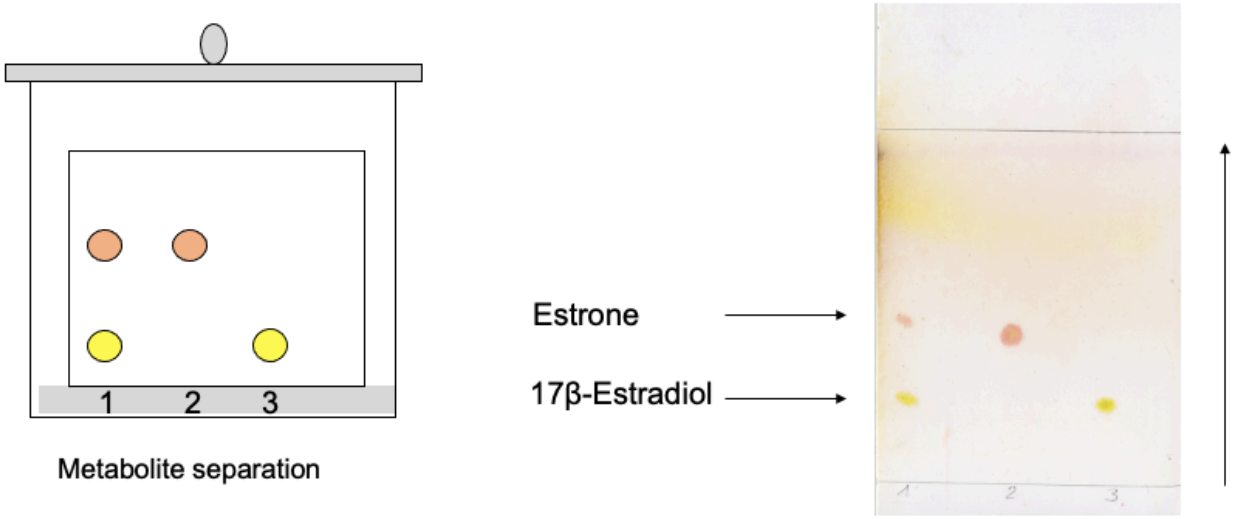

Fig. 8: Thin-layer chromatography (TLC) of estrone (E1) and 17β-estradiol (E2) derived from estrone-sulfate (E1S). Solvent system toluene/ ethanol (93:7; v:v). Spotted on plastic backed silica gel TLC plates (Ref. 805013, 20 cm x 20 cm, Macherey-Nagel). Own work.

2.2.4 Inhibition of steroid sulfatase to prevent E1 and E2 formation from E1S

Hydrolysis of E1S into the product E1 is catalyzed by the enzyme steroid sulfatase (STS). As a control for enzymatic formation and for the hydrolysis of E1S by STS, human anagen scalp hair roots were incubated with different concentrations of the specific STS inhibitor estrone sulfamate. Compound concentrations varied from 0.1 nanomolar (nM) to 0.1 μM. Hair roots were incubated with and without inhibitor in order to demonstrate the involvement of STS.

After evaporating the appropriate amount of estrone sulfamate, the necessary amount of [6,7-^{3}H(N)] E1S was dried completely, both in a vacuum concentrator. For untreated samples, the volume of solvent without inhibitor was used to exclude solvent effects. The dried inhibitor and steroid were resolubilized in MEM and were incubated for 30 minutes shaking at 37 °C to let the inhibitor and steroid dissolve completely in substrate solution. Further preparations of scalp hair roots and incubation settings were equal to that described in 2.2.2.

2.2.5 DNA determination in hair roots

DNA concentration of anagen scalp hair roots was determined according to a modification by Kissane and Robins (Kissane and Robins 1958) of the Doebner-Miller quinoline synthesis (Wehner and Schweikert 2014). Briefly, N-glycosidic bonds of purine deoxynucleotides are cleaved under heating, releasing the corresponding purine from deoxyribose. 3,5-diamino benzoic acid dihydrochloride (DABA) reacts with the liberated deoxyribose, yielding a fluorescent product (quinoline), that can be determined. Since ribose, in contrast to deoxyribose, is substituted at position C2, the reaction is DNA-specific.

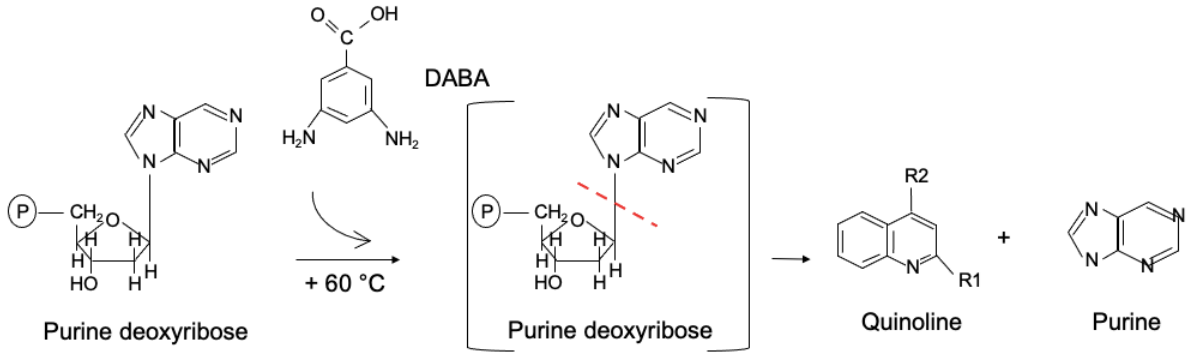

Fig. 9: Reaction of purine deoxynucleotide with DABA, yielding quinoline. Own work.

The DNA standard stock solution was prepared by dissolving 40 μg of genomic DNA from murine liver in 1 ml 0.4 N ammonium hydroxide (NH_4OH, Sigma). DNA stock solution was stored at 4 °C. Working standards were prepared freshly prior to use, by diluting the stock solution in 0.4 N NH_4OH. A standard curve was built from 0, 0.4, 0.6, 0.8, 1, 1.6, 2, 2.6, 3 and 4 μg DNA with a linear trend line with intersection zero. A coefficient of determination (R^2) bigger than 0.95 was considered suitable for further calculations.

A 1.5 M 3,5-diamino benzoic acid dihydrochloride (DABA, Sigma) solution was prepared prior to use by dissolving 0.337 g of DABA in 1 mL bi-distilled H_2O. The dark brown solution was decolorized by successive extraction with 0.1 g per mL activated charcoal (Norit A, Serva) followed by centrifugation at 4000 revolutions per minute (rpm) (3220 relative centrifugal force (rcf), Eppendorf 5810 R) for 20 min at 20 °C and filtration (syringe filter 0.22 μm, Sarstedt), after which the solution got a pale yellowish color. The increase in blank readings can be minimized by protecting the solution from exposure to light (solution stable for almost 3 hours) as described in non-published pre-experiments of Wehner and Schweikert.

250 μL of freshly prepared 1.5 M DABA solution were added to samples and standard. Tubes and cell culture plates were capped and heated at 60 °C for 45 minutes (min) in an oven, protected from light where a fluorescent product was formed by the reaction between DABA and the liberated deoxyribose (liberated from purine deoxynucleotides).

2750 μL of 0.6 N perchloric acid ($HClO_4$, Sigma) and 500 μL bi-distilled H_2O were added to each sample to stop the reaction, samples from cell culture plates were transferred to tubes and samples were mixed and left for incubation on ice for ten minutes to collect precipitates in the lower center of the tubes. 100 μL supernatant were transferred into a black microflour 1 flat bottom 96 well plate (Th. Geyer). Fluorescence was determined with infinite pro 200 software (Tecan) in a microplate reader using excitation wavelength of 396 nm and emission wavelength of 496 nm.

The values for the standard calculated by the software were then illustrated in a XY-plot, where a trendline with intersection zero and its equation served to calculate the DNA-content of samples using the fluorescence intensity of each sample as input. These values were in the end used for normalization of the pmol values calculated as described in 2.2.3 by dividing the pmol values by the DNA amount in μg.

2.2.6 Ribonucleic acid (RNA) extraction

Ribonucleic acid (RNA) was extracted from human anagen scalp hair roots using the RNeasy Micro Kit supplied by Qiagen according to the manufacturer's instructions for purification of total RNA from animal and human tissues. Scalp hair roots were not weighed or counted before disruption and homogenization. Scalp hair roots were not stabilized in reagents like RNAlater™. Furthermore, hair roots were not separated according to the epilation sites. All steps were performed at room temperature (22 - 24 °C). Obtained scalp hair roots were immediately disrupted and homogenized using a homogenisator (Ultra Turrax T25, Janke & Kunkel) in a lysis buffer (supplied with the kit) containing guanidine-thiocyanate and β-mercaptoethanol (β-Me, C. Roth). After spinning down the sample, it was applied to a RNeasy MinElute® spin column supplied with the kit, where RNA bound to the silica membrane. Copurified DNA was removed by DNase I

(supplied with the kit) treatment, resulting in high-quality total RNA. No poly-A RNA was used as carrier RNA. RNA was eluted in 14 μL RNase-free water.

Nucleic acids absorb ultraviolet light (UV-light). RNA quality was determined by measuring the absorbance of samples at 260 nm (A260) and 280 nm (A280) in a spectrophotometer (Nano Drop, Thermo), where the amount of absorbed light correlates with the nucleic acid concentration. The 260:280 ratio, determined in spectrophotometric analysis, enables to draw conclusions on protein, phenol, salt or alcohol contaminations of the measured samples, since these contaminants absorb light at 280 nm. Thus, spectrophotometric analysis supports in evaluating RNA quality.

2.2.7 RNA agarose gel electrophoresis

RNA agarose gel electrophoresis served to determine RNA integrity, by excluding RNase-induced degradation of RNA samples. Spectrophotometric analysis and RNA gel electrophoresis complement each other for quality control of RNA samples.

A two-percentage agarose gel was prepared by dissolving 1.8 g of universal agarose (PeqLab) in 90 mL of bi-distilled H_2O. HDGreen Plus DNA stain supplied by Intas is a fluorescent dye used for visualization of nucleic acids on agarose gels by UV-light. The fluorescent dye was added to the dissolved gel solution according to the manufacturer's instructions (3 μL per 100 mL gel solution). After addition of 6 mL of 20x 3'morpholinopropanesulfonic acid (MOPS) buffer (0.4 M MOPS, 0.1 M sodium acetate - 3 H_2O (NaOAc), 0.02 M disodium ethylenediaminetetraacetate (Na_2EDTA), diethyl pyrocarbonate (DEPC) treated H_2O, pH 7.0) and 12 mL formaldehyde (37 %, Merck) to the prepared gel solution, it was transferred into a prepared electrophoresis chamber for polymerization. A defined amount of RNA was diluted in RNase-free water supplemented with 2x RNA loading dye (95 % formamide, 0.025 % sodium dodecyl sulphate (SDS), 0.025 % bromophenol blue, 0.025 % xylene cyanol FF, 0.025 % ethidium bromide, 0.5 mM ethylenediaminetetraacetic acid (EDTA), Thermo Scientific). Formamide is a denaturing agent that helps to separate RNA molecules according to their size only. Samples were mixed well, heated for ten minutes at 60 °C and chilled on ice for five minutes afterwards, to maintain an unfolded state of RNA samples.

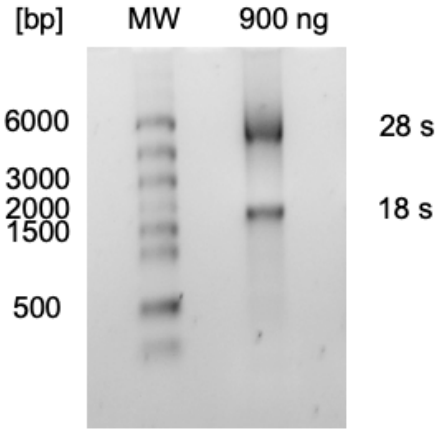

Fig. 10: RNA agarose gel. Molecular weight (MW), base pairs (bp), hours (h), volt (V), milli ampere (mA). RiboRuler High Range RNA Ladder (SM1823, Thermo Fisher) used as reference. 28s ribosomal RNA, 18 s ribosomal RNA. Own work.

2.2.8 3'-mRNA-Sequencing

3'-mRNA sequencing and sample quality control was performed by the Next Generation Sequencing (NGS) Core Facility of the Medical Faculty of the University of Bonn at the Life & Brain Center in Bonn, Germany. Libraries were prepared and samples were enriched using the QuantSeq 3'-mRNA Seq Fw. Library Prep Kit (Lexogen, New Hampshire, United States) and the data was processed using the options recommended by the manufacturer. The RNA Integrity Number (RIN) of all samples was determined using a TapeStation 4200 (Agilent, Santa Clara, California) by the NGS Core Facility. RIN values of all samples were larger than 7. 3'-mRNA sequencing was performed on the NovaSeq 6000 (Illumina) by the NGS Core Facility with read lengths of 1 x 100 bp and a sequencing depth of 10 M read pairs per sample on average.

Further data processing was carried out by Dr. Simon Bohleber and Prof. Dr. Ulrich Schweizer. Raw reads were clipped, mapped to the human genome and aligned against GRCh38. Statistical analysis was done by Dr. Simon Bohleber and Prof. Dr. Ulrich Schweizer using the R-package DESeq2 as recommended by the provider (normalization of raw counts, dispersion estimation and negative binomial Wald test with Benjamini-Hochberg multiple test correction).

2.2.9 Quantitative real time polymerase chain reaction (qRT-PCR)

RNA extraction was done as described in 2.2.6

2.2.9.1 cDNA-synthesis

The synthesis of cDNA from RNA was performed using iScript™ cDNA Synthesis Kit (Bio-Rad) according to the manufacturer's instructions.

Reaction setup and reaction protocol as described in table 10.

Tab. 10: Reaction setup and protocol for cDNA synthesis

Reaction setup	Reaction Protocol	
1 μg RNA template	Priming	25 °C - 5 min
4 μL 5x iScript Reaction Mix	Reverse transcription	46 °C - 20 min
1 μL iScript Reverse Transcriptase	RT inactivation	95 °C - 1 min
ad 20 μL Nuclease-free water	Optional	4 °C - hold

2.2.9.2 qRT-PCR

qRT-PCR was performed in triplicate values. Reaction setup and reaction protocol as described in table 11. Corresponding primer sequences are mentioned in table 12.

Tab. 11: Reaction setup and protocol for qRT-PCR Analysis

PCR Reaction	PCR Program		
5 μL cDNA (1:10 diluted cDNA)	Takyon™ Activation	95 °C - 15 min	
0.25 μL 10 μM Primer forward (fwd)	Denaturation	95 °C - 30 sec	40 cycles
0.25 μL 10 μM Primer reverse (rev)	Annealing	60 °C - 45 sec	
12.5 μL SYBR® Blue	Extension	72 °C - 30 sec	
7 μL Nuclease-free water		72 °C - 3 min	

Tab. 12: Oligonucleotide sequences for qRT-PCR

Oligonucleotide	Nucleotide sequence forward 5’ -> 3’	Nucleotide sequence reverse 5’ -> 3’
hHSD17B7	CATCTCGCAGTGCAAGGAAA	ATATTGCCGGCATCAACAGC
hESR2	GAGTCTGGTCGTGTGAAGGA	ACTTCTCTGTCTCCGCACAA
hLARS2	AAACTGTATGAGGCTGGGCT	AATCCAGTGGGCTTGCATG

2.2.10 Statistical analysis and graphical arrangements

Calculations, graphical evaluations and arrangements were performed with GraphPad Prism 6 (GraphPad Software) and Microsoft Excel from 2020 and 2021 for Macintosh. Figures for overview were created with reMarkable 2 from 2020.

Statistical significance for comparing two groups was calculated by two-tailed and one-tailed unpaired t-test as mentioned in the corresponding figure legends in GraphPad Prism 6.

Group comparisons for more than two groups were evaluated by using ordinary one-way ANOVA and Dunnett’s multiple comparisons test in GraphPad Prism 6.

Group comparisons for age were evaluated by using Mann Whitney U-test with a confidence interval of 95 % in GraphPad Prism 6.

Based on the obtained results, data were considered significant when $P < 0.05$.

Participants were included by age (range 19 - 72) and by type of hair growth disorder, as described before in 2.2.1.

3. Results

3.1 Group assignment and demographic data

This project served to test the hypothesis that disordered hair growth is correlated with impaired local steroid metabolism in hair roots. In this approach disordered hair growth and healthy hair growth were compared. Scalp hair was assigned to control, androgenetic alopecia (AGA) and diffuse alopecia (DA) groups according to visual diagnosis, pull-test and the anagen to telogen ratio observed in the pluck trichogram (see 2.2.1. methods). Women who showed both, a diffuse hair thinning and an elevated telogen rate, only in the frontal head area were assigned into the group of AGA. A positive family history for hair growth disorders underlined the diagnosis, but was not mandatory. Women who had an elevated telogen rate both in frontal and occipital area and showed a uniformly diffuse hair thinning of scalp hair in frontal, parietal and occipital areas of the head, were assigned into the group of DA. Also in this case, a positive family history for hair growth disorders supported the diagnosis, but was not strictly necessary. Neither the exact subtype of DA, nor the progress stage of AGA were estimated in the current project.

In total, 39 female volunteers donated scalp hair roots for this project. Personal data were replaced by a code consisting of letters and numbers, so that no data can be assigned to a specific person. By this classification, the DA group consisted of 15 participants with six individuals younger than 50 years and nine females older than 50 years and a median age of 30.7 and 60.8, respectively (Tab. 15). The group of AGA consisted of eight volunteers with three individuals younger than 50 years and five females older than 50 years and a median age of 43.3 and 58, respectively. The remaining 16 individuals served as healthy controls with nine individuals younger than 50 years and seven females older than 50 years with a median age of 31.3 and 59.6. The median age for females older than 50 years was similar in all three groups. The median age for females younger than 50 years was similar for controls and DA, but was slightly increased in the AGA group.

Tab. 13: Demographic data. AGA androgenetic alopecia, DA diffuse alopecia. n absolute number, h relative fraction in the study population. Approved by the ethics committee of the University of Bonn, reference number 272/16.

		Control n = 16; h = 0.410	AGA n = 8; h = 0.205	DA n = 15; h = 0.385
Age < 50 years		9	3	6
Median age		31.3	43.3	30.7
Age > 50 years		7	5	9
Median age		59.6	58	60.8
Eating habits	Balanced	8	8	6
	Low meat	5	0	6
	Vegetarian	1	0	1
	Not specified	2	0	2
Family history of hair growth disorders		5	4	6
General Medication		9	7	5

3.2 Synthesis of estrone (E1) and 17β-estradiol (E2) from estrone-3-sulfate (E1S) in healthy and disturbed hair growth

Developmental changes in the growth of human body hair are initiated by rising steroid hormone levels during sexual development (Grymowicz et al. 2020, Schiffer et al. 2019, Schweikert and Wilson 1974, Sinclair 1998), but not much is known about the exact molecular mechanisms underlying hair loss and the role of the local steroid hormone metabolism in the hair follicle. Based on the results obtained by Wehner and Schweikert (Wehner and Schweikert 2014) on the local steroid metabolism in healthy hair, this approach served to test the hypothesis that the enzymatic conversion of E1S into E2 might be impaired in hair growth disorders. To work on the question whether there is a different metabolization pattern of estrogens in disturbed hair growth, E1 and E2 formation from the substrate [6,7-^{3}H(N)] E1S was investigated in anagen scalp hair roots obtained from 39 female volunteers, grouped into controls, AGA and DA (Tab. 13).

Hydrolysis of E1S yielded moderate amounts of E1 in both, control and disordered hair growth (AGA and DA) samples (Fig. 11 A). It was shown that there was no statistically significant difference between the group of hair growth disorders and control samples concerning the synthesis of E1 from E1S (Fig. 11 A). Separation of the group with hair growth disorders into AGA and DA reflected partly this observation. The data showed an equal amount of E1 formed from E1S in control and DA samples (Fig. 11 B). In AGA samples, two clusters for E1 synthesis formed, one with a higher and one with a lower amount of E1 released from E1S. The cluster with the lower E1 rate showed equivalent E1 levels as seen for control and DA samples. The increase in E1 formation of the higher cluster in AGA samples was statistically significant in comparison to the control group (Fig. 11 B). E1 is predominantly present in postmenopausal women (Samavat and Kurzer 2015) leading to the assumption that samples with a higher E1 formation might represent women older than 50 years. But the higher rate in metabolization to E1 showed no age-relation indicated as red dots for women older than 50 years in the graph (Fig. 11 B). Considering the low sample number in the AGA group, it is worth mentioning, that the data might therefore not be reliable.

In line with the starting hypothesis, E2 formation from E1S was significantly decreased in case samples (AGA and DA) compared to control samples (Fig. 11 C), noting that sample variation in the control group was higher for E2 formation and a homogenous distribution of case samples was visible (Fig. 11 C). Separation of the case group into AGA and DA did not change this observation (Fig. 11 D). The overall amount of formed E2 was many times lower than that measured for E1. Group comparison showed a significant decrease in E2 formation in DA samples compared to the control group (Fig. 11 D). Note that the y-axis differs between figures 11 C and D, resulting in a compressed presentation of values in D (Fig. 11 C and D). E2 formation from E1S was not different between AGA and DA groups. The observation that the difference compared to control was only significant in the DA group may be associated with the lower number of participants in the AGA group.

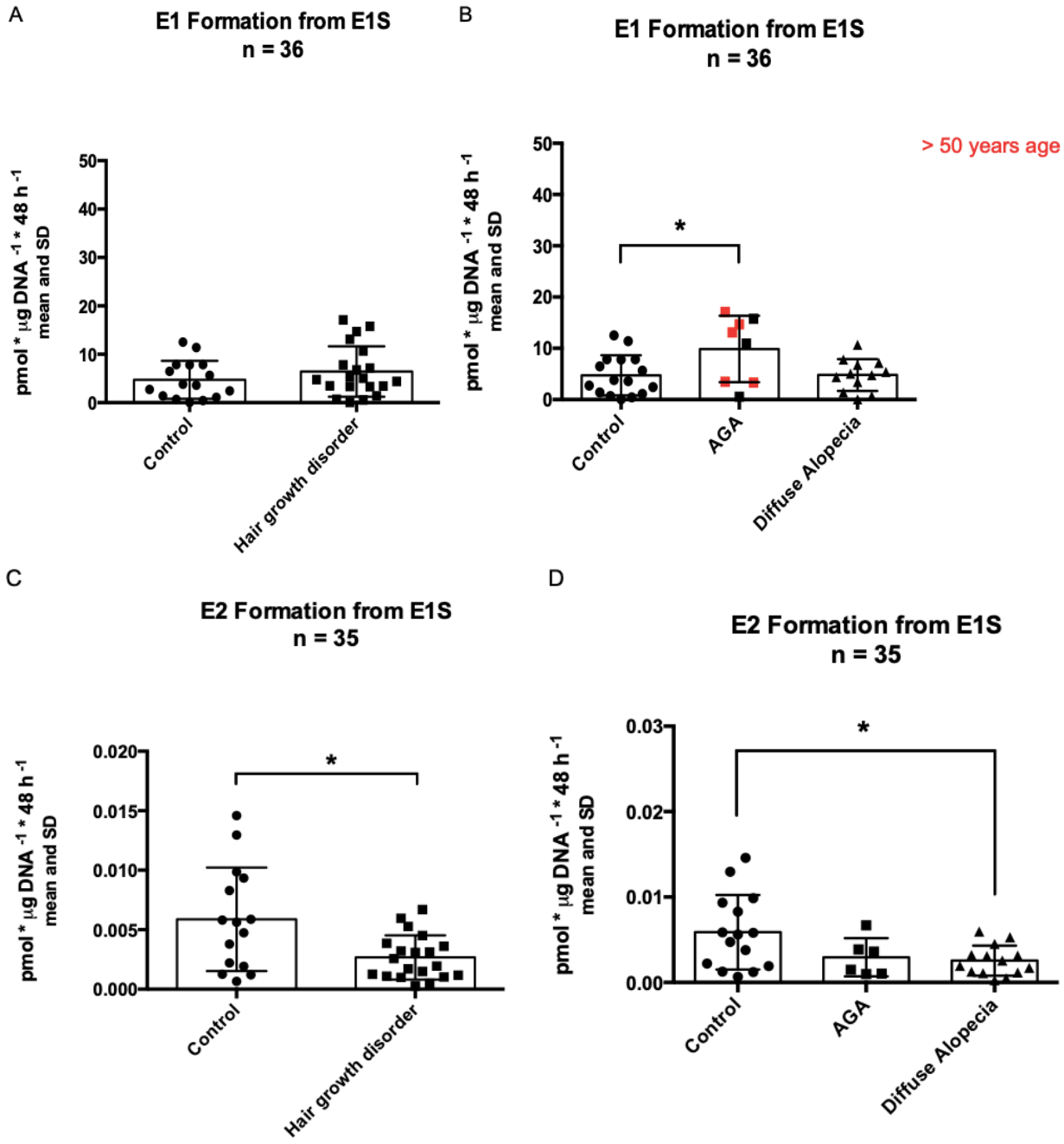

Fig. 11: Formation of estrone (E1) and 17β-estradiol (E2) from [6,7-3H(N)] estrone-3-sulfate (E1S) in isolated anagen scalp hair roots. Six hair roots per hair donor were incubated with [6,7-^{3}H(N)] E1S. Formation of E1 and E2 was determined via thin-layer chromatography (TLC) and the amount of E1 and E2 was normalized on the DNA content. **A** and **B** Comparison of E1 formation from [6,7-^{3}H(N)] E1S in control and disordered hair growth samples. Anagen hair roots from 16 controls (women age range 19 – 72 years, mean 43.69 years), eight androgenetic alopecia (AGA) cases (women age range 41 – 65 years, mean 52.5 years) and 12 diffuse alopecia (DA) cases (women age range 21 – 66 years, mean 50.42 years). **B** Individuals older than 50 years are indicated in red color. **C** and **D** Comparison of E2 formed from [6,7-^{3}H(N)] E1S in control and disordered hair growth samples. Anagen hair roots from 15 controls (women age range 19 – 72 years,

mean 44.67 years), six AGA cases (women age range 44 – 65 years, mean 54.33 years) and 14 DA cases (women age range 21 – 66 years, mean 50.57 years). E2 formation from [6,7-^{3}H(N)] E1S is decreased in disordered hair growth, especially in case of DA (D). Samples displayed hair roots from the frontal scalp area. Each point represents the mean value of three determinations (triplicate) for one individual. Ordinary one-way ANOVA + Dunnett's multiple comparisons test were used for statistical analysis of B and D with only using the higher cluster of AGA samples in comparison to the control group for the analysis in D. Mann-Whitney U-test was used for statistical analysis in C. SD Standard deviation. * $P < 0.05$.

To determine if metabolite formation is an age-related process, as seen in the results of Wehner and Schweikert (Wehner and Schweikert 2014), an age cut-off was set at 50 years, approximating the natural transition period between a premenopausal and a postmenopausal state. This age threshold divided the groups (control, AGA, DA) into individuals younger and older than 50 years.

No age-related effect was detectable for E1 or E2 formation from E1S, neither within the control, AGA or DA group, nor in comparison between all three observation groups (control, AGA, DA) (Fig. 12 A and B). So, it was not possible to confirm an age-dependent steroid metabolism in hair roots as suggested by Wehner and Schweikert (Wehner and Schweikert 2014) in this approach.

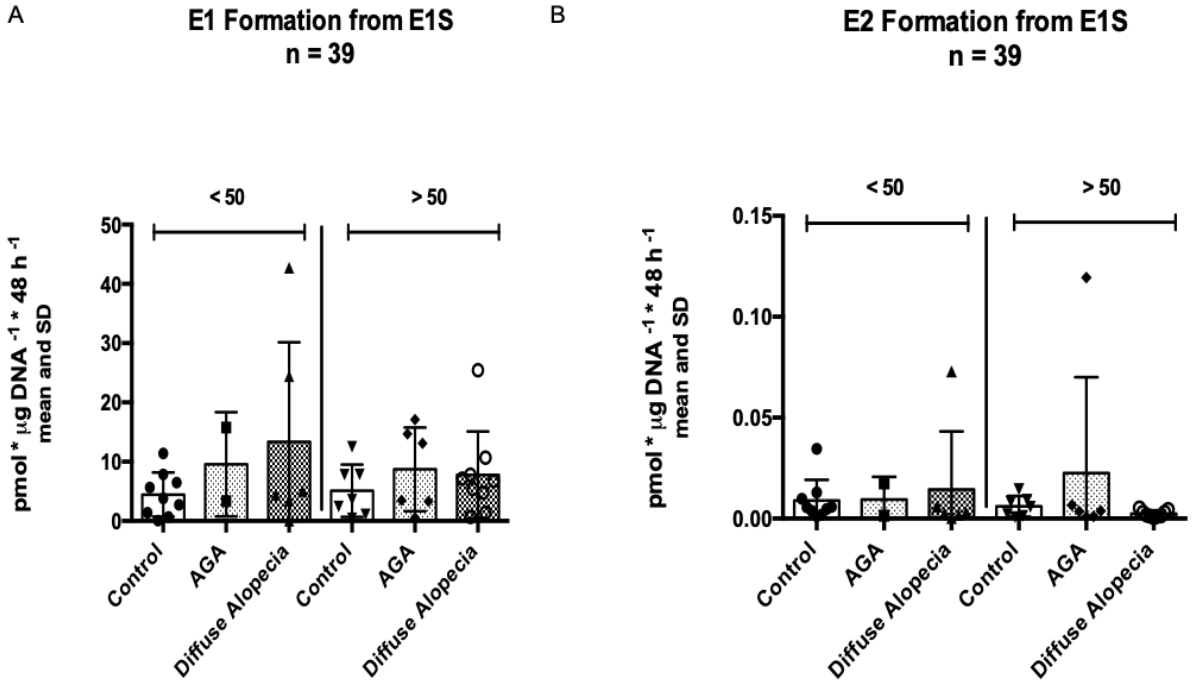

Fig. 12: Test on potential age-dependency in the formation of estrone (E1) and 17β-estradiol (E2) from [6,7-3H(N)] estrone-3-sulfate (E1S). Six hair roots per hair donor were incubated with [6,7-^{3}H(N)] E1S. Formation of E1 and E2 was determined via thin-layer chromatography (TLC) and the amount of E1 and E2 was normalized on the DNA content. **A** E1 and **B** E2 formation from [6,7-^{3}H(N)] E1S in anagen scalp hair roots from the frontal scalp area of women grouped according to an age cut-off of 50 years and according to control, androgenetic alopecia (AGA) and diffuse alopecia (DA) groups. Anagen hair roots from 16 controls (women age range 19 – 72 years, mean 43.69 years), eight androgenetic alopecia (AGA) cases (women age range 41 – 65 years, mean 52.5 years) and 15 diffuse alopecia (DA) cases (women age range 21 – 66 years, mean 48.8 years). Each point represents the mean value of three determinations (triplicate) for one individual. SD standard deviation. No significant differences were found.

3.3 Inhibition of the hydrolysis of E1S into E1 and E2 by the STS inhibitor estrone sulfamate

To verify the experimental setup and to confirm that really the local enzymatic conversion of E1 and E2 from E1S in scalp hair roots was measured, estrone sulfamate served as specific inhibitor of the enzyme steroid sulfatase (STS) which catalyzes the conversion of sulfated steroids, like E1S into its unconjugated product E1 (Hilborn et al. 2017, Kurogi et al. 2019, Mueller et al. 2015). The inhibitor was used to impair the hydrolysis of E1S, yielding less E1.

Estrone sulfamate inhibited the conversion of E1S to E1 in hair roots in a dose-dependent manner, confirming that the hydrolysis of E1S in hair roots is catalyzed by STS, with an estimated half-maximal response of the compound (EC_{50}) at 100 nM for inhibiting E1 formation (Fig. 13 A). Thereby verifying the experimental procedure. The results show that hair roots exposed to estrone sulfamate synthesize less E1 than the untreated control (Fig. 13 A - B), underlining the efficiency of the compound. The roughly five-fold amount of estrone sulfamate (500 nM) efficiently prevented E1 and E2 formation from E1S in anagen scalp hair roots (Fig 13 B and C). So, this experiment confirms that the conversion of E1S into E1 and E2 can be inhibited by estrone sulfamate-mediated inhibition of STS and therefore supports the proposition of enzymatic E2 production from E1S in hair follicles.

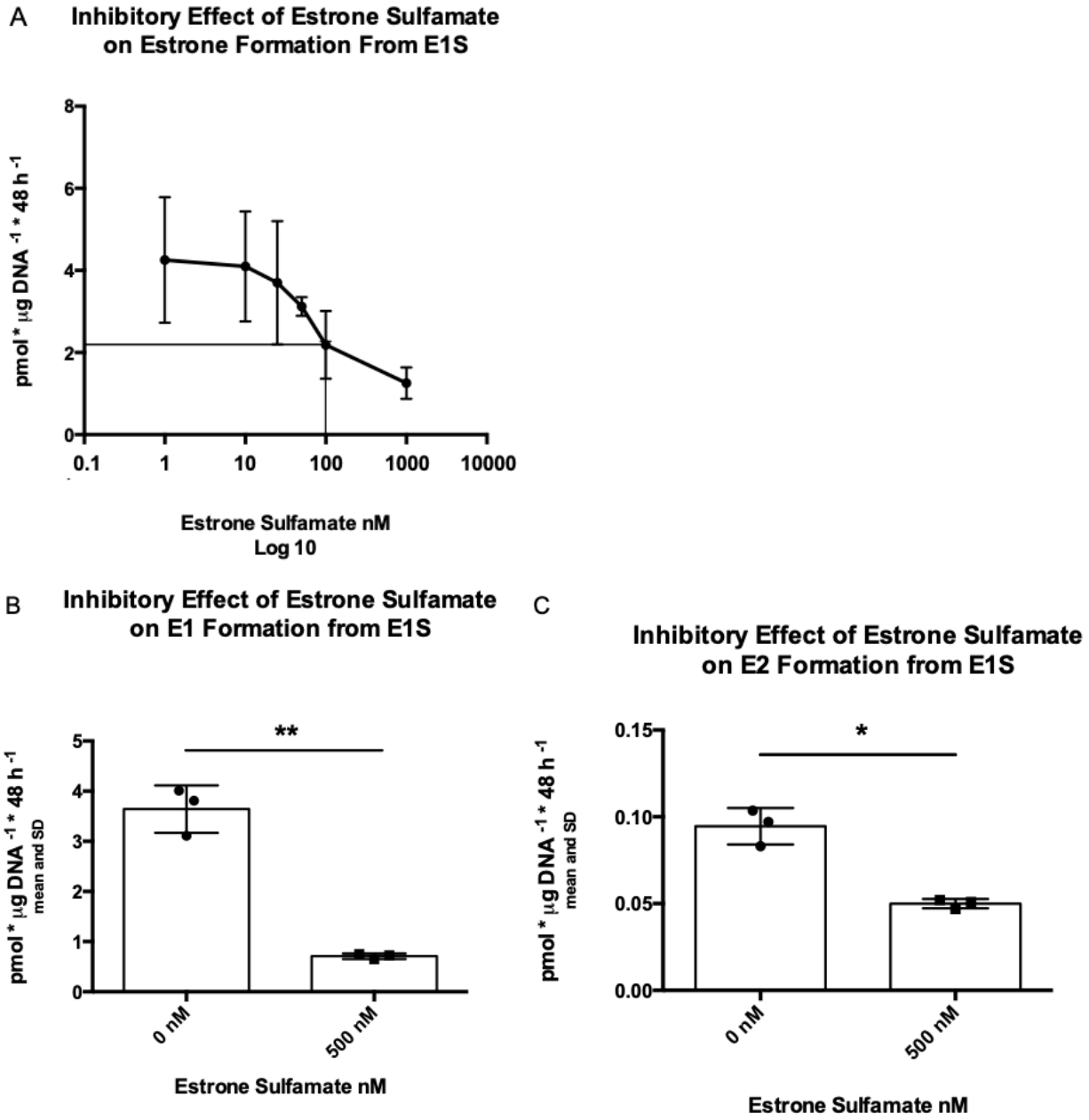

Fig. 13: Effect of estrone sulfamate on the formation of estrone (E1) and 17β-estradiol (E2) from [6,7-3H(N)] estrone-3-sulfate (E1S) in anagen scalp hair roots. Six hair roots per hair donor were incubated with [6,7-^{3}H(N)] E1S. Formation of E1 and E2 was determined via thin-layer chromatography (TLC) and the amount of E1 and E2 was normalized on the DNA content. **A** Formation of E1 from E1S was dose-dependently inhibited by estrone sulfamate with a calculated EC_{50} at 100 nM estrone sulfamate. **B** Inhibition of E1 release from [6,7-^{3}H(N)] E1S by estrone sulfamate. **C** Inhibition of E2 formation from [6,7-^{3}H(N)] E1S. Hair roots were donated by the same female volunteer (34-years old) for all three experiments. Each point represents the mean value of three determinations (triplicate) of one experiment. The experiment was repeated twice. Unpaired one-tailed t test was used for the statistical analysis of B and C. SD standard deviation, * $P < 0.05$, ** $P < 0.01$.

3.4 Analysis of a potential season-dependency of E1 formation from E1S or of the appearance of hair loss

Some animals shed fur in preparation for the warm seasons and develop thicker fur in preparation for colder months, due to a synchronized hair growth cycle (Pierard-Franchimont and Pierard 2013). This season-dependency served as basis for considerations on a potential season-dependency in human hair growth.

The following pilot experiment was carried out three times over a seven months period for one individual. Anagen scalp hair roots were donated by a female volunteer who had no history of hair growth disorders. The volunteer practiced scalp skin massages and used topical application of a solution containing ginkgo and biotin.

As previously done for E1 formation from E1S, six isolated human anagen scalp hair roots were incubated with 50 nM of [6,7-^{3}H(N)] E1S over 48 hours. Experiments were performed once in April, once in September and once in October, each time in triplicate values.

Results indicated that E1 formation from E1S was lower in September and October, compared to April (Fig. 14 A), leading to the impression that E1 formation from E1S varied season-dependently. This finding may serve as inspiration for further research studies.

The recruitment process of volunteers showed no season-dependency, since the appearance of controls and cases was homogenously distributed all over the year (Fig. 14 B). Linear regression of all E1 formation rates did not support a significant effect of season on the results of the study (Fig. 14 C).

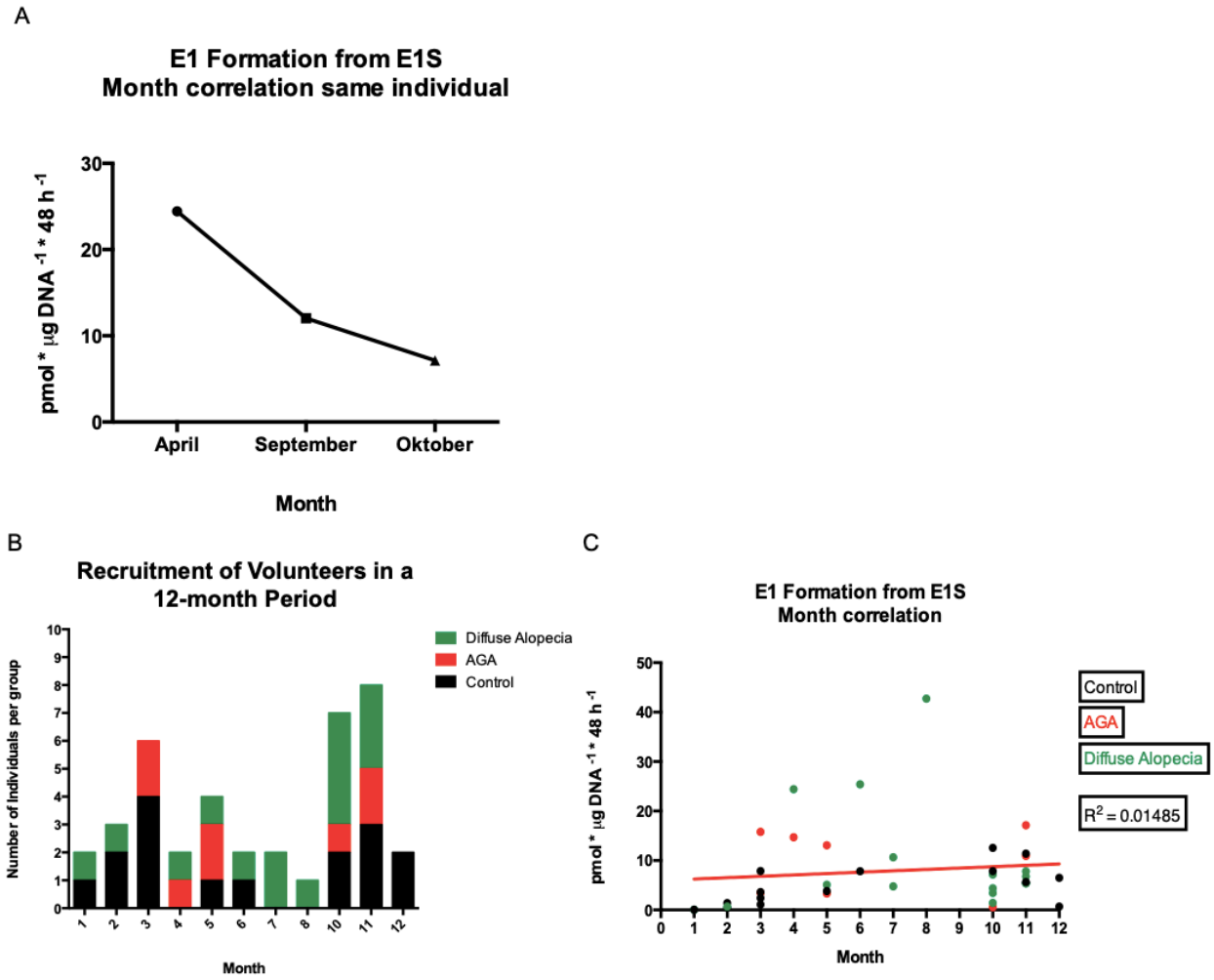

Fig. 14: Analysis of a potential season correlation of hair loss. A Formation of estrone (E1) from [6,7-^{3}H(N)] estrone-3-sulfate (E1S) in isolated anagen hair roots seems to follow a seasonal rhythm. Hair roots were donated from the frontal scalp area of a 34-year-old female volunteer who had no history of hair growth disorders. Six hair roots per hair donor were incubated with [6,7-^{3}H(N)] E1S. Formation of E1 and E2 was determined via thin-layer chromatography (TLC) and the amount of E1 and E2 was normalized on the DNA content. **B** Recruitment of volunteers over a 12 months period with separation of monthly participants into the three observation groups (black = control, red = androgenetic alopecia (AGA), green = diffuse alopecia (DA)). Hair roots were donated by 16 controls (women age range 19 – 72 years, mean 43.69 years), eight androgenetic alopecia (AGA) cases (women age range 41 – 65 years, mean 52.5 years) and 15 diffuse alopecia (DA) cases (women age range 21 – 66 years, mean 48.8 years). **C** Linear regression of E1 formation in dependence of the month. R^2 = R square, control = black, AGA = red and DA = green dots. Trendline = red.

3.5 Establishing an assay for the formation of androstenediol from DHEA in hair roots

Dehydroepiandrosterone (DHEA) is one of the most abundant steroid hormones of the adrenal cortex (Hernandez-Pando et al. 1998, Kohalmy et al. 2007, Schiffer et al. 2018, Turcu and Auchus 2015). In this context, it is important to consider, that its sulfate ester, dehydroepiandrosterone sulfate (DHEAS), is by far the steroid with the highest plasma concentration (Mueller et al. 2015, Schiffer et al. 2019). Reduction of DHEA by HSD17B1 results in formation of androstenediol (Hilborn et al. 2017). Since androstenediol shows binding affinity for both nuclear estrogen receptors α and β (ERα, ERβ), this pathway could provide a route for weak estrogenic activity in hair roots originating from DHEA (Chen et al. 2022, Fuentes and Silveyra 2019, Miller et al. 2013, Paterni et al. 2014). So, the following experiments served to test the hypothesis that an impaired conversion of DHEA into androstenediol may occur in hair growth disorders. First, an assay to test the conversion of DHEA to androstenediol was set up. In this case, anagen scalp hair roots obtained from a female volunteer, who had no history of hair growth disorders, were incubated with different concentrations of the substrate [1,2,6,7-^{3}H(N)] DHEA.

Analogous to the findings by Wehner and Schweikert (Wehner and Schweikert 2014), the analysis was carried out with six anagen scalp hair roots over a time period of 48 hours. Results show that androstenediol formation from DHEA was highest at concentrations around 50 and 100 nM (Fig. 15 A). So, based on this result, all further experiments were carried out with 100 nM [1,2,6,7-^{3}H(N)] DHEA.

In order to set up the activity assay, also the time period in which andostenediol formation from DHEA shows a linear increase needed to be determined. As described before, anagen scalp hair roots were obtained from a female volunteer, who had no history of hair growth disorders, and were incubated over four, six, 24 and 48 hours with 100 nM [1,2,6,7-^{3}H(N)] DHEA as substrate. Androstenediol formation was linear up to six hours of incubation, but increased up to 48 hours measurement (Fig. 15 B).

According to these results, further experiments were carried out with 100 nM substrate over an incubation period of five hours.

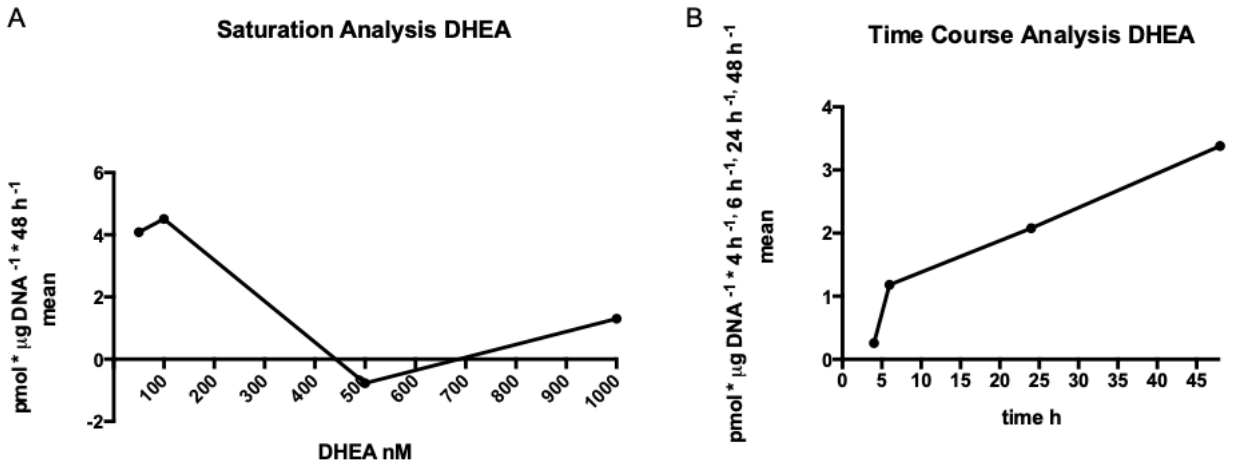

Fig. 15: Standardization of assay conditions. A Saturation analysis of the formation of androstenediol in isolated anagen scalp hair roots at varying [1,2,6,7-^{3}H(N)] dehydroepiandrosterone (DHEA) concentrations in 48 hours. Anagen hair roots were obtained from the frontal scalp region of a 34-year-old female volunteer. The [1,2,6,7-^{3}H(N)] DHEA concentrations ranged from 50 nM to 1000 nM. **B** Time course of the formation of androstenediol from 100 nM [1,2,6,7-^{3}H(N)] DHEA in isolated anagen scalp hair roots over a time period of 48 hours and analysis time points at four, six, 24 and 48 hours. Each data point represents one determination in one experiment.

3.6 Impact of hair growth disorders on the synthesis of androstenediol from DHEA

After determining the experimental setting for the analysis of androstenediol formation from DHEA, all further experiments on this issue were carried out with six isolated anagen scalp hair roots, that were exposed to 100 nM of [1,2,6,7-^{3}H(N)] DHEA over a time period of five hours.

The case samples were not different from controls in androstenediol formation (Fig. 16 A). Sample values were homogenously distributed in case samples, variation of control samples seemed to be higher, building two groups, one with a higher and one with a lower androstenediol formation (Fig. 16 A). The amount of androstenediol synthesized from DHEA was in the lower picomolar range (Fig. 16 A). When separating case samples into AGA and DA, still no difference in between the three observation groups (Fig. 16 B) was visible. As mentioned in 2.2.2 a negative control without hair roots was subtracted as background from values obtained from samples containing hair roots. For androstenediol measurements, these calculations sometimes led to negative values in the corresponding graphical analysis. Taken together, the data show that androstenediol formation from

DHEA did not differ between control and disordered hair growth and therefore it was not possible to confirm the hypothesis that an impaired conversion of DHEA into androstenediol may occur in hair growth disorders. To determine, if androstenediol formation is age-dependent, an age cut-off was set at 50 years, as described in 3.2 for E1 and E2 formation from E1S. No age-related effect was detectable for androstenediol formation from DHEA, neither within the control, AGA or DA groups, nor in comparison of all three observation groups (control, AGA, DA) (Fig. 16 C).

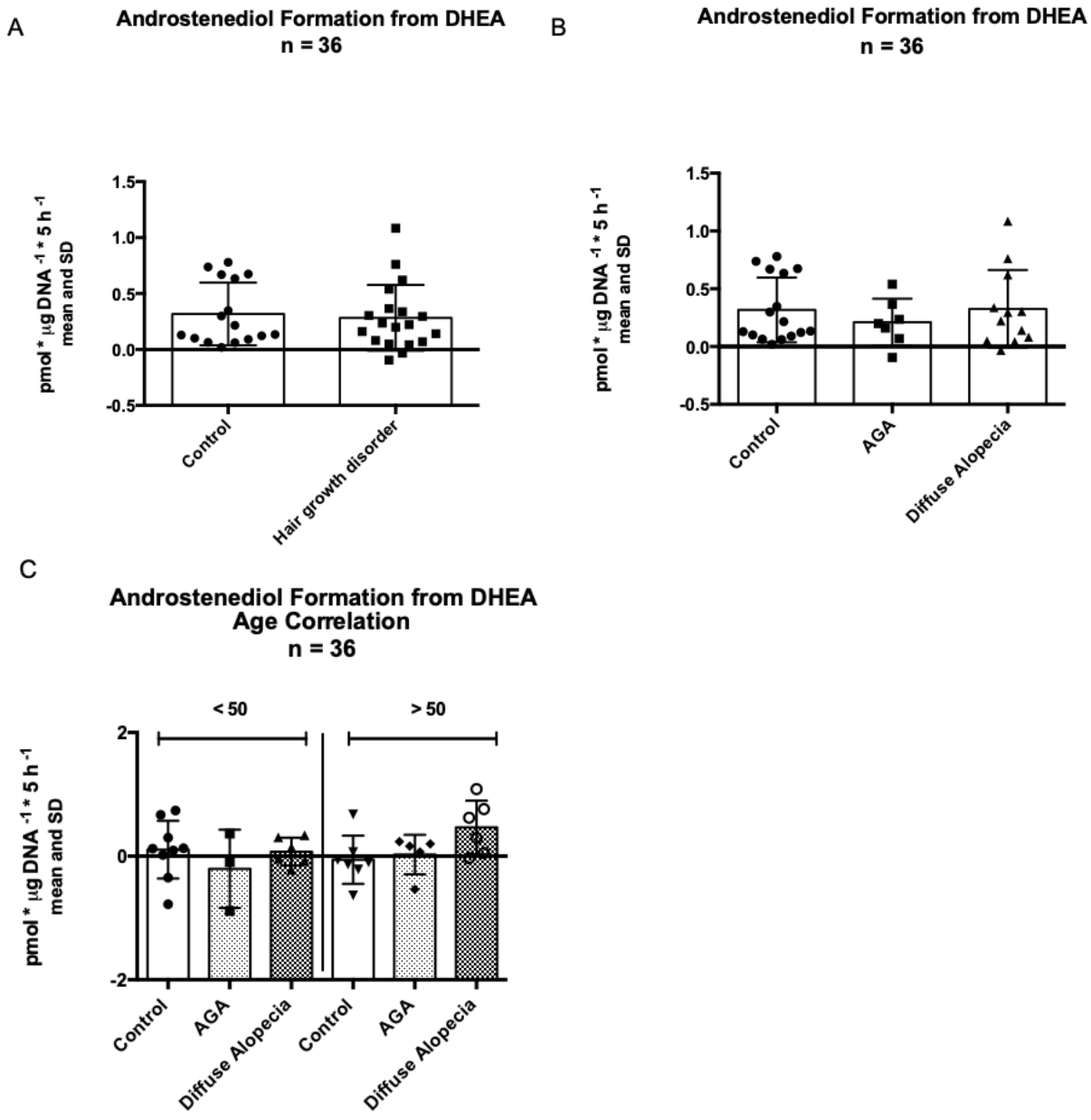

Fig. 16: Formation of androstenediol from [1,2,6,7-3H(N)] dehydroepiandrosterone (DHEA) in isolated anagen scalp hair roots. A and **B** Comparison of androstenediol

formation from [1,2,6,7-^{3}H(N)] DHEA in control and disordered hair growth samples (androgenetic alopecia (AGA) and diffuse alopecia (DA)). Hair roots were donated from 16 controls (women age range 19 – 72 years, mean 43.69 years), eight AGA (women age range 41 – 65 years, mean 52.5 years) and 12 DA cases (women age range 21 – 66 years, mean 46.25 years). **C** Test on connection of the formation of androstenediol from [1,2,6,7-^{3}H(N)] DHEA and age. No age-dependency determined in the formation of androstenediol from [1,2,6,7-^{3}H(N)] DHEA. Each point represents the mean value of three determinations (triplicate) of one individual. Statistical analysis of A was carried out with Mann Whitney U-test with a confidence interval of 95 %. Ordinary one-way ANOVA and Dunnett's multiple comparisons test were used for statistical analysis of the data in B. SD standard deviation. No significant differences were found.

3.7 Analysis of enzyme expression patterns in scalp hair roots from controls, AGA and DA

The data of this project showed a decrease in E2 formation from E1S in disordered hair growth compared to the control group, whereas E1 formation from E1S and androstenediol formation from DHEA seemed to be unaffected in control and case samples (AGA, DA). As described before in 1.2.2 (introduction), the synthesis of steroid hormones involves various enzymes of the CYP450 and HSD families (Mostaghel 2013, Penning 2011, Rizner and Penning 2014, Schiffer et al. 2019). These enzymes mediate the oxidation or reduction of steroid hormones, whereby some enzymes favor the oxidation and some the reduction, respectively. This led to the question, whether the observed decrease in the formation of E2 from E1S in disordered hair growth might be a consequence of changed enzyme expression. Of special interest were here the enzyme STS, which catalyzes the formation from E1S to E1 (Hilborn et al. 2017, Mueller et al. 2015), and the enzymes HSD17B7 and HSD17B1, that mediate the reduction of E1 to E2 (Hilborn et al. 2017, Miller and Auchus 2011, Nokelainen et al. 1998, Ramos and Miot 2015, Samavat and Kurzer 2015, Schiffer et al. 2019), the latter also being involved in the formation of androstenediol from DHEA (Hilborn et al. 2017, Rainey and Nakamura 2008, Rege et al. 2013).

Since Wehner and Schweikert worked on the comparison of the metabolism in anagen and telogen hair (Wehner and Schweikert 2014), the interest here first was on the comparison of mRNA expression patterns of relevant enzymes in anagen and telogen hair. Therefore, RNA was extracted from hair roots obtained by trichogram and 3'-mRNA-sequencing was carried out. Hair roots for these experiments were donated by two female

volunteers who had no history of hair growth disorders and the experiments were carried out independently from the comparison of case and control groups. One of these female volunteers also served for the comparison of HSD17B7 expression of anagen and telogen hair at two time points (Fig. 17 E). No significant difference was observed for expression of CYP19A1, HSD17B1 and STS, maybe since samples from only two volunteers were investigated. If the sample number would have been higher, the single results may turn out to be significant. Interestingly, the data indicated, that HSD17B7 expression might be down regulated in telogen samples compared to anagen samples (Fig. 17 D and E). The enzyme is involved in the conversion of E1 into E2 (Ferrante et al. 2020). This result further underlines the idea of Wehner and Schweikert, that changes in the steroid metabolism (E2) may occur within the hair growth cycle (Wehner and Schweikert 2014), in particular since down regulation of *HSD17B7* would reduce the availability of E2 in the hair root.

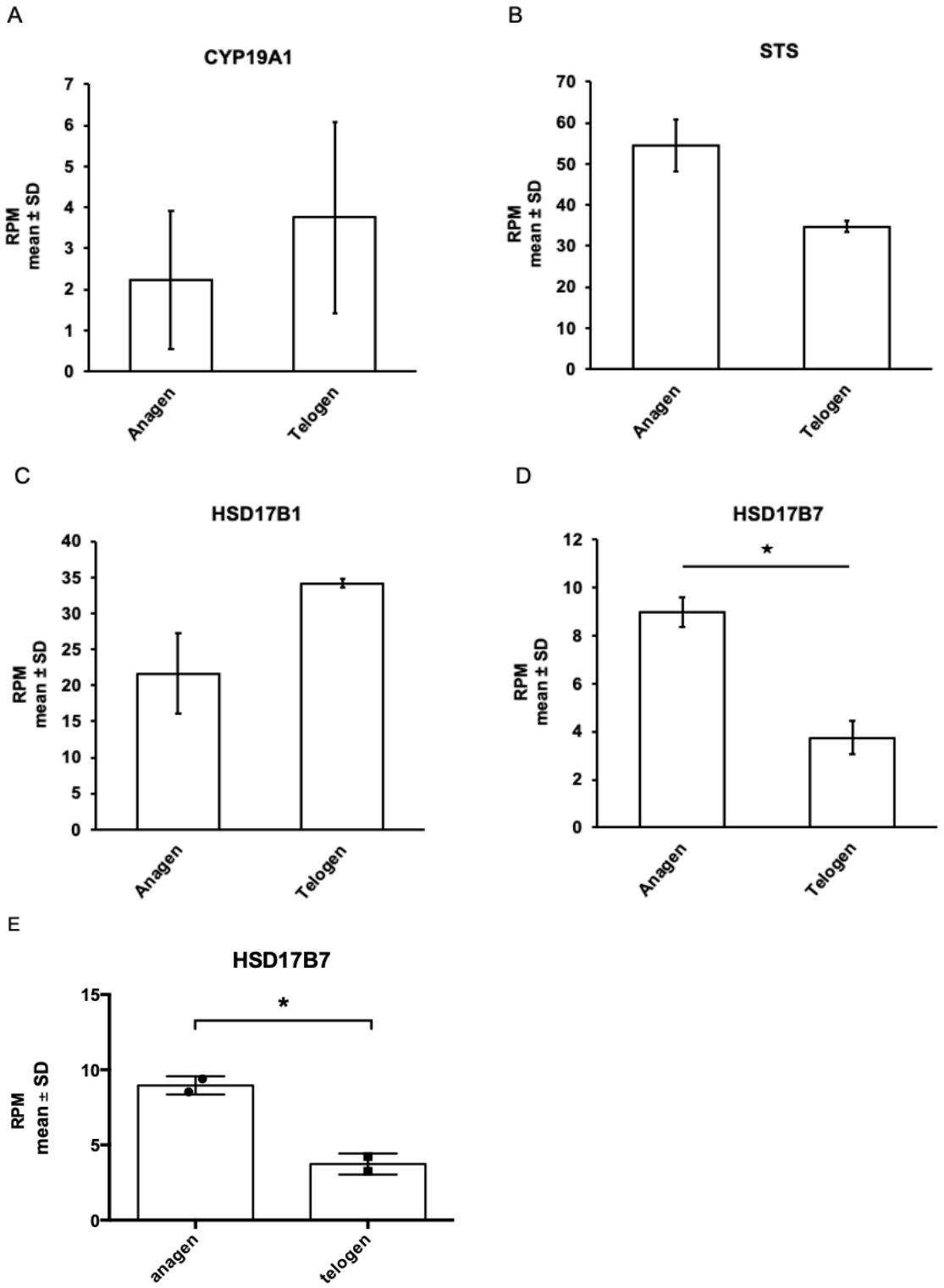

Fig. 17: Expression patterns of relevant enzymes in the hair growth cycle. Expression of **A** CYP19A1, **B** STS, **C** HSD17B1 and **D** HSD17B7 in anagen and telogen hair, donated by two female volunteers without any history of hair growth disorders. **E** Expression of HSD17B7 in anagen and telogen hair, donated by one female volunteer without any history of hair growth disorders at two time points. D and E Expression of HSD17B7 (in reads per million mapped reads (RPM)) depends on the hair growth cycle. SD standard deviation. 3'-mRNA sequencing. * $P < 0.05$. Two sample t-test was used for the statistical analysis of the data in A - D. One-tailed t-test was used for statistical analysis of the data in E. HSD hydroxysteroid dehydrogenase. CYP cytochrome P450s. STS steroid sulfatase.

Thereupon, the next aim was to investigate whether the mRNA expression patterns of relevant enzymes differed between case groups (AGA and DA) and controls. Therefore, 3'-mRNA-sequencing was carried out as before with samples from controls and disordered hair growth. The investigations were supposed to elucidate, if a lower or higher metabolization rate as illustrated in figure 11 (Fig. 11 A-D) may correlate with a lower or higher transcript expression. In these experiments only anagen hair roots were used for the comparison of case and control samples.

Principal component analysis (PCA) was performed in order to see whether the samples clustered in groups. PCA served to flatten the whole data set with lots of dimensions to two dimensions, so that it was easier to look at it graphically. The two-dimensional PCA plot showed, that the data for disordered hair growth (A) and controls (Ctrl) was uniformly distributed from up to down and from left to right, indicating that there was no internal correlation of the two groups on the expression level (Fig. 18), meaning that the group of disordered hair growth did not differ from the control group. If there was a similar transcription pattern of samples in the hair loss group different to that presented in the control group, then a clustering would be visible for samples from disordered hair growth on the one hand and, different to that, another clustering for control samples. Principal component 1 (PC1) accounted for 23.3 % of the total variation around the PCs while PC2 only accounted for 13.5 %. But although PC1 and PC2 only accounted for 36.8 % of the variation in total, both could still be used to identify clusters of data or, like in this case, both can be used to exclude any clustering of samples or sample features in the two-dimensional PCA plot. In summary, the PCA indicates that there are no significant differences between the groups concerning the expression of relevant enzymes in general.

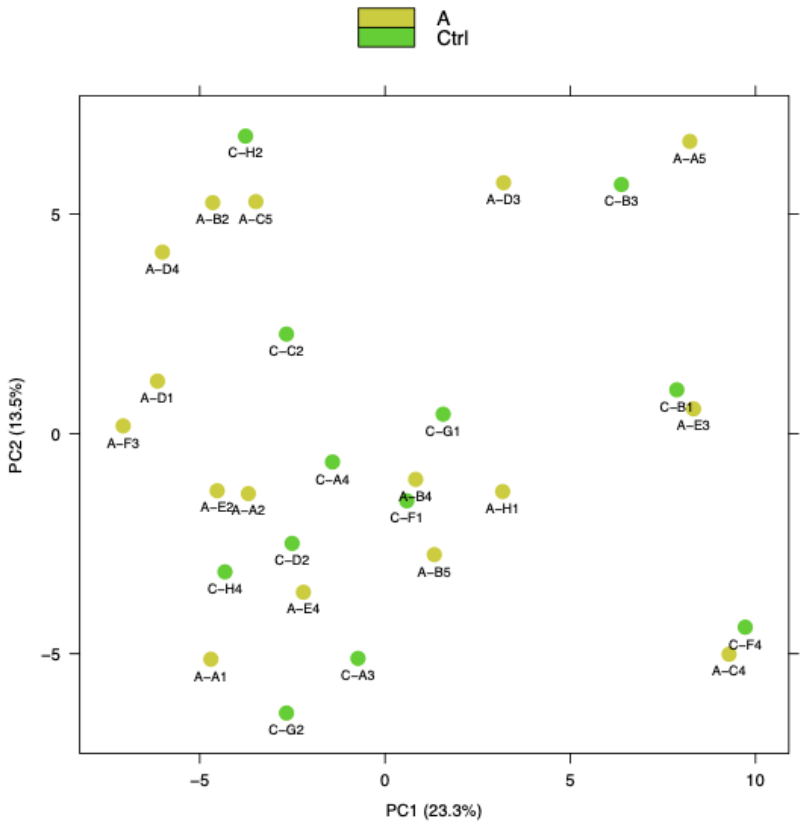

Fig. 18: *Principal component analysis* (PCA) of 3'-mRNA-sequencing data. PCA of all samples distinguished into control (ctrl) and disturbed hair growth samples (A), each point represents one individual and the indicated names correspond to the group (control and disturbed hair growth) and the sample position on the 96-well plate. C (n = 12), A (n = 16). PC1 principal component 1, PC2 principal component 2. No significant differences between C and A found.

Since all participants in this approach do have scalp hair, it was not surprising that the results of mRNA samples from hair roots did not show big differences between control and disordered hair growth in general. So, a deeper and more precise look into the data set concerning the conversion of the substrates E1S and DHEA into their corresponding products E1, E2 and androstenediol was necessary for the further analysis of both observation groups. Therefore, an explorative data analysis was applied to compare disordered hair and healthy hair growth.

A heatmap helped to visualize the data. The heatmap is arranged in rows, representing genes encoding for the enzymes, and columns, representing the observation group (A = hair loss, C = control) (Fig. 19). Numerical values are colored according to the color scale

shown in the figure (Fig. 19), correlating a red color with a higher, than average, gene expression and a blue color with a lower, than average, gene expression. The heatmap indicates that there was no strong up or down regulation among the genes in the comparison of both observation groups, showed by the color code, where most samples center around +/- 2 on the color scale (Fig. 19). The heatmap also indicates, that the data for controls and the data for hair loss are not tightly grouped, otherwise the color code would not differ much in the C and in the A group, assuming variation in between the groups (Fig. 19). Since there were no big differences between both observation groups on average, the single rows had to be analyzed in more detail. Particularly, how strong STS, HSD17B1 and HSD17B7 (all bold) differ from the average. The color code for STS indicated that samples in group C did not clearly show a tendency for a higher or lower regulation of STS, since samples varied in a 50 to 50 ratio (Fig. 19). In the A group it seemed as if STS was down regulated on average, despite a few samples, where the color code indicated a rate between zero and 2 on the color scale (Fig. 19). The consequence for both groups is quite similar, as the enzyme STS did not differ from the average (Fig. 19).

Controversial results were seen regarding the regulation profile of the enzyme HSD17B7, which seemed to be barely expressed in group C, whereas group A showed a ratio of 50 to 50 for barely and low regulation concerning color code and color scale (Fig. 19). Taken together, also this approach showed no significant differences between both groups.

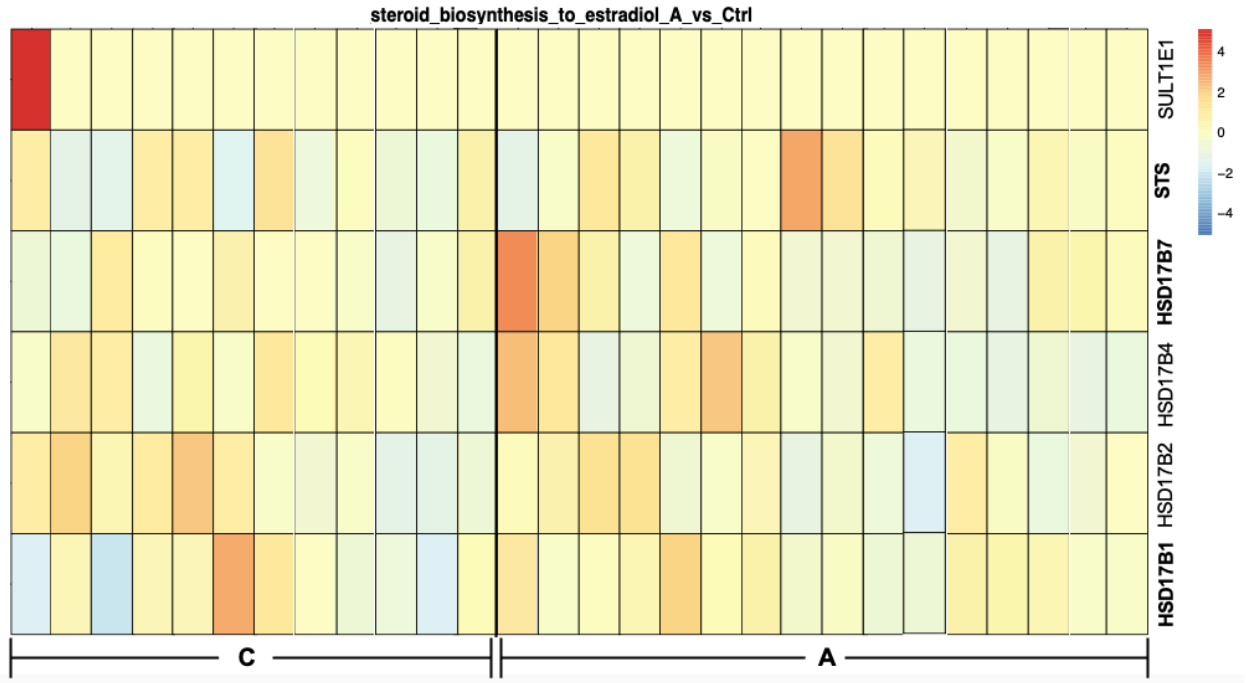

Fig. 19: Heatmap of candidate genes involved in the conversion of estrone-3-sulfate (E1S) into 17β-estradiol (E2). 3'-mRNA sequencing data. A disordered hair growth, C control. Color code as log2 scale. HSD17B1, HSD17B3, HSD17B2, HSD17B4 hydroxy dehydrogenases 17B1, 17B7, 17B2, 17B4, STS steroid sulfatase, SULT1E1 sulfotransferase family 1E member 1. Vs versus. Ctrl control. C (n = 12), A (n = 16). No significant differences between C and A found.

The heatmap illustrated in figure 20 consistently showed, that there still was no significant difference in the regulation of genes that may be involved in the conversion of DHEA into androstenediol (Fig. 20).

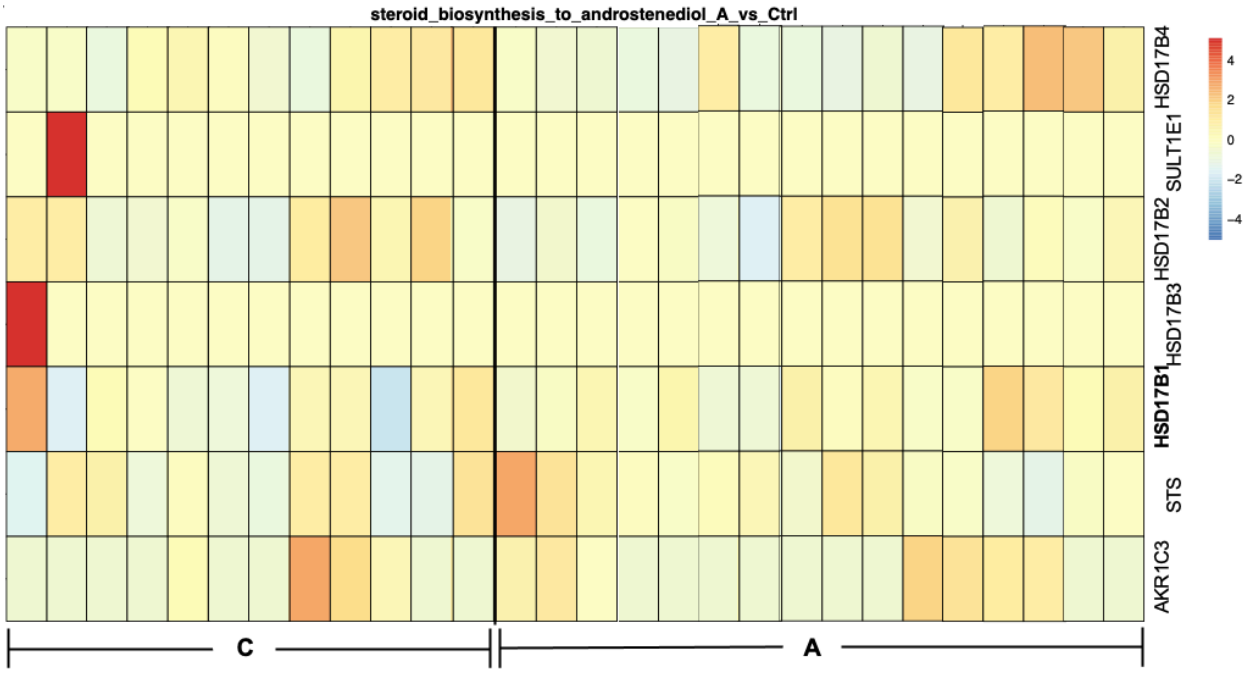

Fig. 20: Heatmap of candidate genes involved in the conversion of dehydroepiandrosterone (DHEA) into androstenediol. 3'-mRNA sequencing data. A disordered hair growth, C control. Color code as log2 scale. Vs versus. HSD17B1, HSD17B3, HSD17B2, HSD17B4 hydroxy dehydrogenases 17B1, 17B3, 17B2, 17B4, STS steroid sulfatase, AKR1C3 aldo keto reductase 1C3, SULT1E1 sulfotransferase family 1E member 1. C (n = 12), A (n = 16). No significant differences between C and A found.

Next, the expression of different enzymes was compared between control, AGA and DA in order to assess, if these candidate genes were differentially regulated in between the three groups. Calculating the fold change suggested, that HSD17B7 showed the highest variability compared to all other enzyme profiles in this graph (Fig. 21 A), indicating that this gene might be deregulated in some of the hair donors. Figure 21 B illustrated all single values for the expression profile of only HSD17B7 and revealed again, that there was a strong variation of the sample values for DA and AGA, but no significant difference between case and control samples (Fig. 21 B).

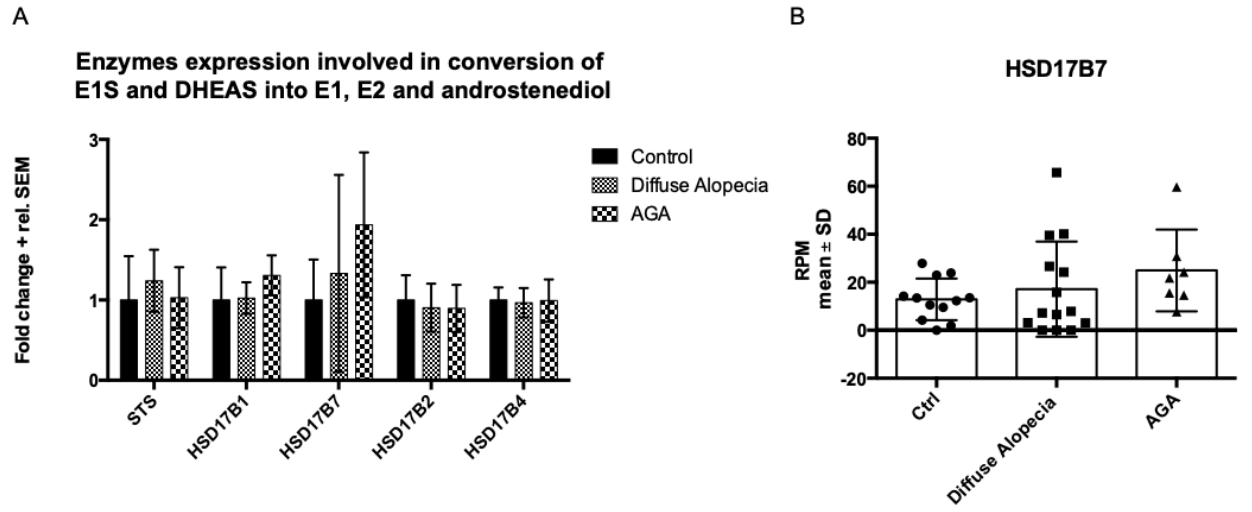

Fig. 21: Gene expression of candidate genes involved in the conversion of dehydroepiandrosterone (DHEA) into androstenediol and estrone-3-sulfate (E1S) into estrone (E1) and 17β-estradiol (E2). 3'-mRNA sequencing data. AGA androgenetic alopecia. Rel. SEM relative standard error of the mean. RPM reads per million mapped reads. AGA androgenetic alopecia. Ctrl control. SD standard deviation. HSD17B1, HSD17B7, HSD17B2, HSD17B4 hydroxy dehydrogenases 17B1, 17B7, 17B2, 17B4, STS steroid sulfatase, DHEAS dehydroepiandrosterone sulfate. A High sample variation for HSD17B7 indicates that HSD17B7 might be deregulated in some samples.

qRT-PCR served to determine, if expression of *HSD17B7* differed between the control and AGA group. Controversially, the data indicated that human *HSD17B7* (hHSD17B7) was lower expressed in AGA samples than in the control group (Fig. 22), mentioning that the standard deviation was high.

So, both methods, 3'-mRNA sequencing and qRT-PCR, indicated that there was no difference in the expression profile of HSD17B7 in the group comparison.

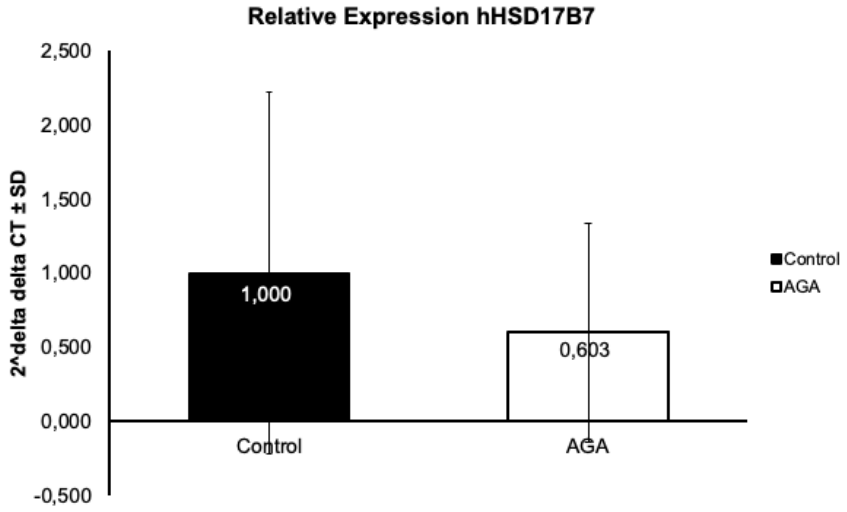

Fig. 22: Quantitative real-time polymerase chain reaction (qRT-PCR) of human hydroxy dehydrogenase 17 B7 (HSD17B7, hHSD17B7). Data represent the relative expression ($2^{\Delta\Delta CT}$) and standard deviations (SD) from five control and five androgenetic alopecia (AGA) samples. CT cycle threshold.

3.8 Analysis of steroid receptor and steroid transporter expression in scalp hair roots from controls, AGA and DA

Up to this point, the here presented experiments showed that E2 formation from E1S was lower in samples from hair growth disorders compared to the control group, whereas E1 formation from E1S and androstenediol formation from DHEA seemed to be unaffected in both groups. 3'-mRNA sequencing failed to detect any different transcript expression levels of enzymes that are involved in the conversions from the substrates E1S and DHEA into their products E1, E2 and androstenediol, indicating that the decreased E2 formation in disordered hair growth might not be subject to a malfunction of enzymes involved in the synthesis of steroid hormones, although the impact of the enzyme HSD17B7 on hair growth may be a potential topic for a follow-up research project.

Steroid hormone actions are mediated through their interaction with their nuclear receptors. Since E1, E2 and androstenediol show binding affinity for both nuclear estrogen receptors α and β (ERα, ERβ) (Chen et al. 2022, Fuentes and Silveyra 2019, Miller et al. 2013, Paterni et al. 2014), the next aim was to investigate if ER expression differed between case and control samples. Data revealed that there was no significant up or down regulation of ESR1 (ERα) or ESR2 (ERβ,) in AGA or DA in comparison to the control

group (Fig. 23 A and B), indicating that at least on the expression level ESR1 was not impaired in one of the observation groups. The data also indicated, that the mean value in the expression profile of ESR2 was higher in AGA samples than the mean value of the control group (Fig. 23 B). But sample variation was high in the groups of DA and AGA, suggesting that all three observation groups might show an equal expression of the receptors. Data on the relative expression of ESR2 obtained by qRT-PCR showed no difference in the expression of ESR2 in control and AGA samples (Fig. 23 C).

So, at least for the here presented observation groups, there seemed to be no difference in the expression profiles of steroid receptors among normal hair growth (control) and disordered hair growth (AGA and DA), assuming normal functionality on steroid hormone receptor level.

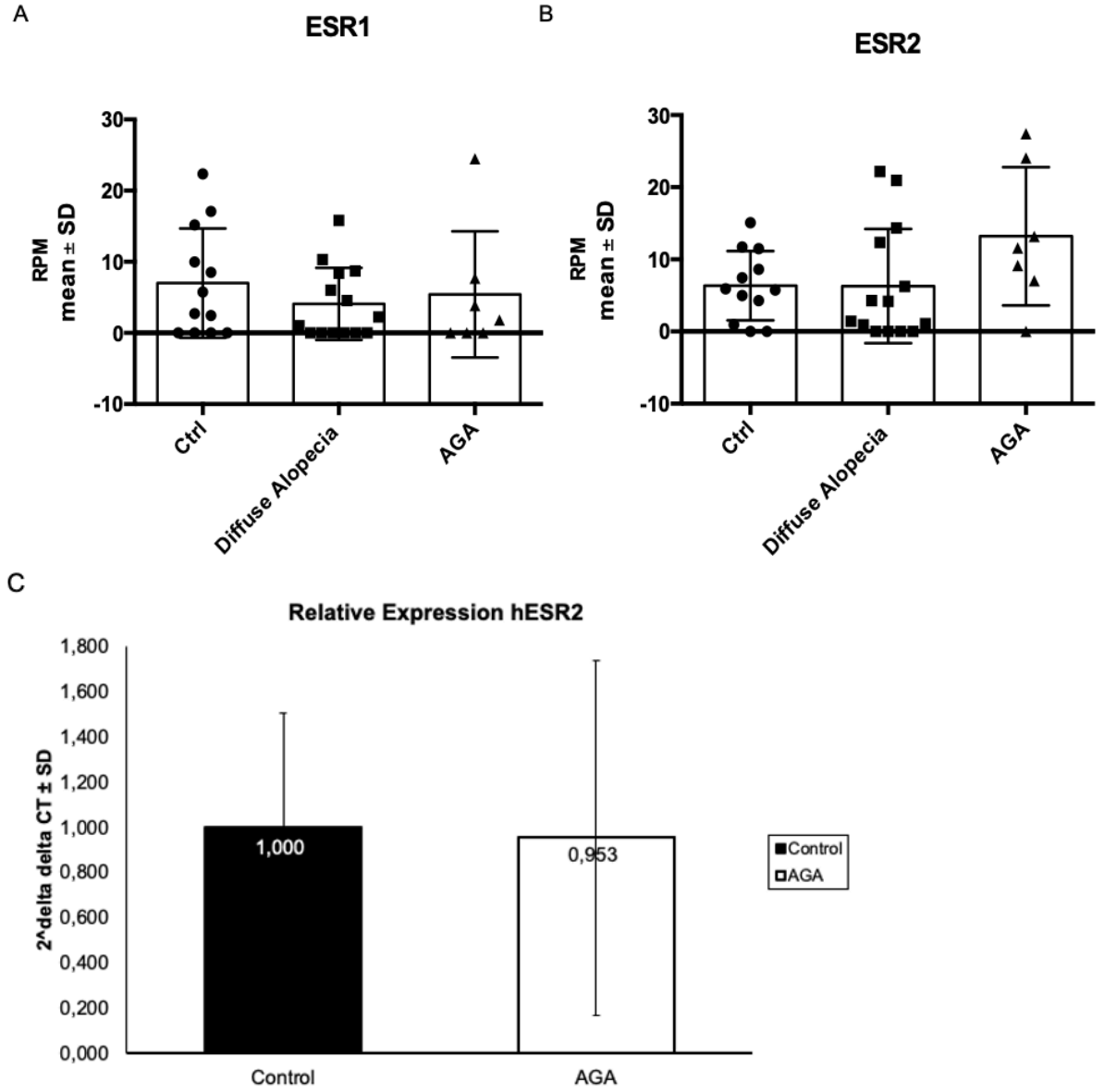

Fig. 23: Expression analysis of steroid hormone receptors. A Comparison of the expression of estrogen receptor α (ESR1) and **B** estrogen receptor β (ESR2). Data represent mean and standard deviation (SD) from 12 control (ctrl), 14 diffuse alopecia (DA) and seven androgenetic alopecia (AGA) samples. **C** Real-Time quantitative polymerase chain reaction (qRT-PCR) of ESR2 in control and AGA samples. Data represent the relative expression ($2^{\Delta\Delta CT}$) and SD from five control and five AGA samples. CT cycle threshold. No significant differences found between control and disordered hair growth (DA, AGA).

Now, it had to be excluded that less E2 was built as a consequence of less available substrate (E1S). Cellular influx of sulfated steroids like E1S requires active transport mechanisms mediated by solute carrier organic anion transporters (SLC) like SLCO2B1 (OATP2B1) which substrate is E1S (Medwid et al. 2021, Mueller et al. 2015, Roth et al. 2012).

Interestingly, expression of SLCO2B1, which is involved in the cellular uptake of endogenous compounds such as steroid hormone conjugates, seemed to be down regulated in DA and AGA compared to the control group (Fig. 24), although this effect was not statistically significant and data showed high sample variation as indicated by the standard deviation.

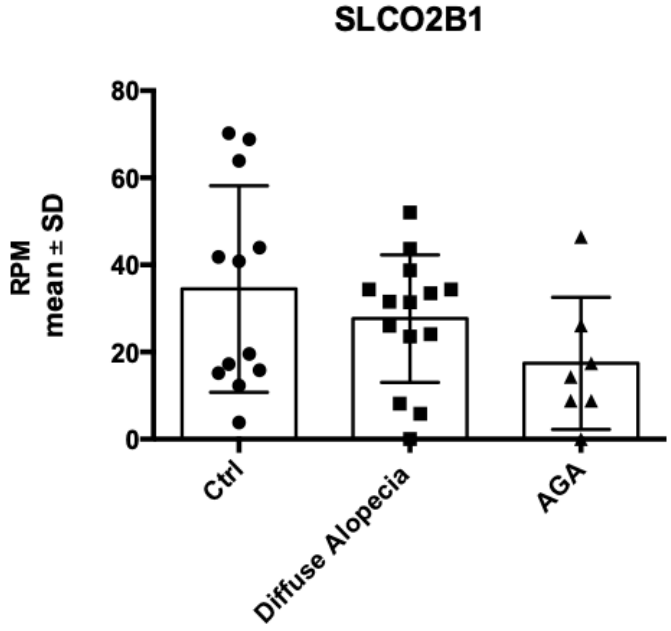

Fig. 24: Expression analysis of solute carrier organic anion transporter family member 2B1 (SLCO2B1) in control (ctrl), androgenetic alopecia (AGA) and diffuse alopecia (DA) samples. SLCO2B1 seems to be lower expressed in AGA (not significant). Data represent mean and standard deviation (SD) from 12 control, 14 DA and seven AGA samples. Ordinary one-way ANOVA and Dunnett's multiple comparisons test were used for statistical analysis of the data. * $P < 0.05$. 3'-mRNA sequencing. RPM reads per million mapped reads.

3.9 Analysis of FGF5 and EDA expression in scalp hair roots from control, AGA and DA

Several genes are described that seem to be involved in *male pattern baldness* (MPB) as mentioned in 1.4.1 (introduction). Transcript expression of these candidate genes served to determine, if there were similarities between MPB and AGA or DA in women.

Data indicated a down regulation of fibroblast growth factor 5 (FGF5) expression in DA and AGA compared to control samples (Fig. 25 A), indicating that DA, or even AGA, may show similarities to MPB, but more samples would be necessary for the AGA group to make further statements on a potential significance of the down regulation of FGF5.

Expression analysis also revealed a slight down regulation of ectodysplasin A (EDA) in anagen scalp hair roots from AGA and DA in comparison to the control group (Fig. 25 B). Due to low sample amounts these results were not verified by qRT-PCR.

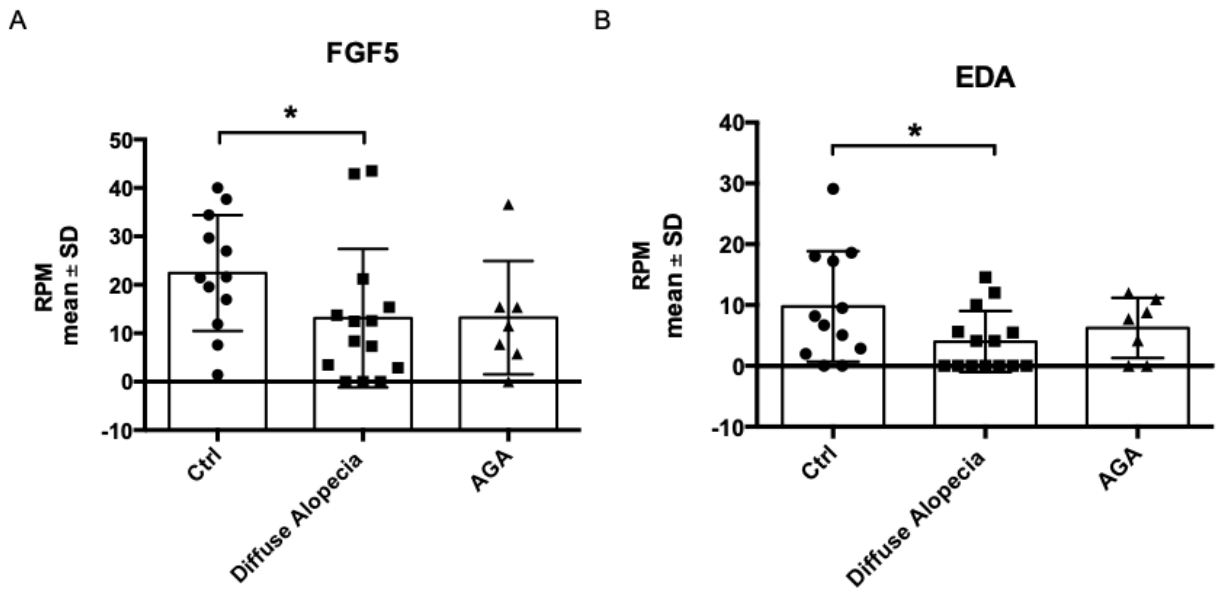

Fig. 25: Expression analysis of candidate genes for male pattern baldness (MPB) A fibroblast growth factor 5 (FGF5) and B ectodysplasin A (EDA) in control (ctrl), androgenetic alopecia (AGA) and diffuse alopecia (DA) samples. Expression of FGF5 and EDA is significantly lower in DA samples compared to the control group. Data represent mean and standard deviation (SD) from 12 control, 14 DA and seven AGA samples. One-tailed t-test was used for statistical analysis of the differences between the control group and the group of DA in A and B. * $P < 0.05$. RPM reads per million mapped reads.

3.10 Analysis of mitochondrial transfer RNA (tRNA) transcript expression in control, AGA and DA

Interestingly, as an incidental finding, a set of genes associated with mitochondrial translation, was noted in the 3'-mRNA sequencing data. These genes were down regulated in the AGA group.

As seen in and described for figure 19, the heatmap is arranged in rows, representing genes encoding for the tRNA genes, and columns, representing the observation group (A = hair loss, C = control) (Fig. 26). Numerical values are colored according to the color scale shown in the figure, correlating a red color with a high gene regulation and a blue color with a low gene regulation. The heatmap indicated that transcript levels for mitochondrial tRNA genes and mitochondrial processing tRNA genes were decreased on average in samples from hair growth disorders (A) compared to the control (C) as shown by the color scale (Fig. 26). This includes mitochondrial encoded tRNA Leucin 1 (MT-TL1), mitochondrial encoded tRNA serin 1 (MT-TS1), and mitochondrial encoded tRNA isoleucine (MT-TI), as well as mitochondrial processing tRNAs tRNA methyltransferase 10 C (TRMT10C) and Leucyl-tRNA synthetase 2 (LARS2).

So, the heatmap indicated a clustering of the samples, building two different groups, one group for the C samples and one group for the A samples. Both clusters showed a different transcript regulation for some mitochondrial encoded genes.

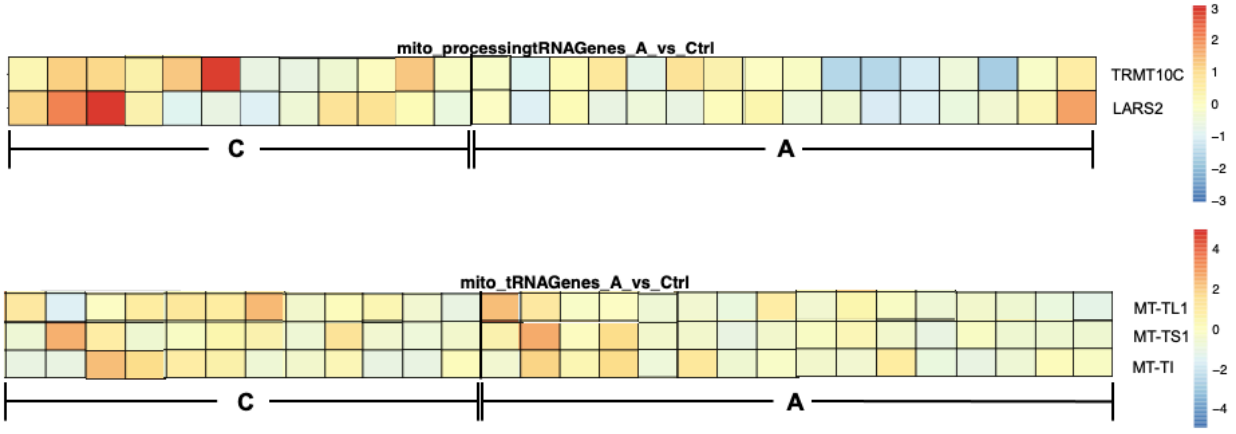

Fig. 26: Expression analysis of mitochondrial (mito) transfer ribonucleic acid (tRNA) transcripts in control and disordered hair growth (androgenetic alopecia (AGA) and diffuse alopecia (DA)) samples. Data include 12 control (C), 14 DA and seven AGA (A) samples. 3'-mRNA sequencing. Ctrl control. tRNA methyltransferase 10

C (TRMT10C), Leucyl-tRNA synthetase 2 (LARS2), tRNA Leucin 1 (MT-TL1), tRNA serin 1 (MT-TS1), tRNA isoleucine (MT-TI). Color code log2 scale.

Separating the group of disordered hair growth into DA and AGA revealed, that the levels for MT-TL1 (Fig. 27 A), MT-TS1 (Fig. 27 B) and MT-TI (Fig. 27 C) were down regulated in AGA samples, which was not the case for the control group. Furthermore, the DA group showed equivalent transcript levels to that of the control samples (Fig. 27 A - C). Transcript expression for tRNA methyl transferase 10 C (TRMT10C), which is involved in the 5’ end removal of the tRNA biogenesis (Phizicky and Hopper 2023), showed a significant decrease in the AGA group when compared to the control group, as illustrated in figure 27 D (Fig. 27 D). In contrast to this, the DA group showed no significant difference to the control group (Fig. 27 D).

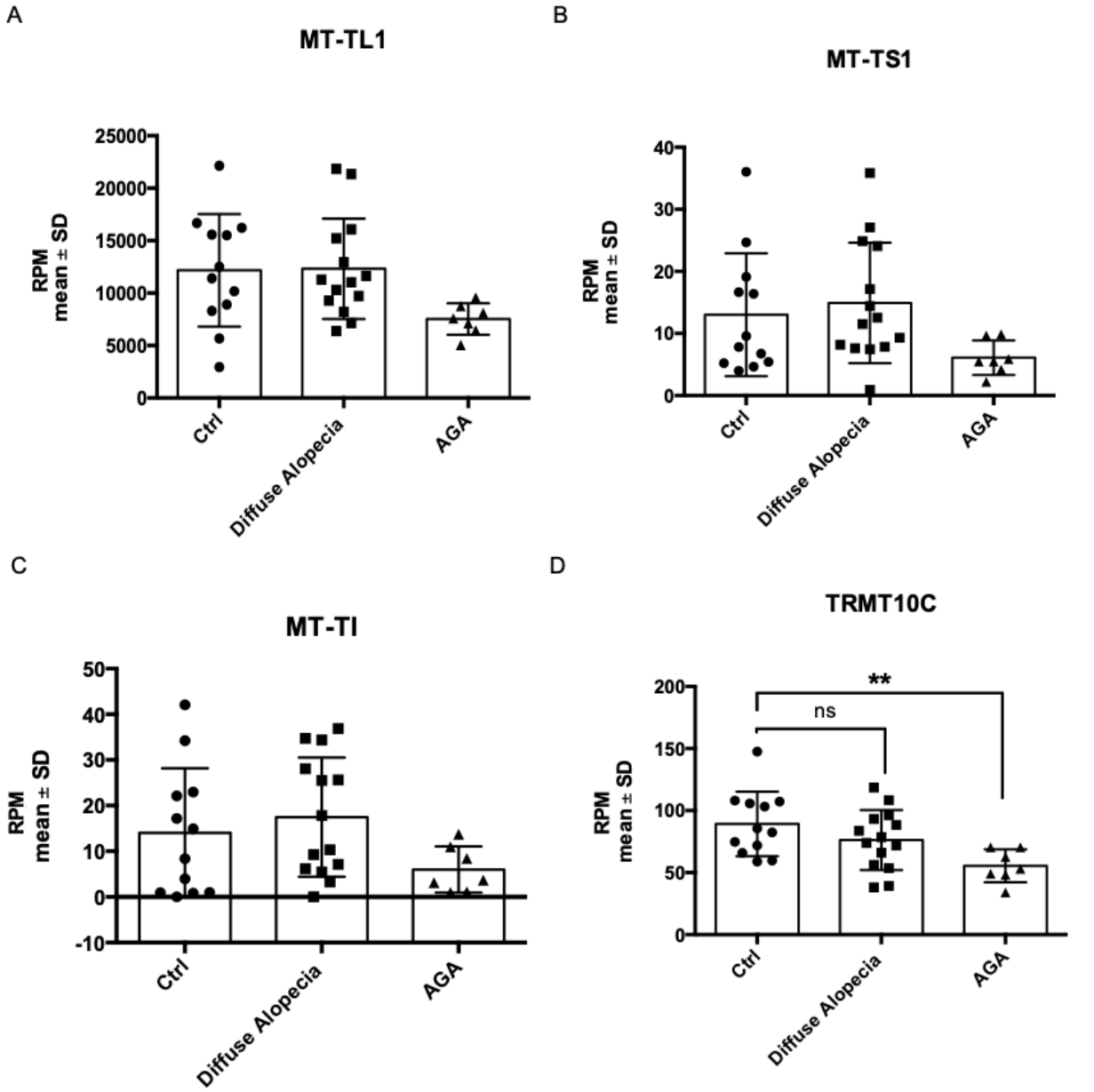

Fig. 27: Expression analysis of mitochondrial genes associated with translation. **A** mitochondrial encoded transfer ribonucleic acid (tRNA) Leucin 1 (MT-TL1), **B** mitochondrial encoded tRNA serin 1 (MT-TS1), **C** mitochondrial encoded tRNA isoleucine (MT-TI), **D** tRNA methyl transferase 10 C (TRMT10C). A - D Mitochondrial genes seem to be lower expressed in AGA, whereas the effect is not visible for DA. 3'-mRNA sequencing. RPM reads per million mapped reads. SD standard deviation. Ctrl control, AGA androgenetic alopecia. Ordinary one-way ANOVA and Dunnett's multiple comparisons test were used for statistical analysis of the data in A - D. * $P < 0.05$, ** $P < 0.01$, ns not significant.

In contrast to this, data for Leucyl-tRNA synthetase 2 (LARS2) showed no significant difference between the control group and AGA or DA (Fig. 28 A). Data obtained from qRT-PCR implicated that relative expression of human LARS2 was slightly down regulated in AGA samples compared to control samples, although this result was not statistically significant and standard deviations indicated a high sample variation in both groups (Fig. 28 B).

So, the qRT-PCR result for LARS2 displays the findings from the 3'-mRNA sequencing data for LARS2.

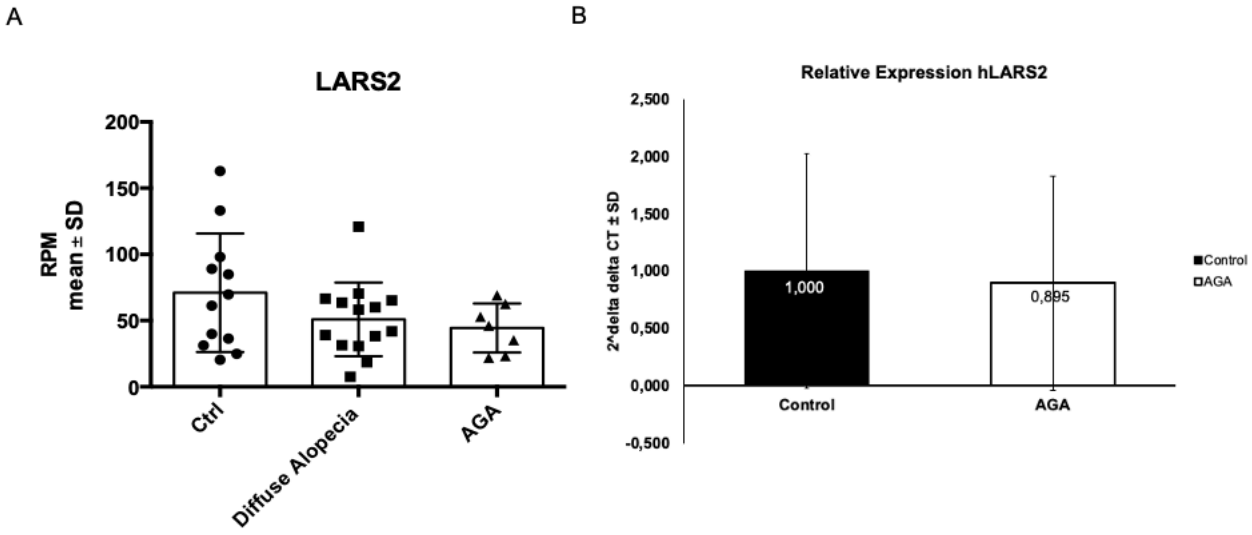

Fig. 28: Expression analysis of Leucyl-tRNA synthetase 2 (LARS2) in control (ctrl), androgenetic alopecia (AGA) and diffuse alopecia (DA) samples. A Data represent mean and standard deviation (SD) from 12 control, 14 DA and seven AGA samples. Mitochondrial genes seem to be lower expressed in AGA. 3'-mRNA sequencing. RPM reads per million mapped reads. **B** Quantitative real-time polymerase chain reaction (qRT-PCR) analysis of human LARS2 (hLARS2) in control and AGA samples. Data represent relative expression ($2^{\Delta\Delta CT}$) and standard deviation (SD) from five control and five AGA samples. Ordinary one-way ANOVA and Dunnett's multiple comparisons test were used for statistical analysis of the data in A. Data not significant. CT cycle threshold.

Considering now all the data presented in this approach (metabolite experiments and 3'-mRNA sequencing), the data from the metabolite experiments, as well as the data for FGF5 and EDA (Fig. 25) and LARS2 (Fig. 28) indicated, that AGA and DA may differ from the control, but may not be different from each other, assuming that both, AGA and DA, may show similarities. But the data presented in figures 26 and 27 now indicated, that the

AGA group may be different from DA and control concerning mitochondrial function. These observations could lead to a potential new research project, namely the impact of mitochondria on hair growth.

In summary, the comparison of disordered hair growth and healthy hair growth are in line with the idea, that hair growth disorders may be correlated with an impaired local E2 metabolism in the hair root, since the conversion of E1S into E2 was lower in hair growth disorders than in the healthy control. In this context, the enzyme HSD17B7 might display a key enzyme, since the data indicate that down regulation of *HSD17B7* may occur in telogen hair.

It was not possible to confirm the hypothesis, that hair growth disorders may be correlated with an impaired androstenediol formation from DHEA.

Furthermore, results indicate that hair growth disorders, especially DA, may show similarities to MPB, since the candidate genes for MPB, FGF5 and EDA, are down regulated in hair growth disorders.

The data also raises the question, whether AGA may be correlated with impaired mitochondrial features.

The here presented results led to ideas for potential follow-up research projects concerning (1) the impact of warm and cold seasons on estrogen metabolism in hair growth and (2) the impact of mitochondria on hair growth.

4. Discussion

4.1 Summary

Hair loss is a symptom that affects both, men and women, at different ages. The extend of and the cause for loosing hair can vary (Lutz 2012), which makes it even more difficult to find the right diagnosis and treatment. The impact of steroid hormones on hair development and hair loss thereby displays an important research field, since hair growth is dependent on the local androgen concentration in the skin (Schiffer et al. 2018).

This project served to test the hypothesis that disordered hair growth may be correlated with impaired local steroid metabolism in hair roots. Based on the results obtained by Wehner and Schweikert (Wehner and Schweikert 2014) on the local steroid metabolism in healthy hair, this approach served to test the hypothesis that the enzymatic conversion of estrone-3-sulfate (E1S) into 17β-estradiol (E2) might be different in hair growth disorders. And indeed, results show, that the conversion of E1S into E2 is significantly decreased in diffuse alopecia (DA). It was also possible to confirm the local conversion in isolated hair roots by inhibiting steroid sulfatase (STS) leading to a decreased conversion of E1S into estrone (E1) and E2.

3'mRNA-sequencing furthermore showed a lower expression of the enzyme *HSD17B7* in telogen compared to anagen hair. The enzyme mediates the reduction of E1 into E2 (Hilborn et al. 2017, Miller and Auchus 2011, Nokelainen et al. 1998, Ramos and Miot 2015, Samavat and Kurzer 2015, Schiffer et al. 2019). In anagen hair, 3'mRNA-sequencing revealed no significant differences between control and disordered hair growth groups. But an explorative approach indicated that fibroblast growth factor 5 (FGF5) and ectodysplasin A (EDA), both being candidate genes for *male pattern baldness* (MPB), are significantly decreased in anagen hair in the group of hair growth disorders.

It was not possible to confirm the hypothesis that the conversion of dehydroepiandrosterone (DHEA) into androstenediol may be different in hair growth disorders.

4.2 Study group

Despite difficulties in the recruitment of hair donors, probably partly a result of the SARS-CoV-2-pandemic situation, it was possible, with the help of Dr. med. Gerhard Alfons Lutz to include 39 female volunteers for the project. Since Dr. Lutz has specialized in the field of alopecia (Lutz 2012, Lutz 2018), he carried out the trichograms according to his own descriptions (Lutz 2001). His diagnostics revealed that several hair donors did not suffer from androgenetic alopecia (AGA), but from diffuse alopecia (DA), so volunteers were assigned into control, AGA and DA groups (Tab. 13). Since Dr. Lutz was the only person carrying out the anamnesis interview and visual diagnosis, as well as the pull-test and the trichogram, it was possible to exclude inter-individual differences in the assignment of hair donors. This helped to create a homogenous group distribution concerning the hair state. It further helped to minimize group variation, that could be otherwise a result of probably wrongly diagnosed volunteers. Median age for volunteers older than 50 years is similar among the three groups (Tab. 13). Since hair develops with age (Robbins et al. 2012) and also the amounts of circulating steroids change with age (Mueller et al. 2015, Schiffer et al. 2019), a similar median age makes a comparison among the groups easier, because a potential age-dependent effect in the analysis of steroid metabolism could be minimized. Unfortunately, the AGA group of younger women is characterized by a higher median age (43.3) than the two other groups (median age 31.3 and 30.7) (Tab. 13). Together with the overall lower number of participants in the AGA group in comparison to the control or DA groups, the higher median age may result in higher sample variation. A higher group number (n) may lead to a more homogenous group distribution and may contribute to a lower variation between the groups.

4.3 Biochemical assay

On the basis of the experimental design published by Wehner and Schweikert (Wehner and Schweikert 2014), anagen scalp hair roots were incubated in cell culture medium containing either [6,7-^{3}H(N)] E1S or [1,2,6,7-^{3}H(N)] dehydroepiandrosterone (DHEA) over 48 hours (E1S) or five hours (DHEA), respectively, followed by extraction of the conditioned media and subsequent separation of steroids via thin-layer chromatography (TLC). Colored spots representing estrone (E1), 17β-estradiol (E2) and androstenediol,

were scratched off from the TLC-plate and corresponding energies of each scratched spot were analyzed. Results, given as counts per minute (cpm), in combination with the specific activities of the substrates were used to normalize the amount of formed product on the DNA content of the hair roots.

Following these experimental designs, it was possible to confirm a local metabolization of E1S to E1 and E2 in isolated scalp hair roots, as it was described before by Wehner and Schweikert (Wehner and Schweikert 2014). Hydrolysis of E1S yielded moderate amounts of E1, nearly as much as shown in the results by Wehner and Schweikert (Wehner and Schweikert 2014, Fig. 2 A), indicating that the biochemical assay worked nearly as good as in their experiments. Measurable, but much lower amounts of E2 were detectable (Fig. 11). Comparable results were shown by Wehner and Schweikert, although the overall amount of E2 was much lower than presented by Wehner and Schweikert (Wehner and Schweikert 2014, Fig. 2 B). Reduction of E1 yielded 3 % E2 in their experiments (Wehner and Schweikert 2014, Fig. 2 B) and approximately 0.1 % in the here presented results (Fig. 11). It is known that some hormone levels are subject to variation during the day (Oster 2014) and also steroid hormones show variable levels during the menstrual cycle (Rassow et al 2012). To rule out that enzymes involved in the conversion of the substrates E1S and DHEA into their products E1, E2 and androstenediol may be subject to a circadian expression pattern, hair roots were always epilated between 9 AM and 11 AM, so that the experiments always started at the same time period of a day. Differences in the amounts of formed metabolites between the experiments of Wehner and Schweikert (Wehner and Schweikert 2014) and the here presented project may be a result of differences in the experimental setup between this approach and the settings from Wehner and Schweikert. Briefly, Wehner and Schweikert described that after separation of steroids via TLC, the resulting spots and the spaces in between were cut off and analyzed (Wehner and Schweikert 2014). In this approach, only the resulting spots were scratched off and analyzed, not the spaces in between (see 2.2.2). It may happen that the steroid mixture did not separate completely or accurately, so that not all of the formed E2 centered in the colored E2 spot. This would mean that some of it might still be detectable in the space between starting line and E2 spot. This would mean, that only part of the formed E2 was scratched and analyzed. This aspect cannot be totally excluded concerning this approach, since the steroid mixture runs upwards on the TLC plate for

separation. In all instances, E1 formation is higher than E2 formation (Fig. 11) and this supports the data presented by Wehner and Schweikert (Wehner and Schweikert 2014). Since the amount of E2 formed from E1S were low, someone could also assume, that experiments on E2 formation did not work properly. Assuming this, due to trace amounts of measurable E2 in the samples (Fig. 11 C and D), it should also be the case for experiments on E1 formation, because the synthesis of E1 and E2 were measured within the same experiment, same sample and same TLC lanes and runs. But results reveal moderate amounts of formed E1, assuming that the experiments did work correctly.

So, it was possible to confirm a local metabolization of the sulfated steroid E1S into its products E1 and E2 in human scalp hair roots, as it was presented by Wehner and Schweikert (Wehner and Schweikert 2014).

4.4 E2 formation in women suffering from hair loss

Another goal of this project was to compare the metabolism of E1S in healthy women and women suffering from hair loss, in order to possibly uncover potential differences in the formation of E2 from E1S.

The comparison of the local synthesis of steroid hormones in control and disordered hair growth (AGA and DA) shows that E1 formation from E1S might be higher in the AGA group than in control or DA samples (Fig. 11 A and B). This might indicate a higher STS activity in AGA samples, since STS is involved in the conversion of sulfated steroids like E1S (Hilborn et al. 2017, Mueller et al. 2015). But due to the low number of participants and the sample variation within the AGA group, the data may not be reliable. It might be possible that a higher sample number may lead to more precise and more homogenous results. As indicated in the graph, the group with a higher E1 formation from E1S does not exclusively contain samples from women older than 50 years, although E1 is said to be predominantly present in postmenopausal women (Samavat and Kurzer 2015). Wehner and Schweikert compared E1 formation in healthy women younger and older than 50 years and they showed that E1 formation is lower in scalp hair from women older than 50 years (Wehner and Schweikert 2014). Considering their results (Wehner and Schweikert 2014), it then seems plausible that the higher E1 formation in the AGA group is not related

to higher aged participants, but it might indicate that part of the AGA group may differ from the other AGA samples, maybe in an aspect that was not identified during this project.

Taken together, the experiments of the here presented project cannot confirm an age-dependency in the metabolization of E1S to E1 and E2 in women, like it was described before by Wehner and Schweikert (Wehner and Schweikert 2014), neither in the control group, nor in the group of disordered hair growth, although composition of the control group (age < 50, n = 9, age > 50, n = 7) is comparable to the study by Wehner and Schweikert (age < 50, n = 8, age > 50, n = 8).

In contrast to Wehner and Schweikert, who determined anagen and telogen scalp hair in healthy volunteers (Wehner and Schweikert 2014), only anagen hair roots served for the comparison of healthy and disturbed hair growth in this approach. Wehner and Schweikert showed, that much more telogen than anagen hair was necessary for their experiments (Wehner and Schweikert 2014), but due to the possibility that the epilation of hair from the scalp might be painful, the experiments focused on anagen hair. Although hair loss is characterized by a higher rate of telogen hair (Lutz 2001, Lutz 2012), at least for AGA, the duration of the anagen phase was described to be shorter than in the normal hair growth cycle (Paus and Cotsarelis 1999). A shorter anagen phase might then be a promising aspect in the comparison of estrogen metabolism in AGA and control group. But the results indicate that there is no difference in the synthesis of E1, assuming proper STS-functionality in all observation groups. Furthermore, returning to the E1 formation in telogen hair, the results presented by Wehner and Schweikert revealed, that E1 formation does not differ between the anagen and telogen state of scalp hair roots (Wehner and Schweikert 2014). Another reason, why this approach excluded telogen hair from the analysis a priori. But Wehner and Schweikert showed, that E2 formation from E1S is almost abolished in telogen hair (Wehner and Schweikert 2014). In this context, the overall aim of the current project was to test the hypothesis that hair loss may be correlated or even caused by a reduced enzymatical conversion of sulfated steroids into E2 in the human scalp hair root. The data show indeed, that the conversion of E2 from E1S is reduced in anagen hair roots in disordered hair growth (AGA and DA) (Fig. 11 C and D). A reduced conversion of E1 to E2 in anagen hair roots in case of hair loss now suggests, that E2 may be involved in the transition of anagen to telogen phase, a hypothesis that

was already suggested by Wehner and Schweikert, based on their finding that E2 formation is almost abolished in telogen hair (Wehner and Schweikert 2014). Together with the reduced expression of *HSD17B7* in telogen hair (Fig. 17), it strengthens the impression that hair loss may be correlated to a reduced conversion of sulfated steroids in hair roots. The decreased E2 levels in hair growth disorders therefore underline the hypothesis of Wehner and Schweikert that E2 might play a critical role in the maintenance of anagen phase and physiological hair development (Wehner and Schweikert 2014). In this case, AGA and DA show comparable amounts in E2 formation (Fig. 11 D), assuming, in disordered hair growth, impaired functionality of enzymes of the HSD family, namely HSD17B1 and/ or HSD17B7, that mediate the reduction of E1 to E2 (Hilborn et al. 2017, Miller and Auchus 2011). The data also indicate that AGA and DA do not differ much concerning the metabolization of estrogens (Fig. 11), although both diseases appear clinically different from each other (Lee et al. 2015, Qi and Garza 2014). In all instances, the group size is low and more AGA cases would have been helpful and necessary to make more precise statements on this result, but within 13 months it was not possible to include more AGA cases.

AGA is a disease that can be present in different stages, each characterized with an increase in the severity of the phenotype, according to the classifications on hair loss patterns occurring in men and women from Hamilton, Norwood and Ludwig (Hadshiew 2022, Ludwig 1977). In this project, AGA cases were not examined on activity stages or the severity of the phenotype due to the low number of AGA cases in this project in general. So, if a stronger or weaker stage of the disease might reflect its activity in a higher or lower estrogen metabolization, no further statements can be made, regarding this aspect, only on the basis of the here presented experiments and results, but it could be a potential future aspect for further research in this field.

It was not possible to confirm an age-dependency in the estrogen production as shown by Wehner and Schweikert, neither for the control group, nor for the AGA or DA groups (Fig. 12 A and B), although the group size, at least for the control, was comparable to the number of participants in the study by Wehner and Schweikert (Wehner and Schweikert 2014).

The metabolization of a substrate into its product always involves enzymatical action. The enzyme STS catalyzes the hydrolysis of sulfated steroids like E1S and dehydroepiandrosterone sulfate (DHEAS) (Hilborn et al. 2017, Mueller et al. 2015) and estrone sulfamate is described to be specific in inhibiting STS (Kurogi et al. 2019). The results of the current project show, that hair roots exposed to estrone sulfamate synthesize less E1, the direct product of E1S, than the untreated control (Fig. 13 A - B), thereby underlining the efficiency of the compound on the enzyme STS (Kurogi et al. 2019). These results therefore confirm that E1 and E2 are enzymatically formed from the substrate E1S during the experiments. The internal background control (without hair roots) described in the methods (2.2.2) serves to make sure, that only the local, hair root-mediated, E1 and E2 formation from E1S is observed.

4.5 Season-dependency

Figure 14 A indicates that E1 formation from [6,7-^{3}H(N)] E1S in a healthy female donor is lower in autumn than in spring (Fig. 14 A), suggesting that estrogen levels, at least concerning E1 formation, might show a season-dependency. Actually, the hair growth cycle in humans follows an asynchronous rhythm, so that the hair density is supposed to remain relatively stable all over the year (Natarelli et al. 2023, Pierard-Franchimont and Pierard 2013). Different to that, it is known that some animals show variable fur growth patterns in warm and cold seasons, due to a synchronized hair growth cycle (Pierard-Franchimont and Pierard 2013). This is an aspect that might partly reflect the today's differences between humans and animals. The reason that leads to the synchronization of the hair growth cycle in some animals is not completely understood. Maybe it is an evolutionary mechanism that helped to survive, but the underlying basic biochemical or endocrinological mechanism remains unknown. Since this was just a pilot experiment with only one individual, the number of data also needs to be increased to allow further statements on this issue. But indeed, it is an interesting finding. Since the result is not statistically significant, it is potentially a not reliable finding that human hair growth may follow a seasonal effect as known for animals (Pierard-Franchimont and Pierard 2013). There could also be other reasons why the amount of E1 formed from E1S varies among these consecutive experiments (for example (e.g.) use of dietary supplements in the

meantime), concluding that only data for E1 formation do not provide any reliable information on this issue. It would have been interesting and strictly necessary to see data for E2 formation for this time period, since E2 formation, following the data in this project, is suggested to be affected in hair growth disorders and in telogen hair, as shown by Wehner and Schweikert (Wehner and Schweikert 2014). Further considering a potential season-dependency in the occurrence of hair loss, figure 14 B and C indicate that there is no correlation between the recruitment of hair loss cases and colder months (Fig. 14 B and C). The recruitment process followed a random principle, since the assignment to one of the groups was first carried out when meeting potential hair donors. So, it was not known in advance, if a volunteer serves as a control or case (see 2.2.1). Regarding the whole project and the interviews with the volunteers concerning personal experiences on hair growth, it is also not surprising that hair loss cases are well distributed over the observed 12 months period and that they are not clustering in warmer months. People suffering from AGA recognized years ago that they are losing hair, indicating that the disease developed over a long time rather than being a sudden issue that develops according to changes in the weather. This is the case for AGA, but it does not mean vice versa, that another sudden hair loss could not be related to seasonal differences. For example, vitamin D is implicated to be involved in alopecia (Conic et al. 2021). The effect of vitamin D on hair growth is not well understood, but mice lacking the vitamin D-receptor (VDR -/- mice) were described to develop alopecia (Li et al. 1997). And serum vitamin D is one parameter medically determined in case of hair loss (Conic et al. 2021). People living beyond the 48th latitude may develop a kind of vitamin D-deficiency in terms of winter, due to the low number of hours, where the sun shines and probably also because they spend more time inside than outside in nature with less skin exposure to UV-light (Blum und Müller-Wieland 2020). It though may be interesting to compare serum vitamin D levels in case of hair loss in relation to winter months and the severity of the hair loss in another future project.

4.6 DHEA

The data of the current project further indicate, that androstenediol formation from DHEA is concentration- and time-dependent (Fig. 15 A and B). These results resemble the data

for E1 and E2 formation from E1S presented by Wehner and Schweikert (Wehner and Schweikert 2014). The data illustrate, that androstenediol formation from DHEA is highest at 100 nM substrate (Fig. 15 A). Actually, one would expect a plateau, if the maximum of the amount of formable androstenediol has already been reached in the measurement. Or one would at least expect as much as the maximum input of isotope-labeled substrate, in this case 100 nM, because the energy measured should rather be lower and not exceed the input activity. All substrate preparations include 100 nM of [1,2,6,7-^{3}H(N)] DHEA, but samples for 500 nM and 1000 nM are filled up to the aimed concentration with non-labeled substrate. Of course, it cannot be totally excluded that this mixture for the higher concentrations were incorrectly carried out, but since the substrate is evaporated to dryness before it is resolubilized in the cell culture medium, at least a solvent effect can be excluded. If it is not a mistake in the preparation, maybe the non-labeled substrate is somehow interfering with the isotope-labeled substrate, but this issue has not been further analyzed. The amount of androstenediol formed in 48 hours from 100 nM substrate, is, concerning the exact value, lower in figure 15 B than illustrated in figure 15 A (Fig. 15 B), but since the experiments were carried out with hair roots from the same woman, inter-individual effects can be excluded. Daily fluctuations could explain the different measurable amounts since the experiments were not carried out on the same day (Fig. 15 A and B). The data show, that a metabolization of DHEA to androstenediol can be determined using the adapted experimental conditions (see 2.2.2 and Fig. 15 A and B). The measurable amount of DHEA-derived androstenediol is even higher (approximately 0.3 pmol * μg DNA^{-1} * 5 hours^{-1}) than the amount of E1S-derived E2 (0.005 pmol * μg DNA^{-1} * 48 hours^{-1}). DHEA is one of the most abundant steroid hormones of the adrenal cortex (Kohalmy et al. 2007, Schiffer et al. 2018, Turcu and Auchus 2015) and androstenediol can serve as a ligand for the ER (Miller et al. 2013, Paterni et al. 2014). But the comparison of control and disordered hair growth clearly shows, that androstenediol formation from DHEA is not different in disordered hair growth (Fig. 16 A and B). Wehner and Schweikert suggested that estradiol might play a key role in hair formation, since they found that E2 formation in telogen hair roots from healthy donors is almost abolished (Wehner and Schweikert 2014). Regarding this and since androstenediol can also serve as a ligand for the estrogen receptor (Miller et al. 2013, Paterni et al. 2014), it would have been interesting to see a comparison of the androstenediol formation in anagen and telogen hair. But as mentioned

before, due to the restricted amount of material and since anagen phase is supposed to be shorter in AGA than in normal hair growth (Paus and Cotsarelis 1999), all experiments in this project concerning the comparison of healthy and disordered hair growth included anagen and excluded telogen hair roots. Furthermore, it was not possible to confirm an age-dependency in androstenediol formation from DHEA (Fig. 16 C) like it was described for E1S-derived E1 and E2 in the experiments of Wehner and Schweikert (Wehner and Schweikert 2014).

4.7 Expression of steroid biosynthetic genes

To uncover potential transcriptional differences between anagen and telogen hair, 3'-mRNA sequencing was performed. The analysis revealed no significantly different expression patterns of enzymes that are involved in the conversion of E1S or DHEA into E1, E2 or androstenediol (Fig. 17 A - C). An explorative analysis of the data focused on candidate genes involved in the processes studied in this work. Interestingly, expression of HSD17B7 is significantly reduced in telogen hair (Fig. 17 D and E). HSD17B7 is involved in the conversion of E1 into E2 (Hilborn et al. 2017, Miller and Auchus 2011). The reduction of HSD17B7 expression in telogen hair (Fig. 17 D and E) is in line with the observation of Wehner and Schweikert on E2 formation being decreased in telogen hair (Wehner and Schweikert 2014). These data might suggest that a low expression of HSD17B7 in anagen hair may underline the observed reduction in E2 formation from E1S in volunteers suffering from hair loss (Fig. 11 D). These data would again underline the hypothesis of Wehner and Schweikert on E2 playing a role in the termination of the hair growth cycle (Wehner and Schweikert 2014). These observations may also correlate hair loss with a reduced enzymatical conversion of sulfated steroids like E1S into E2. This strengthens the impression that changes in steroid metabolism may be involved in the hair growth cycle.

The comparison of gene expression patterns of control, AGA and DA samples suggest that there are no significant differences between the groups in general (Fig. 18 - 20). Particularly, the expression patterns of STS, HSD17B1 and HSD17B7 are here of special interest, since these are the enzymes involved in the downstream conversions from E1S to E1 to E2 (Hilborn et al. 2017, Miller and Auchus 2011, Mueller et al. 2015, Nokelainen

et al. 1998, Ramos and Miot 2015, Samavat and Kurzer 2015, Schiffer et al. 2019). But the results indicate again, that there is no difference in the expression patterns of control and disordered hair growth samples (Fig. 19 - 20). But if there is no significant difference in the expression patterns of enzymes involved in the metabolization of E1S to E1 and E2 or of DHEA to androstenediol, why is the amount of E1S-derived E2 lower in samples from disordered hair growth in the here presented results? It must have been a different enzymatical conversion, because otherwise the lower E2 amount cannot be explained. The comparison of the regulation of candidate genes (enzymes involved in E1S and DHEA metabolism to E1, E2 and androstenediol) shows, that again HSD17B7 showed the highest variability among the two hair loss groups (AGA and DA) (Fig. 21 A). It is worth mentioning, that comparing all the enzyme expression profiles, it is visible that the differences between the three observation groups are not as strong for STS, HSD17B1, HSD17B2 and HSD17B4 as for HSD17B7 (Fig. 21 A - B). The high variability in the AGA or DA group concerning the expression of HSD17B7 might indicate, that this gene may be deregulated in some volunteers suffering from hair loss. These data reflect the status in hair roots from anagen phase, but the data do not differ between the frontal and occipital scalp area, where the hair roots were epilated. Hair roots used for the analysis were epilated from frontal and occipital part of the head and were afterwards mixed for the sample preparation for 3'-mRNA sequencing. As mentioned before, hair loss may show different activities (Lutz 2012) and AGA and DA differ from each other in their hair loss pattern. Briefly, the AGA group shows a high telogen rate in the frontal scalp area, whereas the DA group is characterized by a uniformly shedding of scalp hair in the frontal and occipital scalp area (see 2.2.1 and Lutz 2012). It cannot be excluded, that a sample contained more anagen hair from the occipital part than from the frontal epilation site. But the data presented by Wehner and Schweikert indicate, that E1S-derived E1 and E2 formation do not significantly differ between the epilation sites on the scalp (Wehner and Schweikert). The high variability of the HSD17B7 expression in comparison to the other enzyme expression patterns (Fig. 21 A) is especially noticeable, in particular, when reminding that the analysis did not differ between frontal and occipital anagen scalp hair roots. So, this might also explain the high variation in between the groups. By the way, expression analysis does also not give any information on the translation process, so it is not sure, if the information on HSD17B7 obtained from the mRNA gains functional HSD17B7 protein. Furthermore,

it was not possible to confirm these results on qRT-PCR level (Fig. 22). Controversially, qRT-PCR suggests a lower relative expression of HSD17B7 in AGA than in control samples (data not significant), which may be correlated with the lower E2 formation in AGA and DA in metabolite experiments, since HSD17B7 mediates the conversion from E1 into E2 (Hilborn et al. 2017, Miller and Auchus 2011). It could be that the samples measured in qRT-PCR were not properly enough prepared in advance, since Ct values actually should be similar in between a group, although each sample represents a different individual. It could also be that the primer used for the analysis was not properly enough designed. Due to the restricted sample amount, the analysis was only carried out once, therefore only serving as a kind of pilot experiment, that should give further hints on the expression of HSD17B7 in the human hair root. So, in order to draw further conclusions on the expression of HSD17B7 in the human hair root, qRT-PCR actually needs to be repeated at least twice, to check if the here presented result can be reproduced. So, this result does not help in the understanding of hair loss and it does not provide any information about potential differences in the expression patterns of enzymes in samples from controls and hair loss, but it might suggest a role for HSD17B7 to be somehow involved in this process. Shehu et al. described in 2011 that estradiol stimulated HSD17B7 expression on protein and mRNA level (Shehu et al. 2011). Furthermore, they found that upregulation of hsd17b7 by estradiol is an ER-mediated event, since tamoxifen, as a selective ER antagonist, blocked these effects (Shehu et al. 2011). In a study with 112 female patients with breast cancer, alopecia was attributed to tamoxifen treatment in 37 cases (33 %) (Freites-Martinez et al. 2018). If upregulation of hsd17b7 is ER-mediated (Shehu et al. 2011), the next effort in this project was, to compare the expression patterns of steroid receptors in the observation groups, to uncover potential transcriptional differences between the three observation groups. Expression analysis has demonstrated that mediators of estrogen action, including (i) the estrogen receptor (ER) isoforms ERα and ERβ (Fig. 23) and (ii) enzymes of the 17β-hydroxysteroid dehydrogenases (17β-HSD) are expressed within human anagen scalp follicles. Expression analysis indicates that, at least for the here presented observation groups, there seems to be no difference in the expression profiles of the estrogen receptors α and β among normal hair growth (control) and disordered hair growth (AGA and DA), assuming normal functionality on receptor

level. Also in this case, expression analysis gives no information about the translation of gene into (functional) protein.

Solute carrier organic anion transporters (SLC transporters) are considered to mediate the influx of substrates (Roth et al. 2012). One member of the SLC transporter family is SLCO2B1 and one well-studied substrate of SLCO2B1 is E1S (Medwid et al. 2021). Results indicate, that expression of SLCO2B1 is down regulated in AGA samples (Fig. 24). If down regulation of SLCO2B1 expression may lead to an impaired influx of E1S in disordered hair growth, one would assume, that the lower local substrate availability consequently leads to a lower product amount, which is the case for E2 in the here presented metabolite experiments (Fig. 11 C and D). But since E1 formation remains nearly unaffected in control and AGA groups, this idea is challenged, because E1S is enzymatically converted to E1 by the enzyme STS and not to E2 (Hilborn et al. 2017, Mueller et al. 2015). Above all, the decrease in the expression level between control and AGA is not statistically significant. SLCO2B1 has been previously shown to be responsible for the cellular availability of iron (Unlu et al. 2022). As mentioned in the introduction, several factors, including iron, are assumed to be involved in the regulation of the hair growth cycle and CYP450 enzymes, involved in the synthesis of steroid hormones, contain a heme group with iron (Guo and Katta 2017, Lutz 2012, Mellon and Griffin 2002, Natarelli et al. 2023). But the exact mechanism how iron deficiency affects hair growth remains unknown (Guo and Katta 2017). Iron is described to act as a cofactor for the enzyme ribonucleotide reductase, which is a rate-limiting enzyme in the synthesis of DNA (Natarelli et al. 2023). Rapidly dividing cells constantly use this enzyme, as it is the case for rapidly dividing hair follicle cells (Natarelli et al. 2023). So, it is suggested, that iron deficiency may lead to a decrease in the efficiency of the enzyme ribonucleotide reductase, thereby leading to the association to disordered hair growth (Natarelli et al. 2023). Due to the complexity of this topic, further considerations are challenging only on the basis of the here presented results. Still, the high variation of sample values in between the observation groups does not clarify, if there is really a different expression pattern of SLCO2B1 between the groups. Although, the high variation might also indicate, that the expression of SLCO2B1 is deregulated in some of the samples. A higher number of participants may minimize the variability to clarify, if there are different expression patterns of SLCO2B1 in control and disordered hair growth or not. Other methods for

analyzing the impact of iron in local steroid metabolism would be necessary to draw further conclusions in this research field.

4.8 Known candidate genes and hair loss

Several genes are described that seem to be involved in *male pattern baldness* (MPB) (Heilmann-Heimbach et al. 2017). Could these genes also be involved in female hair loss? The data indicate, that fibroblast growth factor 5 (FGF5) is statistically significant lower expressed in DA than in control samples (Fig. 25 A). Also in the AGA group, expression of FGF5 seems to be lower in comparison to the control group (Fig. 25 A), although this result is not statistically significant. FGF5 is assumed to be involved in the deregulation of the development from anagen phase to the transition (catagen) phase (Heilmann-Heimbach et al. 2017, Higgins et al. 2014). It is also suggested, that FGF5 determines hair length in human hair follicles (Higgins et al. 2014). If this would be the case, it raises the question whether a lower expression of FGF5 may correlate with shorter hair or a shorter anagen phase. The hair growth cycle, actually anagen phase, determines the length of hair, since anagen is the state with the longest duration within the hair growth cycle (Duverger and Morasso 2014, Grymowicz et al. 2020, Ota et al. 2002). Since AGA is described to be characterized by a shorter anagen phase (Paus and Cotsarelis 1999), results then suggest that the effect of FGF5 in disordered hair growth may be an interesting future research field. If the number of samples analyzed would have been higher, the result may also be significant for the AGA group. Figure 25 B illustrates that also expression of ectodysplasin A (EDA) is decreased in hair growth disordered samples (DA and AGA) compared to the control group (Fig. 25 B). Even in this case, the reduction in the expression of EDA in the DA group, but not in the AGA group, is statistically significant compared to the control group (Fig. 25 B). EDA is necessary for a proper hair formation and is furthermore assumed to be affected in human hair growth disorders (Duverger and Morasso 2014, Heilmann-Heimbach et al. 2016). Clarke et al. described in 1987, that mutations in EDA lead to hypohidrotic ectodermal dysplasia (HED), which is characterized by failed development of hair and teeth (Clarke et al. 1987). If mutations in EDA lead to decreased levels of functional EDA, this would be in line with the here presented observation of a decrease of EDA in disordered hair growth.

In summary, results indicate, that DA and AGA may show correlations to MPB at least on gene expression level. Quite interesting is, that Lutz described in 2018 that female pattern hair loss may be distinguished in a female and a male type, the latter more often presenting with hyperandrogenemia (Lutz 2018). Together with the results obtained in this project, it then seems possible that hair loss diseases may have even more similarities, although they are distinguished clinically by their phenotypes and sometimes also by their origin. This again underlines the difficulties in the classification and treatment of hair loss, but may open up the possibility for disease over-lapping treatment options. This aspect would need to be further investigated.

4.9 Incidental findings

Quite interesting, although found as a coincidence, is the finding that certain mitochondrial genes, meaning nuclear genes expressed in mitochondria, as well as mitochondrially coded genes including mt-tRNAs, seem to be lower expressed in disordered hair growth (Fig. 26). Before being further processed to their final structure, pre-tRNAs are enzymatically released from long polycistronic precursor RNAs in the mitochondria (Vilardo et al. 2023). Since tRNAs are involved in the translation process, this incidental finding leads back to the discussion about a potentially different translational process in scalp hair in hair growth disorders, as mentioned before. The data indicate that levels for mitochondrial encoded tRNA Leucin 1 (MT-TL1), mitochondrial encoded tRNA serin 1 (MT-TS1) and mitochondrial encoded tRNA isoleucine (MT-TI) are decreased on average in the AGA group (Fig. 27 A - C). Levels for mitochondrial processing tRNA methyltransferase 10 C (TRMT10C) are even significantly decreased in the AGA group (Fig. 27 D). This effect cannot be seen for the DA group. TRMT10C is involved in the 5’ end removal of the tRNA biogenesis (Phizicky and Hopper 2023). Leucyl-tRNA synthetase 2 (LARS2) levels are also decreased on average in the AGA group, although this result is not statistically significant, probably due to the low sample number in the AGA group and high sample variation within the control group (Fig. 28 A). It was also not possible to confirm this result via qRT-PCR (Fig. 28 B). But these data might suggest, that tRNA processing may not function properly in AGA. Mitochondria play a key role of a cells oxidative phosphorylation process in gaining adenosine triphosphate (ATP) (Feng et al. 2022). A proper function of

the mitochondria drives several cellular processes, and mitochondrial disorders are associated with several diseases (Picard et al. 2016). But do these findings suggest, that there might exist mitochondrial stress in AGA and if so, how may it become noticeable? If there would be a problem in the respiratory efficiency of human scalp hair roots in AGA, it might explain the differences in AGA and DA phenotypes, pluck trichogram or telogen rates. Lower tRNA levels could also indicate lower mitochondria numbers. Vidali et al. investigated in 2014 the impact of thyroid hormones on mitochondria in organ-cultured human scalp hair follicles (Vidali et al. 2014). They found that hair follicles subjected to TSH, T3 and T4 showed an upregulation of mitochondrial biogenesis, indicating that evaluation of thyroid hormone levels might be important when characterizing hair loss (Vidali et al. 2014). In fact, it was already mentioned that thyroid dysfunction may lead to hair loss (Cohen et al. 2023, Deo et al. 2016, Lutz 2012, Natarelli et al. 2023) and laboratory testing in case of hair loss commonly includes thyroid stimulating hormone (TSH), thyroxine (T3) and trijodthyronine (T4) (Wolff et al. 2016). Results presented now in the current project may open up the possibility for new research in the field of hair growth disorders, namely the impact of mitochondria on hair growth. To clarify, if there might exist a respiratory inefficiency in human scalp hair roots in case of AGA, other experimental tests would be necessary, probably measurements on oxygen consumption or extracellular acidification rates using scalp hair roots as input. Due to the restricted amount of sample material, no such experiments were carried out in this approach, therefore no further statements concerning the mitochondrial respiratory state of hair roots in case of hair loss can be made. Since the exact origin of the type of hair loss was not determined in this study, it cannot be completely excluded, that differences in the disease characteristics, leading to high heterogeneity, confound the results. Heterogeneity also includes the absolute abundances between the observation groups with the AGA group (n = 8) being only half of the control group (n = 16) concerning the number of participants (Tab. 13). In this context, it is again worth mentioning that the recruitment process took thirteen months during which time it was possible to include only eight AGA cases out of 39 participants in total.

It would have been interesting to determine, if more data from more individuals would reflect equivalent results as presented here for metabolization and expression analysis, since higher absolute abundances may reflect more precise results.

In this context, it is again worth mentioning, that hair root samples from fronto vertical and occipital scalp areas were pooled for expression analysis due to restricted amounts of sample material. Considering that at least for AGA, anagen to telogen ratios differ in fronto vertical and occipital areas of the scalp, it would have been interesting to distinguish samples in frontal and occipital specimen prior to expression analysis to investigate, if expression patterns also differ at the two considered scalp sites. As mentioned before, AGA is a disease that can be characterized in different stages, according to the extent of the hair loss (Hadshiew 2022). This may complicate the interpretation of the here presented results even more. If different disease states correlate with different metabolization or expression patterns, it could explain greater intra-assay variability in an observation group. In this case, it might have been better to classify AGA not only as AGA, but as AGA according to the precise state of the disease. A more detailed classification of AGA or DA has not been done in this approach.

In summary, premature hair loss, especially from the scalp or even an excess of hair growth, may be a difficult situation for those affected, due to social or psychological aspects that may arise. A more detailed knowledge of local steroid metabolism and involved enzymes in human scalp hair, may open up the possibility of pharmacological intervention, since enzymes can be inhibited, in principle, and topical application may reach the hair follicle inside of the skin. A better understanding of the molecular mechanisms may also be important for all organs and tissues that are regulated by male and female sexual hormones and that possess an enzymatic activity comparable to that in human scalp hair, for example bone, prostate and mamma.

5. Abstract

Hair loss displays a common symptom with a multitude of different origins that complexes diagnostics and therapy.

The basis of the current project was the hypothesis, that hair loss may be correlated or even caused by an impaired local steroid hormone metabolism in scalp hair roots. It is known that human hair growth is regulated by hormones, including steroid hormones (Schweikert and Wilson 1974). In this context it was determined, if the local conversion of the steroid estrone-3-sulfate (E1S) into its products estrone (E1) and 17β-estradiol (E2) may be impaired in hair growth disorders (androgenetic alopecia (AGA) and diffuse alopecia (DA)). Indeed, the conversion of [6,7-^{3}H(N)] E1S into E2 was significantly decreased in the DA group in metabolite experiments. By the use of the steroid sulfatase (STS)-specific inhibitor estrone sulfamate, it was furthermore possible to inhibit the conversion of [6,7-^{3}H(N)] E1S into E1 and E2, thereby confirming that the conversion occurs locally in isolated hair roots. Moreover, 3'-mRNA sequencing data revealed, that expression of the enzyme HSD17B7, which is involved in the conversion of E1 into E2, is decreased in telogen hair.

It was not possible to confirm the hypothesis, that the conversion of dehydroepiandrosterone (DHEA) into androstenediol may be impaired in hair growth disorders.

Concerning the comparison of healthy and disordered hair growth, transcript expression analysis revealed, that there are no significant differences between the control, AGA or DA groups on the gene expression level in general. But an explorative analysis shows, that fibroblast growth factor 5 (FGF5) and ectodysplasin A (EDA), both being candidate genes in *male pattern baldness* (MPB), are significantly lower expressed in DA. This may indicate similarities of AGA and/ or DA to MPB.

Interestingly, found as a coincidence, the data set also suggested, that expression of several mitochondrial genes may be decreased in samples from hair growth disorders, which may open up the possibility for new research in the field of hair growth disorders.

6. List of figures

7. List of tables

8. References

Alemany M. Estrogens and the regulation of glucose metabolism. World J Diabetes 2021; 12(10): 1622-1654

Arias-Santiago S, Arrabal-Polo MA, Buendia-Eisman A, Arrabal-Martin M, Gutierrez-Salmeron MT, Giron-Prieto MS, Jimenez-Pacheco A, Calonje JE, Naranjo-Sintes R, Zuluaga-Gomez A, Serrano Ortega S. Androgenetic alopecia as an early marker of benign prostatic hyperplasia. J Am Acad Dermatol 2012; 66(3): 401-408

Arias-Santiago S, Gutierrez-Salmeron MT, Castellote-Caballero L, Buendia-Eisman A, Naranjo-Sintes R. Androgenetic alopecia and cardiovascular risk factors in men and women: a comparative study. J Am Acad Dermatol 2010; 63(3): 420-429

Arnold JT. DHEA metabolism in prostate: For better or worse? Molecular and Cellular Endocrinology 2009; 301(1-2): 83-88

Auer MK, Birnbaum W, Hartmann MF, Holterhus PM, Kulle A, Lux A, Marshall L, Rall K, Richter-Unruh A, Werner R, Wudy SA, Hiort O. Metabolic effects of estradiol versus testosterone in complete androgen insensitivity syndrome. Endocrine 2022; 76(3): 722-732

Bah SY, Dickinson P, Forster T, Kampmann B, Ghazal P. Immune oxysterols: Role in mycobacterial infection and inflammation. J Steroid Biochem Mol Biol 2017; 169: 152-163

Baulieu EE. Dehydroepiandrosterone (DHEA): a fountain of youth? J Clin Endocrinol Metab 1996; 81(9): 3147-3151

Betz RC, Petukhova L, Ripke S, Huang H, Menelaou A, Redler S, Becker T, Heilmann S, Yamany T, Duvic M, Hordinsky M, Norris D, Price VH, Mackay-Wiggan J, de Jong A, DeStefano GM, Moebus S, Böhm M, Blume-Peytavi U, Wolff H, Lutz G, Kruse R, Bian L, Amos CI, Lee A, Gregersen PK, Blaumeister B, Altshuler D, Clynes R, de Bakker PIW, Nöthen MM, Daly MJ, Christiano AM. Genome-wide meta-analysis in alopecia areata

resolves HLA associations and reveals two new susceptibility loci. Nat Commun 2015; 6: 5966

Blum H und Müller-Wieland D. Stoffwechsel: Kalziummangel (Hypokalzämie). In: Blum H und Müller-Wieland D, Hrsg. Klinische Pathophysiologie. Stuttgart: Georg Thieme Verlag, KG, 2020

Burns KA and Korach KS. Estrogen receptors and human disease: an update. Arch Toxicol 2016; 86(10): 1491- 1504

Cardoso D, Perucha E. Cholesterol metabolism: a new molecular switch to control inflammation. Clin Sci (Lond) 2021; 135(11): 1389-1408

Carr BR, MacDonald PC, Simpson ER. The role of lipoproteins in the regulation of progesterone secretion by the human corpus luteum. Fertility and Sterility 1982; 38(3): 303-311

Chen JF, Lin PW, Tsai YR, Yang YC, Kang HY. Androgens and Androgen Receptor Actions on Bone Health and Disease: From Androgen Deficiency to Androgen Therapy. Cells 2019; 8(11)

Chen P, Li B, Ou-Yang L. Role of estrogen receptors in health and disease. Front Endocrinol (Lausanne) 2022; 13: 839005

Choi N, Shin S, Song SU, Sung JH. Minoxidil Promotes Hair Growth through Stimulation of Growth Factor Release from Adipose-Derivd Stem Cells. Int J Mol Sci 2018; 19(3): 691

Clarke A, Phillips DI, Brown R, Harper PS. Clinical aspects of X-linked hypohidrotic ectodrmal dysplasia. Arch Dis Child 1987; 62: 989-996

Cohen B, Cadesky A, Jaggi S. Dermatologic manifestations of thyroid disease: a literature review. Front Endocrinol (Lausanne) 2023; 14: 1167890

Colardo M, Martella N, Pensabene D, Siteni S, Di Bartolomeo S, Pallottini V, Segatto M. Neurotrophins as Key Regulators of Cell Metabolism: Implications for Cholesterol Homeostasis. Int J Mol Sci 2021; 22(11): 5692

Conic RRZ, Piliang M, Bergfeld W, Atanaskova-Mesinkovska N. Vitamin D Status in Scarring and Non-Scarring Alopecia. J Am Acad Dermatol 2021; 85(2): 478-480

Contreras-Jurado C, García-Serrano L, Martínez-Fernández M, Ruiz-Llorente L, Paramio JM, Aranda A. Impaired hair growth and wound healing in mice lacking thyroid hormone receptors. PLoS One 2014; 9(9): e108137

Coulson-Thomas VJ, Gesteira TF, Esko J, Kao W. Heparan sulfate regulates hair follicle and sebaceous gland morphogenesis and homeostasis. J Biol Chem 2014; 289(36): 25211-25226

Cui J, Shen Y, Li R. Estrogen synthesis and signaling pathways during aging: from periphery to brain. Trends Mol Med 2013; 19(3): 197-209

Davis DS and Callender VD. Review of quality of life studies in women with alopecia. Int J Womens Dermatol 2018; 4(1): 18-22

Deo K, Sharma YK, Wadhokar M, Tyagi N. Clinicoepidemiological Observational Study of Acquired Alopecias in Females Correlating with Anemia and Thyroid Function. Dermatol Res Pract 2016; 2016: 6279108

Dufort I, Rheault P, Huang XF, Soucy P, Luu-The V. Characteristics of a highly labile human type 5 17beta-hydroxysteroid dehydrogenase. Endocrinology 1999; 140(2): 568-574

Duverger O and Morasso MI. To grow or not to grow: Hair morphogenesis and human genetic hair disorders. Seminars in Cell & Developmental Biology 2014; 25-26: 22-33

Elmlinger MW, Mayer I, Schnabel D, Schuett BS, Diesing D, Romalo G, Wollmann HA, Weidemann W, Spindler KD, Ranke MB, Schweikert HU. Decreased expression of IGF-II and its binding protein, IGF-binding protein-2, in genital skin fibroblasts of patients with complete androgen insensitivity syndrome compared with normally virilized males. J Clin Endocrinol Metab 2001; 86(10): 4741-4746

Enkavi G, Javanainen M, Kulig W, Róg T, Vattulainen I. Multiscale Simulations of Biological Membranes: The Challenge To Understand Biological Phenomena in a Living Substance. Chem Rev 2019; 119(9): 5607-5774

Fabbrocini G, Cantelli M, Masara A, Annunziata MC, Marasca C, Cacciapuoti S. Female pattern hair loss: A clinical, pathophysiologic, and therapeutic review. Int J Womens Dermatol 2018; 4(4): 203-211

Feng S, Wan S, Liu S, Wang W, Tang M, Bai L, Zhu Y. LARS2 Regulates Apoptosis via ROS-Mediated Mitochondrial Dysfunction and Endoplasmic Reticulum Stress in Ovarian Granulosa Cells. Oxid Med Cell Longev 2022; 2022: 5501346

Ferrante T, Adinolfi S, D'Arrigo G, Poirier D, Daga M, Lolli ML, Balliano G, Spyrakis F, Oliaro-Bosso S. Multiple caalytic activities of human 17β-hydroxysteroid dehydrogenase type 7 respond differently to inhibitors. Biochimie 2020; 170: 106 - 117

Förster C, Mäkela S, Wärri A, Kietz S, Becker D, Hultenby K, Warner M, Gustafsson JA. Involvement Of estrogen receptor β in terminal differentiation of mammary gland epithelium. Proc Natl Acad Sci U S A 2002; 99(24): 15578-15583

Foradori C D, Weiser MJ, Handa RJ. Non-genomic actions of androgens. Front Neuroendocrinol 2008; 29(2): 169-181

Freites-Martinez A, Shapiro J, Chan D, Fornier M, Modi S, Gajria D, Dusza S, Goldfarb S, Lacouture ME. Endocrine Therapy-Induced Alopecia in Patients With Breast Cancer. JAMA Dermatol 2018; 154(6): 670-675

Fuchs E. Scratching the surface of skin development. Nature 2007; 445(7130): 834-842

Fuentes N, Silveyra P. Estrogen receptor signaling mechanisms. Adv Protein Chem Struct Biol 2019; 116: 135-170

Geyer J, Bakhaus K, Bernhardt R, Blaschka C, Dezhkam Y, Fietz D, Grosser G, Hartmann K, Hartmann MF, Neunzig J, Papadopoulos D, Sanchez-Guijo A, Scheiner-Bobis G, Schuler G, Shihan M, Wrenzycki C, Wudy SA, Bergmann M. The role of sulfated steroid hormones in reproductive processes. J Steroid Biochem Mol Biol 2017; 172: 207-221

Giorgi EP, Stein WD. The transport of steroids into animal cells in culture. Endocrinology 1981; 108(2): 688-697

Goldstein JL and Brown MS. A Century of Cholesterol and Coronaries: From Plaques to genes to Statins. Cell 2015; 161(1): 161-172

Gonzalez GA, Hofer MP, Syed YA, Amaral AI, Rundle J, Rahman S, Zhao C, Kotter MRN. Tamoxifen accelerates the repair of demyelinated lesions in the central nervous system. Sci Rep 2016; 6: 31599

Grymowicz M, Rudnicka E, Podfigurna A, Napierala P, Smolarczyk R, Smolarczyk K, Meczekalski B. Hormonal Effects on Hair Follicles. Int J Mol Sci 2020; 21(15)

Guo EL and Katta R. Diet and hair loss: effects of nutrient deficiency and supplement use. Dermatol Pract Concept 2017; 7(1): 1-10

Hadshiew I. Androgenetische Alopezie (AGA). In: Sterry W, Czaika V, Drecoll K, Hadshiew I, Kiecker F, Papakostas D, Philipp S, Stefania R, Stieler K., Hrsg. Kurzlehrbuch Dermatologie. Stuttgart: Thieme, 2022

Hammes A, Andreassen TK, Spoelgen R, Raila J, Hubner N, Schulz H, Metzger J, Schweigert FJ, Luppa PB, Nykjaer A, Willnow TE. Role of endocytosis in cellular uptake of sex steroids. Cell 2005; 122(5): 751-762

Heilmann-Heimbach S, Hochfeld LM, Paus R, Nothen MM. Hunting the genes in male-pattern alopecia: how important are they, how close are we and what will they tell us? Exp Dermatol 2016; 25(4): 251-257

Heilmann-Heimbach S, Herold C, Hochfeld LM, Hillmer AM, Nyholt DR, Hecker J, Javed A, Chew EGY, Pechlivanis S, Drichel D, Heng XT, del Rosario RCH, Fier HL, Paus R, Rueedi R, Galesloot TE, Moebus S, Anhalt T, Prabhakar S, Li R, Kanoni S, Papanikolaou G, Kutalik Z, Deloukas P, Philpott MP, Waeber G, Spector TD, Vollenweider P, Kiemeney LALM, Dedoussis G, Richards JB, Nothnagel M, Martin NG, Becker T, Hinds DA, Nöthen MN. Meta-analysis identifies novel risk loci and yields systematic insights into the biology of male-pattern baldness. Nat Commun 2017; 8: 14694

Hernandez-Pando R, De La Luz Streber M, Orozco H, Arriaga K, Pavon L, Al-Nakhli SA, Rook GA. The effects of androstenediol and dehydroepiandrosterone on the course and cytokine profile of tuberculosis in BALB/c mice. Immunology 1998; 95(2): 234-241

Hernández-Silva CD, Villegas-Pineda JC, Pereira-Suárez AL. Expression and Role of the G Protein-Coupled Estrogen Receptor (GPR30/GPER) in the Development and Immune Response in Female Reproductive Cancers. Front Endocrinol 2020; 11: 544

Higgins CA, Petukhova L, Harel S, Ho YY, Drill E, Shapiro L, Wajid M, Christiano AM. FGF5 is a crucial regulator of hair length in humans. Proc Natl Acad Sci U S A 2014; 111(29): 10648-10653

Higgins CA, Westgate GE, Jahoda CA. From telogen to exogen: mechanisms underlying formation and subsequent loss of the hair club fiber. J Invest Dermatol 2009; 129(9): 2100-2108

Hilborn E, Stal O, Jansson A. Estrogen and androgen-converting enzymes 17beta-hydroxysteroid dehydrogenase and their involvement in cancer: with a special focus on 17beta-hydroxysteroid dehydrogenase type 1, 2, and breast cancer. Oncotarget 2017; 8(18): 30552-30562

Hobkirk R. Steroid sulfation. Trends in Endocrinology & Metabolism 1993; 4(2): 69-74

Jensen-Jarolim E, Pacios LF, Bianchini R, Hofstetter G, Roth-Walter F. Structural similarities of human and mammalian lipocalins, and their function in innate immunity and allergy. Allergy 2016; 71(3): 286-294

Jimenez JJ, Wikramanayake TC, Bergfeld W, Hordinsky M, Hickman JG, Hamblin MR, Schachner LA. Efficacy and safety of a low-level laser device in the treatment of male and female pattern hair loss: a multicenter, randomized, sham device-controlled, double-blind study. Am J Clin Dermatol 2014; 15(2): 115-127

Kaiser M, Abdin R, Gaumond SI, Issa NT, Jimenez JJ. Treatment of Androgenetic Aloepcia: Current Guidance and Unmet Needs. Clin Cosmet Investig Dermatol 2023; 16: 1387 - 1406

Kapama A, Papadimitriou DT, Mastorakos G, Vlahos NF, Papagianni M. Identification of the Rare Ala871Glu Mutation in the Androgen Receptor Gene Leading to Complete Androgen Insensitivity Syndrome in an Adolescent Girl with Primary Amenorrhea. Children (Basel) 2022; 9(12): 1900

Kissane JM and Robins E. The Fluorometric Measurement of Deoxyribonucleic Acid in Animal Tissues with Special Reference to the Central Nervous System. Journal of Biological Chemistry 1958; 233(1): 184-188.

Kohalmy K, Tamasi V, Kobori L, Sarvary E, Pascussi JM, Porrogi P, Rozman D, Prough RA, Meyer UA, Monostory K. Dehydroepiandrosterone induces human CYP2B6 through the constitutive androstane receptor. Drug Metab Dispos 2007; 35(9): 1495-1501

Kraemer FB, Khor V, Shen WJ, Azhar S. Cholesterol Ester Droplets and Steroidogenesis. Mol Cell Endocrinol 2013; 371(0): 15-19

Kraemer FB, Shen WJ, Azhar S. SNAREs and cholesterol movement for steroidogenesis. Mol Cell Endocrinol 2017; 441: 17-21

Krege JH, Hodgin JB, Couse JF, Enmark E, Warner M, Mahler JF, Sar M, Korach KS, Gustafsson JA, Smithies O. Generation and reproductive phenotypes of mice lacking estrogen receptor β. Proc Natl Acad Sci U S A 1998; 95(26): 15677-15682

Krupp K, Fliegner M, Brunner F, Brucker S, Rall K, Richter-Appelt H. How do Individuals with Complete Androgen Insensitivity Syndrome, Mayer-Rokitansky-Kuster-Hauser Syndrome or Polycystic Ovary Syndrome Experience Contact to Other Affected Persons? Geburtshilfe Frauenheilkd 2012; 72(11): 1009-1017

Kurogi K, Yoshihama M, Williams FE, Kenmochi N, Sakakibara Y, Suiko M, Liu MC. Identification of zebrafish steroid sulfatase and comparative analysis of the enzymatic properties with human steroid sulfatase. J Steroid Biochem Mol Bio 2019; 185: 110-117

Labrie F, Luu-The V, Lin SX, Simard J, Labrie C, El-Alfy M, Pelletier G, Belanger A. Intracrinology: role of the family of 17 beta-hydroxysteroid dehydrogenases in human physiology and disease. J Mol Endocrinol 2000; 25(1): 1-16

Langbein L, Schweizer J. Keratins of the human hair follicle. Int Rev Cytol 2005; 243: 1-78

Lee MJ, Cha HJ, Lim KM, Lee OK, Bae S, Kim CH, Lee KH, Lee YN, Ahn KJ, An S. Analysis of the microRNA expression profile of normal human dermal papilla cells treated with 5alpha-dihydrotestosterone. Mol Med Rep 2015; 12(1): 1205-1212

Levy LL and Emer JJ. Female pattern alopecia: current perspectives. Int J Womens Health 2013; 5: 541-556

Li YC, Pirro AE, Amling M, Delling G, Baron R, Bronson R, Demay MB. Targeted ablation of the vitamin D receptor: An animal model of vitamin D-dependent rickets type II with alopecia. Proc Natl Acad Sci U S A 1997; 94(18): 9831-9835

Lin X, Zhu L, He J. Morphogenesis, Growth Cycle and Molecular Regulation of Hair Follicles. Front Cell Dev Biol 2022; 10: 899095

Ludwig E. Classification of the types of androgenetic alopecia (common baldness) occuring in the female sex. Br J Dermatol 1977; 97(3): 247-254

Lutz GA. Das Trichogramm - Indikation, Durchführung und Interpretation. Der Deutsche Dermatologe 2001; 4: 254-261

Lutz GA. Hair loss and hyperprolactinemia in women. Dermatoendocrinol 2012; 4(1): 65-71

Lutz GA. Alopecia androgenetica der Frau - ein Haarausfall mit vielen Facetten. Gynäkologie + Geburtshilfe 2018; 23: 29-37

Maninger N, Wolkowitz OM, Reus VI, Epel ES, Mellon SH. Neurobiological and neuropsychiatric effects of dehydroepiandrosterone (DHEA) and DHEA sulfate (DHEAS). Front Neuroendocrinol 2009; 30(1): 65-91

Manolagas SC, O'Brien CA, Almeida M. The role of estrogen and androgen receptors in bone health and disease. Nat Rev Endocrinol 2013; 9(12): 699-712

Marjon NA, Hu C, Hathaway HJ, Prossnitz ER. G protein-coupled estrogen receptor (GPER) regulates mammary tumorigenesis and metastasis. Mol Cancer Res 2015; 12(11): 1644- 1654

Marko HL, Hornig NC, Betz RC, Holterhus PM, Altmüller J, Thiele H, Fabiano M, Schweikert HU, Braun D, Schweizer U. Genomic variants reducing expression of two endocytic receptors in 46,XY differences of sex development. Hum Mutat 2022; 43(3): 420-433

Martin SG, Lebot MN, Sukkarn B, Ball G, Green AR, Rakha EA, Ellis IO, Storr SJ. Low expression of G protein-coupled oestrogen receptor 1 (GPER) is associated with adverse survival of breast cancer patients. Oncotarget 2018; 9(40): 25946-25956

Martini C, Pallottini V. Cholesterol: from feeding to gene regulation. Genes Nutr 2007; 2(2): 181-193

Medwid S, Price HR, Taylor DP, Mailloux J, Schwarz Ui, Kim RB, Tirona RG. Organic Anion Transporting Polypeptide 2B1 (OATP2B1) Genetic Variants: In Vitro Functional Characterization and Association With Circulating Concentrations of Endogenous Substrates. Front Pharmacol 2021; 12:713567

Mellon S and Griffin LD. Neurosteroids: biochemistry and clinical significance. Trends Endocrinol Metab. 2002; 13(1): 35-43

Miller KK, Al-Rayyan N, Ivanova MM, Mattingly KA, Ripp SL, Klinge CM, Prough RA. DHEA metabolites activate estrogen receptors alpha and beta. Steroids 2013; 78(1): 15-25

Miller WL, Auchus RJ. The molecular biology, biochemistry, and physiology of human steroidogenesis and its disorders. Endocr Rev 2011; 32(1): 81-151

Mirallas O, Grimalt R. The Postpartum Telogen Effluvium Fallacy. Skin Appendage Disord 2016; 1(4): 198-201

Mistriotis P, Andreadis ST. Hair follicle: a novel source of multipotent stem cells for tissue engineering and regenerative medicine. Tissue Eng Part B Rev 2013; 19(4): 265-278

Mostaghel EA. Steroid hormone synthetic pathways in prostate cancer. Transl Androl Urol 2013; 2(3): 212-227

Mueller JW, Gilligan LC, Idkowiak J, Arlt W, Foster PA. The Regulation of Steroid Action by Sulfation and Desulfation. Endocr Rev 2015; 36(5): 526-563

Natarelli N, Gahoonia N, Sivamani RK. Integrative and Mechanistic Approach to the Hair Growth Cycle and Hair Loss. J Clin Med 2023; 12(3): 893

Naville D, Rainey WE, Mason JI. Corticotropin regulation of 3β-hydroxysteroid dehydrogenase/Δ5→4-isomerase in ovine adrenocortical cells: Inhibition by transforming growth factor β. Molecular and Cellular Endocrinology 1991; 75(3): 257-263

Nestor MS, Ablon G, Gade A, Han H, Fischer DL. Treatment options for androgenetic alopecia: Efficacy, side effects, compliance, financial considerations, and ethics. J Cosmet Dermatol 2021; 20(12): 3759-3781

Nokelainen P, Peltoketo H, Vihko R, Vihko P. Expression cloning of a novel estrogenic mouse 17 beta-hydroxysteroid dehydrogenase/17-ketosteroid reductase (m17HSD7), previously described as a prolactin receptor-associated protein (PRAP) in rat. Mol Endocrinol 1998; 12(7): 1048-1059

Ntshingila S, Oputu O, Arowolo AT, Khumalo NP. Androgenetic alopecia: An update. JAAD Int 2023; 13: 150-158

Ohnemus U, Uenalan M, Inzunza J, Gustafsson JA, Paus R. The hair follicle as an estrogen target and source. Endocr Rev 2006; 27(6): 677-706

Okamoto N, Viswanatha R, Bittar R, Li Z, Haga-Yamanaka S, Perrimon N, Yamanaka N. A Membrane Transporter Is Required for Steroid Hormone Uptake in Drosophila. Dev Cell 2018; 47(3): 294-305 e297

O'Neill KI, Kuo LW, Williams MM, Lind H, Crump LS, Hammond NG, Spoelstra NS, Caino MC, Richer JK. NPC1 Confers Metabolic Flexibility in Triple Negative Breast Cancer. Cancers (Basel) 2022; 14(14): 3543

Oostdijk W, Idkowiak J, Mueller JW, House PJ, Taylor AE, O'Reilly MW, Hughes BA, de Vries MC, Kant SG, Santen GW, Verkerk AJ, Uitterlinden AG, Wit JM, Losekoot M, Arlt W. PAPSS2 deficiency causes androgen excess via impaired DHEA sulfation--in vitro and in vivo studies in a family harboring two novel PAPSS2 mutations. J Clin Endocrinol Metab 2015; 100(4): E672-680

Oster H. Endokrine Rhythmen. In: Lehnert H., Hrsg. Rationale Diagnostik und Therapie in Endokrinologie, Diabetologie und Stoffwechsel. Stuttgart: Georg Thieme Verlag KG, 2014

O'Sullivan F, Laird E, Kelly D, van Geffen J, van weele M, McNulty H, Hoey L, Healy M, McCarroll K, Cunningham C, Casey M, Ward M, Strain JJ, Molloy AM, Zgaga L. Ambient UVB Dose and Sun Enjoyment Are Important Predictors of Vitamin D Status in an Older Population. J Nutr 2017; 147(5): 858-868

Ota Y, Saitoh Y, Suzuki S, Ozawa K, Kawano M, Imamura T. Fibroblast growth factor 5 inhibits hair growth by blocking dermal papilla cell activation. Biochem Biophys Res Commun 2002; 290(1): 169-176

Ouimet M, Barrett TJ, Fisher EA. HDL and Reverse Cholesterol Transport: Basic Mechanisms and their Roles in Vascular Health and Disease. Circ Res 2019; 124(10): 1505-1518

Panchaprateep R, Lueangarun S. Efficacy and Safety of Oral Minoxidil 5 mg Once Daily in the Treatment of Male Patients with Androgenetic Alopecia: An Open-Label and Global Photographic Assessment. Dermatol Ther (Heidelb) 2020; 10(6): 1345-1357

Papotti B, Escola-Gil JC, Julve J, Poti , Zanotti I. Impact of Dietary Lipids on the Reverse Cholesterol Transport: What We Learned from Animal Studies. Nutrients 2021; 13(8): 2643

Paterni I, Granchi C, Katzenellenbogen JA, Minutolo F. Estrogen receptors alpha (ERalpha) and beta (ERbeta): subtype-selective ligands and clinical potential. Steroids 2014; 90: 13-29

Paus R, Cotsarelis G. The biology of hair follicles. N Engl J Med 1999; 341(7): 491-497

Penning TM. Human hydroxysteroid dehydrogenases and pre-receptor regulation: insights into inhibitor design and evaluation. J Steroid Biochem Mol Biol 2011; 125(1-2): 46-56

Phizicky EM and Hopper AK. The life and times of a tRNA. RNA 2023; 29(7): 898-957

Picard M, Wallace DC, Burelle Y. The Rise of Mitochondria in Medicine. Mitochondrion 2016; 30: 105-116

Pierard-Franchimont C, Pierard GE. Alterations in hair follicle dynamics in women. Biomed Res Int 2013; 2013: 957432

Pluciennik F, Verrecchia F, Bastide B, Herve JC, Joffre M, Deleze J. Reversible interruption of gap junctional communication by testosterone propionate in cultured Sertoli cells and cardiac myocytes. J Membr Biol 1996; 149(3): 169-177

Prossnitz ER and Barton M. The G-protein-coupled estrogen receptor GPER in health and disease. Nat Rev Endocrinol 2011; 7(12): 715-726

Qi J, Garza LA. An overview of alopecias. Cold Spring Harb Perspect Med 2014; 4(3): a013615

Rainey WE, Nakamura Y. Regulation of the adrenal androgen biosynthesis. J Steroid Biochem Mol Biol 2008; 108(3-5): 281-286

Ramos PM, Miot HA. Female Pattern Hair Loss: a clinical and pathophysiological review. An Bras Dermatol 2015; 90(4): 529-543

Randall VA. Androgens and human hair growth. Clinical Endocrinology 1994; 40(4): 439-457

Rassow J. Lipoproteine: Transport von Lipiden im Blut. In: Rassow, J., Hauser, K., Netzker, R. und Deutzmann, R., Hrsg. Duale Reihe Biochemie. Stuttgart: Georg Thieme Verlag, KG, 2012: 243-251

Redler S, Messenger AG, Betz RC. Genetics and other factors in the aetiology of female pattern hair loss. Exp Dermatol 2017; 26(6): 510-517

Rege J, Nakamura Y, Satoh F, Morimoto R, Kennedy MR, Layman LC, Honma S, Sasano H, Rainey WE. Liquid chromatography-tandem mass spectrometry analysis of human adrenal vein 19-carbon steroids before and after ACTH stimulation. J Clin Endocrinol Metab 2013; 98(3): 1182-1188

Reinehr T, Sanchez-Guijo A, Lass N, Wudy SA. Higher steroid sulfation is linked to successful weight loss in obese children. Endocr Connect 2018; 7(10): 1020-1030

Reisch N, Taylor AE, Nogueira EF, Asby DJ, Dhir V, Berry A, Krone N, Auchus RJ, Shackleton CHL, Hanley NA, Arlt W. Alternative pathway androgen biosynthesis and human fetal female virilization. Proc Natl Acad Sci U S A 2019; 116(44): 22294-22299

Rizner TL, Penning TM. Role of aldo-keto reductase family 1 (AKR1) enzymes in human steroid metabolism. Steroids 2014; 79: 49-63

Robbins C, Mirmirani P, Messenger AG, Birch MP, Youngquist RS, Tamura M, Filloon T, Luo F, Dawson Jr TL. What women want - quantifying the perception of hair amount: an analysis of hair diameter and density changes with age in caucasian women. Br J Dermatol 2012; 167(2): 324-332

Robinson DP, Klein SL. Pregnancy and pregnancy-associated hormones alter immune responses and disease pathogenesis. Horm Behav 2012; 62(3): 263-271

Roth M, Obaidat A, Hagenbuch B. OATPs, OATs and OCTs: the organic anion and cation transporters of the SLCO and SLC22A gene superfamilies. Br J Pharmacol 2012; 165(5): 1260-1287

Rozmus D, Ciesielska A, Plominski J, Grzybowski R, Fiedorowicz E, Kordulewska N, Savelkoul H, Kostyra E, Cieslinska A. Vitamin D Binding Protein (VDBP) and Its Gene Polymorphism - The Risk of Malignant Tumors and Other Diseases. Int J Mol Sci 2020; 21(21): 7822

Rusidzé M, Adlanmérini M, Chantalat E, Raymond-Letron I, Cayre S, Arnal JF, Deugnier MA, Lenfant F. Estrogen receptor-α signaling in post-natal mammary development and breast cancers. Cell Mol Life Sci 2021; 78(15): 5681-5705

Sahu B, Pihlajamaa P, Dubois V, Kerkhofs S, Claessens F, Jänne OA. Androgen receptor uses relaxed response element stringency for selective chromatin binding and transcriptional regulation *in vivo*. Nucleic Acids Res 2014; 42(7): 4230-4240

Samavat H, Kurzer MS. Estrogen metabolism and breast cancer. Cancer Lett 2015; 356(2 Pt A): 231-243

Santos Z, Avci P, Hamblin MR. Drug discovery for alopecia: gone today, hair tomorrow. Expert Opin Drug Discov 2015; 10(3): 269-292

Schiffer L, Arlt W, Storbeck KH. Intracrine androgen biosynthesis, metabolism and action revisited. Mol Cell Endocrinol 2018; 465: 4-26

Schiffer L, Barnard L, Baranowski ES, Gilligan LC, Taylor AE, Arlt W, Shackleton CHL, Storbeck KH. Human steroid biosynthesis, metabolism and excretion are differentially reflected by serum and urine steroid metabolomes: A comprehensive review. J Steroid Biochem Mol Biol 2019; 194: 105439

Schweikert HU, Milewich L, Wilson JD. Aromatization of androstenedione by isolated human hairs. J Clin Endocrinol Metab 1975; 40(3): 413-417.

Schweikert HU, Wilson JD. Regulation of human hair growth by steroid hormones. I. Testerone metabolism in isolated hairs. J Clin Endocrinol Metab 1974; 38(5): 811-819

Shehu A, Albarracin C, Devi YS, Luther K, Halperin J, Le J, Mao J, Duan RW, Frasor J, Gibori G. The Stimulation of HSD17B7 Expression by Estradiol Provides a Powerful Feed-Forward Mechanism for Estradiol Biosynthesis in Breast Cancer Cells. Mol Endocrinol. 2011; 25(5): 754-766

Sinclair R. Male pattern androgenetic alopecia. BMJ 1998; 317(7162): 865-869

Sinclair R, Torkamani N, Jones L. Androgenetic alopecia: new insights into the pathogenesis and mechanism of hair loss. F1000Res 2015; 4(F1000 Faculty Rev): 585

Soria-Jasso LE, Carino-Cortés R, Muñoz-Pérez VM, Pérez-Hernández N, Fernández-Martínez E. Beneficial and Deleterious Effects of Female Sex Hormones, Oral Contraceptives, and Phytoestrogens by Immunomodulation on the Liver. Int J Mol Sci 2019; 20(19): 4694

Tan MH, Li J, Xu HE, Melcher K, Yong EL. Androgen receptor: structure, role in prostate cancer and drug discovery. Acta Pharmacol Sin 2015; 36(1): 3-23

Trueb RM. Understanding Pattern Hair Loss-Hair Biology Impacted by Genes, Androgens, Prostaglandins and Epigenetic Factors. Indian J Plast Surg 2021; 54(4): 385-392

Turcu AF, Auchus RJ. Adrenal steroidogenesis and congenital adrenal hyperplasia. Endocrinol Metab Clin North Am 2015; 44(2): 275-296

Turcu AF, Auchus RJ. Clinical significance of 11-oxygenated androgens. Curr Opin Endocrinol Diabetes Obes 2017; 24(3): 252-259

Turcu AF, Nanba AT, Auchus RJ. The Rise, Fall, and Resurrection of 11-Oxygenated Androgens in Human Physiology and Disease. Hormone Research in Paediatrics 2018; 89(5): 284-291

Unlu G, Prizer B, Erdal R, Yeh HW, Bayraktar EC , Birsoy K. Metabolic-scale gene activation screens identify SLCO2B1 as a heme transporter that enhances cellular iron availability. Mol Cell 2022; 82(15): 2832-2843.e7.

Unluhizarci K, Hacioglu A, Taheri S, Karaca Z, Kelestimur F. Idiopathic hirsutism: Is it really idiopathic or is it misnomer? World J Clin Cases 2023; 11(2): 292-298

Van Scott EJ, Reinertson RP, Steinmuller R. The growing hair roots of the human scalp and morphologic changes therein following amethopterin therapy. J Invest Dermatol 1957; 29(3): 197-204

Vickers AJ, Savage CJ, Lilja H. Finasteride to Prevent Prostate Cancer: Should All Men or Only a High-Risk Subgroup Be Treated? Journal of Clinical Oncology 2010; 28(7): 1112-1116

Vidali S, Knuever J, Lerchner J, Giesen M, Bíró T, Klinger M, Kofler B, Funk W, Poeggeler B, Paus R. Hypothalamic-pituitary-thyroid axis hormones stimulate mitochondrial function and biogenesis in human hair follicles. J Invest Dermatol 2014; 134(1):33-42

Vilardo E, Toth U, Hazisllari E, Hartmann RK, Rossmanith W. Cleavage kinetics of human mitochondrial RNase P and contribution of its non-nuclease subunits. Nucleic Acids Res 2023; 51(19): 10536-10550

Vincent M and Yogiraj K. A Descriptve Study of Alopecia Patterns and their Relation to Thyroid Dysfunction. Int J Trichology 2013; 5(1): 57- 60

Walther TC and Farese RV Jr. The life of lipid droplets. Biochim Biophys Acta 2009; 1791(6): 459-466

Wardell SE, Nelson ER, McDonnell DP. From empirical to mechanism-based discovery of clinically useful Selective Estrogen Receptor Modulators (SERMs). Steroids 2014; 90: 30-38

Wehner G, Schweikert HU. Estrone sulfate source of estrone and estradiol formation in isolated human hair roots: identification of a pathway linked to hair growth phase and subject to site-, gender-, and age-related modulations. J Clin Endocrinol Metab 2014; 99(4): 1393-1399

Wolff H, Fischer TW, Blume-Peytavi U. The Diagnosis and Treatment of hair and Scalp Diseases. Dtsch Arztebl Int 2016; 113(21): 377- 386

Xu Z, McClure ST, Appel LJ. Dietary Cholesterol Intake and Sources among U.S. Adults: Results from National Health and Nutrition Examination Surveys (NHANES), 2001-2014. Nutrients 2018; 10(6): 771

Xu S, Yu S, Dong D, Lee LTO. G Protein-coupled estrogen receptor: a potential therapeutic target in cancer. Front Endocrinol 2019; 10: 725

Xu T, Ma D, Chen S, Tang R, Yang J, Meng C, Feng Y, Liu L, Wang J, Luo H, Yu K. High GPER expression in triple-negative breast cancer is linked to pro-metastatic pathways and predicts poor patient outcomes. NPJ Breast Cancer 2022; 8:100

Yakin K, Hela F, Oktem O. Progesterone signaling in the regulation of luteal steroidogenesis. Mol Hum Reprod 2023; 29(8): gaad022

Yanagisawa R, He C, Asai A, Hellwig M, Henle T, Toda M. The Impacts of Cholesterol, Oxysterols, and Cholesterol Lowering Dietary Compounds on the Immune system. Int J Mol Sci 2022; 23(20): 12236

Yu K, Shen Y, Jiang YL, Huang W, Wang F, Wu YQ. Two novel ectodysplasin A gene mutations and prenatal diagnosis of X-linked hypohidrotic ectodermal dysplasia. Mol Genet Genomic Med 2021; 9(11): e1824

Zgaga L, Laird E, Healy M. 25-Hydroxyvitamin D Measurement in Human Hair: Results from a Proof-of-Concept study. Nutrients 2019; 11(2): 423

Zhang D, Wang J, Chen H, Yan S. Cytoplasmic G Protein-Coupled Estrogen Receptor 1 as a Prognostic Indicator of Breast Cancer: A Meta-Analysis. Technol Cancer Res Treat 2022; 21: 15330338221131664

Zirkin BR, Papadopoulos V. Leydig cells: formation, function, and regulation. Biol Reprod 2018; 99(1): 101-111

Żylińska LA, Gromadzińska E, Lachowicz L. Short-time effects of neuroactive steroids on rat cortical Ca2+-ATPase activity. Biochimica et Biophysica Acta (BBA) - Molecular and Cell Biology of Lipids 1999; 1437(2): 257-264